LARGE-DIAMETER LOW-PROFILE AIR FORMS USING CABLE NET SUPPORT SYSTEMS FOR CONCRETE DOMES

A Thesis

Submitted to the

Department of Civil & Environmental Engineering

Brigham Young University

In Partial Fulfillment

of the Requirements for the Degree

Master of Science

by

Scott E. Jacobs

June 1996

Large-Diameter Low-Profile Air Forms Using Cable Net Support Systems For Concrete Domes

Scott Jacobs

Department of Civil & Environmental Engineering

M.S. Degree, August 1996

Abstract

The objective of this thesis was to show that a cable net based on the geometry of the Pantheon Roof would control distortions of a large-diameter, low-profile air form. A secondary purpose of this research was too show that this method of construction is cost effective, and optimizes construction time. A model was constructed with a cable net consisting of three primary horizontal cables, and corresponding vertical cables. The cables were attached to the ring beam, and the membrane inflated; the apex deformations in the membrane were measured at 7 inches without cables, and at 0.5 inches with cables. This data proved that the cable net will eradicate the apex deformations in the membrane.

To mitigate a potential distortion problem, it is suggested that the cables be attached to fixed node points on the membrane at all cable intersections. The horizontal cables will also need to be placed in spacing equal to that of the vertical cables at the base of the air form. Using this technology, cable nets will adequately support an 800+ ft diameter air form. Additional research should be conducted to better understand the nonlinear cable membrane interactions. The desire to build large open span structures can now be fulfilled in a quick, efficient and very economic method of construction.

COMMITTEE APPROVAL:

Arnold Wilson, Committee Chair

Reese Goodwin, Committee Member

Kyle Rollins, Committee Member

Woodruff Miller, Graduate Coordinator

This thesis, by Scott E. Jacobs, is accepted in its present form by the Department of Civil & Environmental Engineering of Brigham Young University as satisfying the thesis requirement for the degree of Master of Science.

Arnold Wilson, Committee Chair

Reese Goodwin, Committee Member

Kyle Rollins, Committee Member

7-3-96

Date

Woodruff Miller, Graduate Coordinator

Definitions

h	Thickness of concrete dome
D	Diameter of the dome(ft)
R	Radius of Curvature of the dome(ft)
H	Height of the dome(ft)
ϕ_k	Total angle of the dome from apex to the ring beam
ψ	Angle from ring beam to some point x
α	ϕ_k-ψ
N_θ	Circumferential - horizontal force from membrane analysis
N_ϕ	Radial - vertical force from membrane analysis
Membrane analysis	A simple analysis not considering any moment within the membrane
Membrane	A single-ply material
Node point	A fixed point on the membrane to which the cable's net is connected
Cable net	A system of cables of different geometries that is applied to the outside of the membrane, and then removed from the dome after construction with the membrane.
Tributary area	A specific area on the surface of the membrane that distributes the forces to a specific cable.
Domical structure	A structure that is based on a rotated roman arch.

Thin shell	A structure that spans a distance and has a relative thin material depth
Reinforced concrete	A composite using steel and concrete as the medium
Force component	Any force that can be broken into a set of forces on any assigned axis whose equivalent direction and magnitude are equal to the original force.
Air form	A membrane that is inflated with air pressure and used as a forming system for reinforced concrete domical structures.
Ribs	Beam-Column members placed monolithically with the thin shell to support against concrete thin shelled buckling problems.
Water pressure	A method of measuring the pressure on the interior of the dome.
Distortion	Movement of the air form surface from the projected profile.
Scaling factor	The amount of reduction taken in the model attributes, diameter, height, radius etc.
Geodesic-net	A pattern of octagonal shapes in a cable net.
Web-net	A pattern of horizontal and radial cables.

Table of Contents

Table of Contents (Continued)

List of Figures

List of Tables

Chapter 1
Introduction

Fascination with the arch has been evident in much of the architecture since the early Roman times(2)[1]. An arch rotated 360° is the shape of a dome, and probably the inspiration for many of the early domical structures. The most significant domical structure of the Roman period was the roof structure of the Pantheon. The 142 ft diameter dome required nearly a decade to complete. The forming and placement of the masonry dome were likely very time consuming, but due to slave labor the cost of construction was not a problem. Today the interest in building larger diameter domical structures continues to increase as more effort is made to expand this capability. The high cost of conventional forming and constructing a 300 ft plus diameter dome has deterred many proposed projects from becoming a reality. Through inventive methods, the immense forming costs have been reduced for domes smaller than 260 ft in diameter.

The Kingdome of Seattle Washington is the most recent (1976) addition to the list of large-diameter domical structures. The Kingdome is currently (1996) one of the largest open-span, concrete, thin-shelled structure in the world, and was touted as an economically successful structure. The 65,000-seat structure (2) cost less than $1000/per seat, substantially lower than other structures of comparable sized diameter.

In the early 1940s (5) the idea of using an inflated membrane to form a concrete dome was invented and used efficiently. The use of air forms has progressed significantly. Structures as large as 260 feet in diameter are formed and built with a construction time of

---

[1]This refers to a listed reference

two-three months using this technology. The air forms have become a very quick and efficient method of forming domical structures. Domes larger than 260 feet in diameter have not been attempted due to problems related to the membrane's limited ability to take the forces required to inflate the air forms. The ability to use air form technology to form large diameter domes would create a very effective structure, economically and structurally.

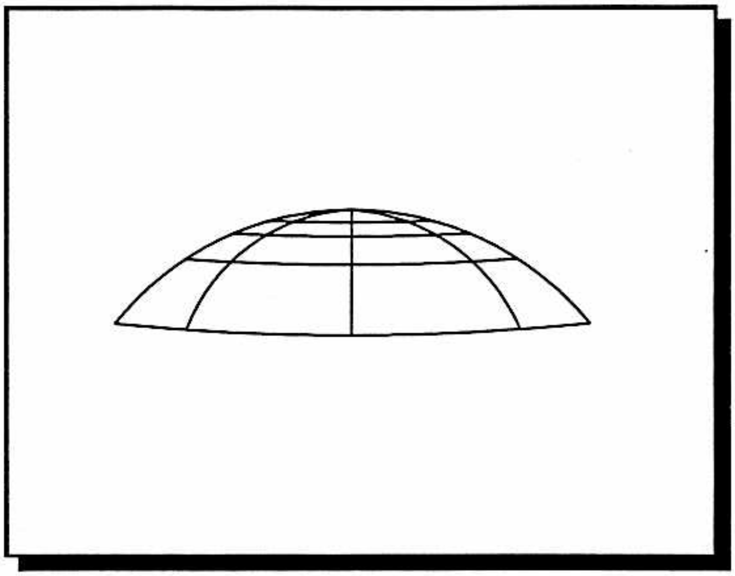
Figure 1.1 Radial-Horizontal Cable Net Geometry

OBJECTIVE

In a pattern similar to that of the Pantheons, radial and horizontal grids spaced in equal leg dimensions, horizontally and vertically, will be used. A cable net will control the air form deflections and make forming larger

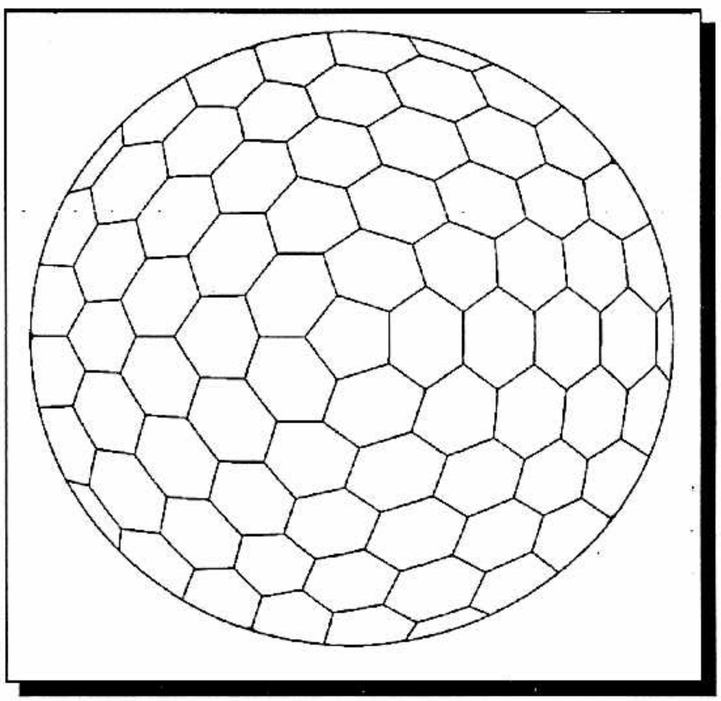
Figure 1.2 Geodesic Cable Net Geometry

diameter domes feasible. The purpose of this thesis is to present research, based on the modeling of low-profile domes using either a radial-horizontal (figure 1.1), or geodesic cable net (figure 1.2). Each cable net system will be tested in terms of membrane deformations and cable tensions, due to applied forces. A dimensional analysis will be used to compare the apex deformation data to air forms constructed in the future. The largest dome constructed to date was about 260 ft in diameter. It is believed that a 300 ft diameter dome could be constructed, using current air form technology. The membrane strength would limit the radius of curvature to 170 ft, based[2] on a generally accepted factor of safety. The research presented here will show the feasibility of using this technology to build 800+ ft large diameter low-profile domes.

This model will show that the use of an air form with a supportive cable-net system will aid in the solution to correct the inherent deflection problems that cause the air form to be unusable for large-diameter domes. The model will also show that cable nets reduce the local stresses within the air form, by reducing the local radius of curvature, and making the air forming system itself feasible. The combination of the membrane and the cable-net system makes the construction of very large dome roof structures feasible both in terms of economics and time.

---

[2]David South - Monolithic Constructors 170 ft radius of curvature limit

Chapter 2
Historical Background

2.1 History of Domes

Domical shaped structures dating from before the time of Christ have interested engineers and architects for centuries. For example the Pantheon (2)[1], constructed of masonry during the Roman era, measured 142 feet in diameter (see figure 2.1), the largest of the Roman masonry domes constructed; however, other smaller diameter dome structures were constructed during that period (2). The Pantheon has particular value in terms of this thesis because of the large diameter and the length of time the structure has endured (2). Like the

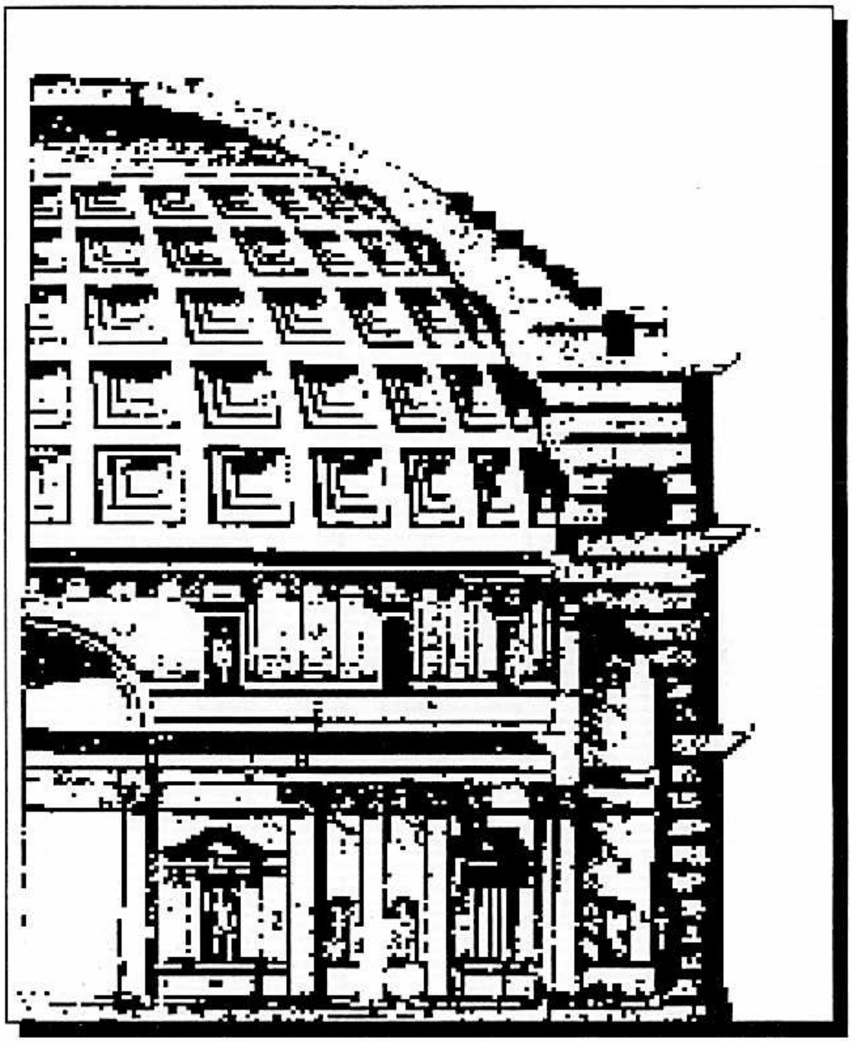

Figure 2.1 Pantheon (2)

[1]This refers to a listed reference

Pantheon, many of the early dome structures are still standing, a strong verification of their durabiltiy with time. Figure 2.2 shows a profile of the significant dome diameters since the time of the Pantheon.

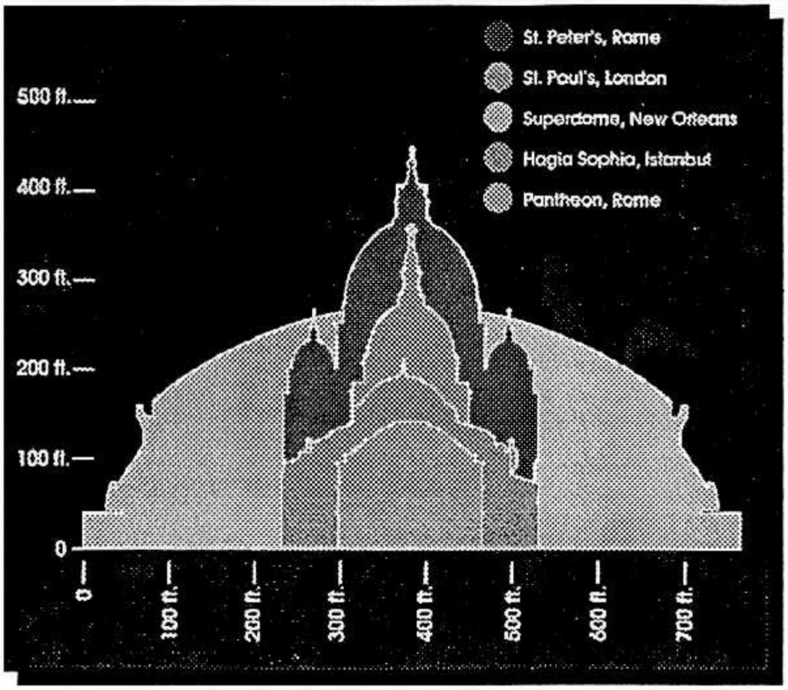

Figure 2.2 Dome Size Comparison (10)

The Pantheon stood as the world's largest diameter dome (2) for centuries. Centennial Hall (figure 2.3) in Breslau, Germany was constructed in 1913 as a domical roof structure. Designed by Max Berg(2), it used radially arranged arches connected by concentric circular ribs to form the dome roof structure, supported on a system of vertical arches. This particular dome is significant, not only because of the large diameter of 213 feet, but because the whole dome was constructed of reinforced concrete.

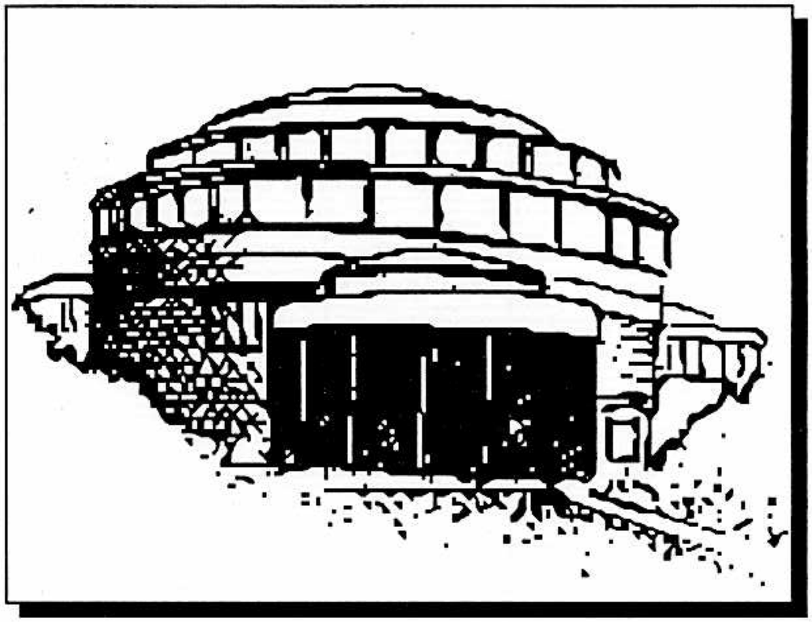
Figure 2.3 Centennial Hall, Germany (2)

Centennial Hall (see figure2.3) the largest diameter dome in 1913(1), was followed by many larger diameter domes. In 1976, the open-span distance traversed by a reinforced concrete, thin- shelled roof structure formed by a reusable forming system, grew to an amazing 660 feet in diameter. This structure and forming system was designed by J. V. Christiansen. The reusable forming system rotated on a rail mounted on the interior wall,

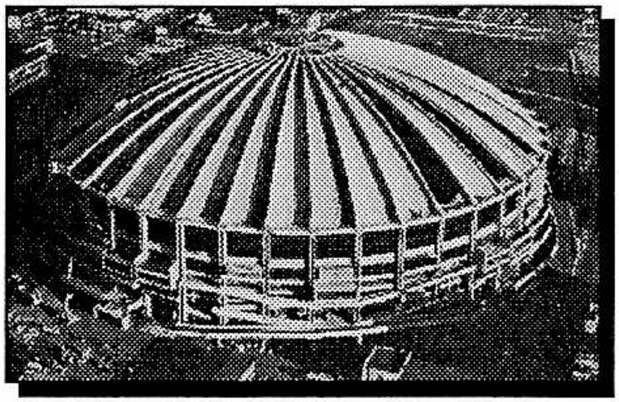

Figure 2.4 Kingdome Roof Construction (1)

and pivoted on a point in the center of the arena. The reusable forming system allowed the forming of four concentric sections simultaneously. Two sections would be formed on symmetric sides of the dome, in order to maintain equilibrium on the structure during construction (see figure 2.4). Maintaining symmetry during construction reduced potential eccentricity problems and increased safety during construction. The reusable forming system gave the project an economic edge, as well as expediting the actual construction process. Melaragho (2) attributes the

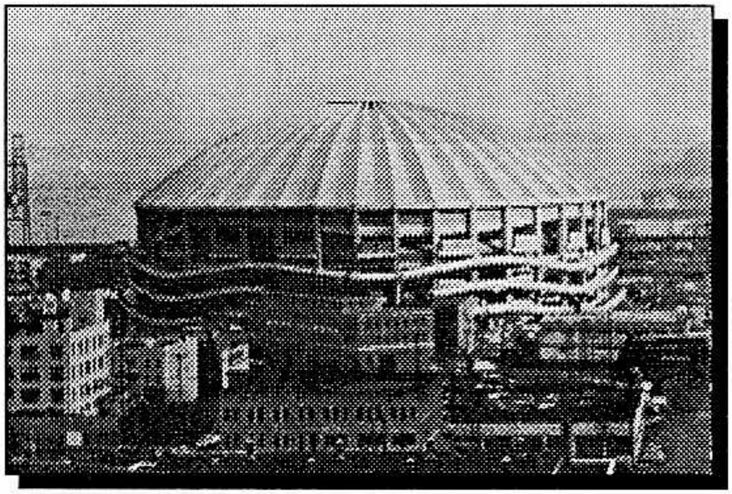

Figure 2.5 Kingdome (1)

overwhelming success of the Kingdome roof (see figure 2.5) structure itself to the quality management and experience of John V. Christiansen, the engineer of record. Melaragho also attributed the reasons for choosing a reinforced concrete dome to be based in economics, including the reduction in potential fire insurance premiums, savings in construction cost, due to no fire proofing necessary in reinforced concrete structures. This list also included minimum maintenance cost, and low roofing requirements. The overall cost ended up substantially lower than that of other comparable sized domical steel structures. The Kingdome demonstrated that a thin shell reinforced concrete dome could be economically feasible in both construction and maintenance.

Modern and ancient thin-shelled structures have proven themselves through time to be very durable in the face of diverse forces, including: seismic, wind, snow and direct impact. During the Second World War, factories were set up under thin-shelled roofs. As quickly as the allied planes would drop bombs crashing through the roof systems, the roofs were, patched and the factory was immediately placed back into operation.

The cost and effort of forming a domical structure have in the past overshadowed all the positive attributes that are traditionally viewed as factors in favor of a domical structure. The time required to form the compound curved structure would often take years to complete. The advent of the use of air forms to form compound curved domical structures reduces the time requirement from years to months. The air form has removed the time constraints, thus making a domical concrete structure more economically feasible.

2.2 Air forms

The use of air forms in small-diameter[2] domes has increased in popularity over the last 20 years, as the advantages of using these forms have become more recognized. The economic benefits are obvious in the current time of high material and labor costs, as well as the fact that most projects are pressured to complete construction at or below a budget. Air-form domes are constructed one tier at a time, with cranes and forklift baskets. The concrete and structural steel are placed on the interior of the membrane surface. The support crew for each crane consists of 10 to 15 persons. Domes smaller than 180 ft only safely allow two cranes in operation at one time. Working from cranes and smaller crews strongly facilitate, the use of double shifts in the construction of air-form domes, thus being able to finish the project in a smaller period of time, again saving money.

The fact that the shell is placed monolithically, with the beams, and that the beams are completely on the interior side of the shell, effectively eliminates any valleys on the top side of the roof, creating a smooth path for the water to drain. The monolithically placed reinforced concrete roof structure theoretically eliminates leaky roof problems, that are currently inherent in most large span roof structures in the country. Being able to control water flow more effectively is yet another structural and economical advantage in favor of using an air form for large-diameter domes.

Along with the positive aspects of using air form construction are a few negative factors that need to be addressed. One of the inherent problems with air forms is that few contractors have the equipment and experience necessary to construct such a structure.

---

[2]260 feet is the largest dome built to date (1996)

Experience is probably the most important factor, because like any other construction procedure the process takes years to develop. The placement of the steel and the application of the concrete include "tricks of the trade"[3] that can only be learned with time and experience. The concrete is applied to the interior of the membrane surface with a special pump and nozzle system. The special nozzle system, is very difficult to operate and requires operators to have at least 400 hours of supervised experience (5). The cranes and shotcrete equipment required is expensive, thus becoming another determent to many would-be contractors. The negative aspects of air-form construction are exclusively related to the contractor and not to the owner-operator of the actual finished structure.

2.2.1 Airform Construction History

The first patent for air forms was issued in the early 1940s to Wallace Neff (5). This patent included the process of inflating a membrane to the desired shape and placing the concrete and the steel on top of the air form. This construction process was not an overwhelming success.

Dante Bini (5) received a patent on air forms in the late 1940s early 1950s based, on placing the concrete and the structural steel on top of the membrane, while still on the ground. Once this was completed, the air form was inflated while the concrete was hopefully still plastic. The steel was loosely tied and placed so that as the membrane rose,

---

[3]Shotcreteing - the process of shoting the concrete onto the interior surface of the membrane through a shotcrete nozzle.

the steel would pull into the designed location. This process was quite successfully used and developed.

In 1972, Lloyd Turner (5) received a patent on an air-form construction process that placed urethane foam on the inside of the inflated membrane. A measuring block is placed into the foam,

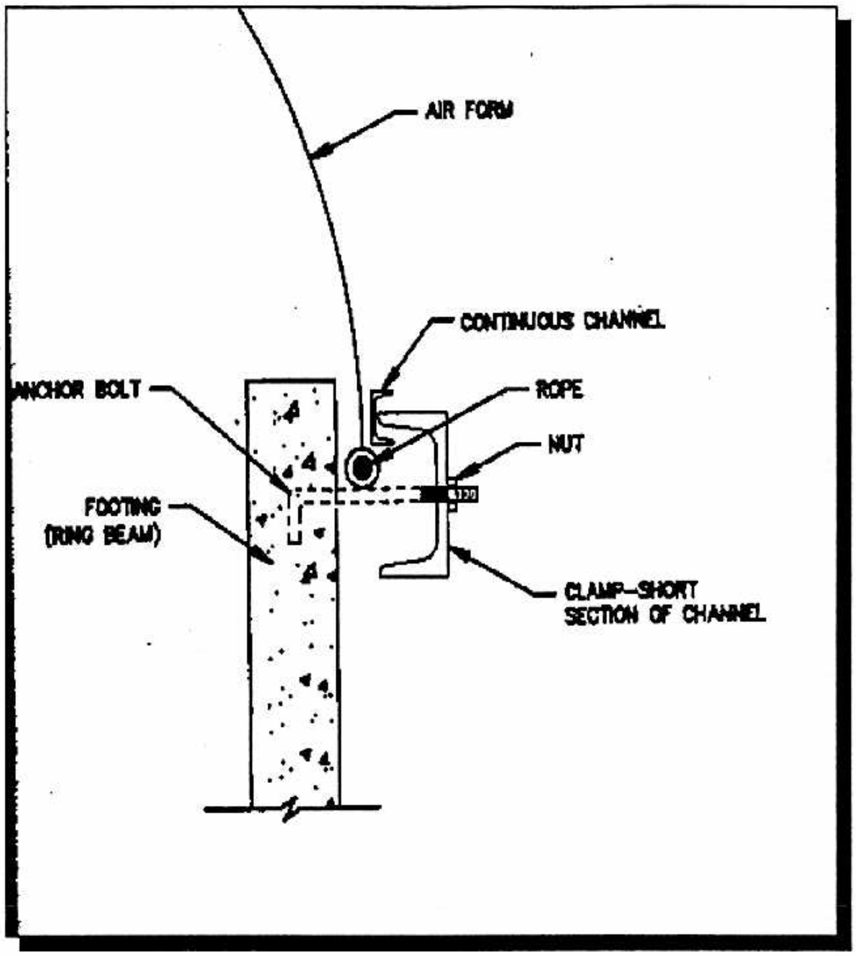

Figure 2.6 foundation connection (9)

to measure the thickness of the foam and concrete as it is applied. This process was never fully developed, but contractors were able to purchase rights to the patent for use in construction of domes.

In 1976, David and Barry South (5) were issued a patent for a construction process that was much like that of Lloyd Turners. This process used a steel depth gage that could be placed right into the urethane foam and used to tie the steel to during construction. The Souths have developed this process and have made it work in hundreds of smaller domes built around the world. Each of the different air form construction methods developed from the 1940s to 1976, was moved toward making air-forming feasible. The South method as outlined in "Construction of Shells Using Air-Supported Forms" (5) specifically includes:

a. Constructing an engineered ring beam and slab capable of handling uplift and horizontal thrust of the air form. The ballooning effect must be taken into consideration because the membrane must be spread over the foundation evenly before fastening it to the foundation (see figure 2.6).

b. Everything that will be used to construct the dome must be placed on the inside of the ring beam prior to spreading the dome membrane over the ring beam-foundation. The membrane manufacture carefully folds the skin at the plant marking clearly the position where the membrane should be laid out. The equipment (5) inside of the ring beam poses a potential hazard for the membrane, so the inflation process must be slow and careful.

c. Special hangers are placed, while spraying a urethane foam on to the membrane which will develop enough stability to begin placing the steel and concrete.

d. A mat typically of #3 bars is attached to the special steel hangers mounted in the urethane foam. This gives the membrane more rigidity, allowing the placement of the larger structural mats of steel. When more than one mat of steel is required, one mat is placed then embedded in concrete, and then another mat is added. The shotcrete is applied layers until the full shell thickness is obtained as required by the engineering design of the structure.

2.2.2 Membrane Materials and Physical Properties

The most important component in the membrane-cable system is the construction of, and strength of the membrane. The membrane must be able to carry the forces to the cables then to the ringbeam or foundation. The membrane is a manufacured matrix composed of a scrim which is the strength of the membrane and a PVC coating that protects the scrim. The scrim is made of polyester fibers tightly woven into a bolt of cloth. The cloth called greygoods is then coated with the PVC material making it secure from the elements. The scrim covered with a hot semi- moltant PVC material is sent through a set of rollers, that impregnates or calanders the matrix permanantly together. The finished material is classified by its unit weight. Typically the scrim is 7 oz/yd^2 and the PVC coating ranges from 27 to 40 oz/yd^2. The material is shipped in bolts of material that are cut into gores coorelating to the dimensions of the air-form to be constructed. The gores are welded together, by overlapping the material 1 3/4" and concentrating hot air on the weld area semi-melting the PVC material and sealing the sections together. The hot air ranges in temperature from 700 F° to 1000 F° and connects two gores together using the calandered PVC material on each section to connect the pieces. The new materials and assembly processes have made the membrane very strong. However the stability of the membrane on an actual job site requires a substantial factor of safety, in order to safely use the air form.

2.3 Air-form Limitations

The larger the diameter of a dome that is being built, the greater force that the membrane is required to carry. As can be seen in Equation 1, the force "T" increases proportional to the increase in the radius of curvature. Therefore the size of air form is limited to the safe force that is feasible within the membrane. The higher forces create a

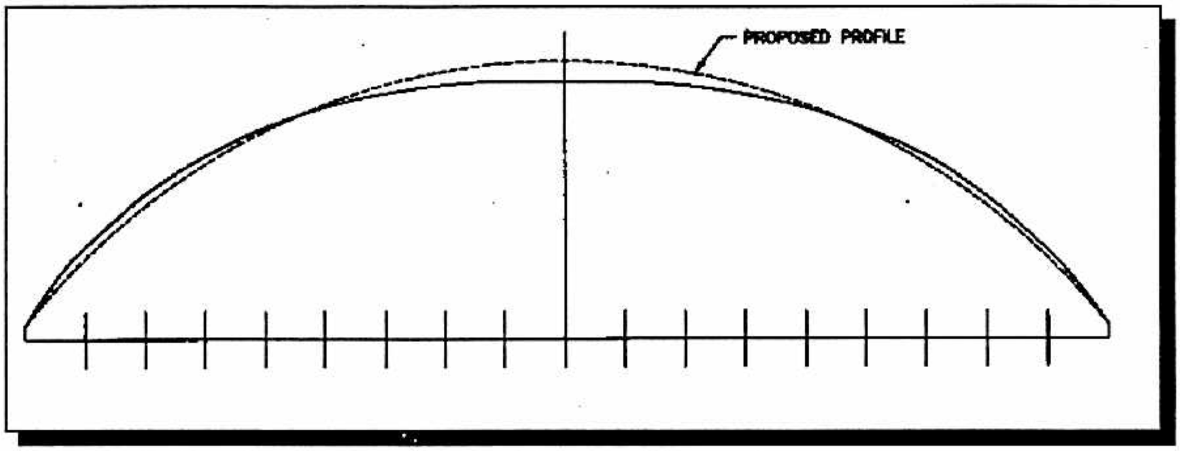

Figure 2.7 Deflection of a nonsupported, low-profile membrane

few problems within the membrane itself. The most critical being, the higher tensions in the membrane. The second is the large deformations at the apex (figure 2.7) and at the lower point on the dome. These distortions create even greater forces in the membrane as the effective radius of curvature is increased. Figure 2.7 shows the deformation of the dome at a pressure equal to 10 inches of water. When the pressure is decreased the

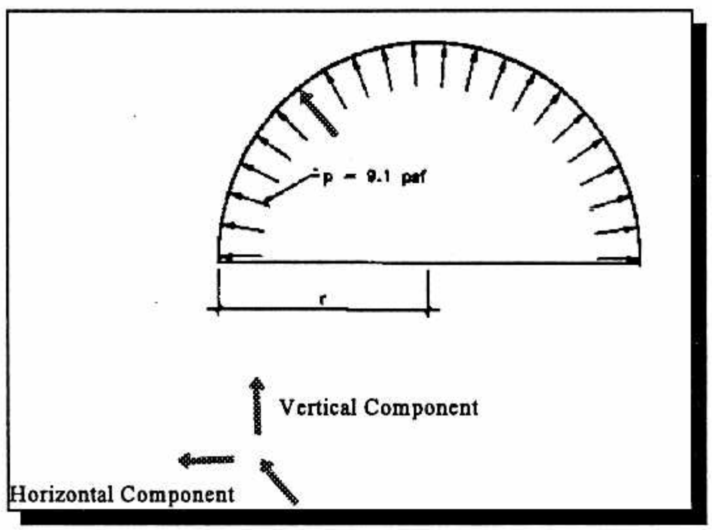

Figure 2.8 Radial pressure

amount of apex deflection is decreased as well. Figure 2.7 also showed that as the apex gets flater the radius of curvature is increased in that particular section. Based on this data these problems seemed to be inter-related in that as the membrane forces are increased the deflections within the membrane are also increased[1]. As the forces increase, the apex deflections become larger effectively increasing the upper membrane tensions even further. The increased tension in the lower membrane must be supported by the air form fabric, which eventually will lead to membrane rupture, if not mitigated.

2.3.1 Membrane Theory

The radius of curvature is the limiting factor in the amount of pressure safely placed within the dome membrane. Equation 1 shows that as the radius of curvature increases, the membrane force "T" also proportionally increases.

$$T=\frac{PR}{2} \qquad \text{Equation 1}$$

T = force in the fabric, lb/ft
R = radius of curvature, ft
P = pressure inside membrane, psf

$$T_{\Theta}=\frac{PR}{2}(2-\frac{r_2}{r_1}) \qquad \text{Equation 2}$$

T_0 = stresses in horizontal plane of the membrane
r_2 = small radius, where the membrane goes from horizontal to vertical
r_1 = large radius, of the top flat region

[1]Appendix A, has all of the data collected showing that the deflections do get worse with increase in pressure

The variable "R" represents the distance from the centroid of the arc to the surface of the membrane (see figure 2.9). Irvine (3) says that as the top of the dome becomes flatter from deflections a larger radius of curvature is developed in the apex of the membrane. As r_2 goes to zero, the membrane tension doubles at the top in magnitude (equation 2).

This additional increase of localized tension (3) in the skin will theoretically redistribute the membrane forces proportional to the new deformed radius of curvature.

The allowable air-form force of 49 lb/in for a 34 oz/yd^2 is generally accepted by most membrane manufacturers. This corresponds to 9.1 psf (9) (see figure 2.8), or 1.75 inches of water pressure for a radius of curvature of 130 feet thus, limiting the allowable hemispherical air form diameter (9) to 260 feet, ($T_\theta = 9.1 * 130 / 2 = 49$ lb/in). The air form manufacturers[2] feel that a radius of curvature of 170 ft would be feasible, depending on the profile of the air form. The larger radius of curvatures could

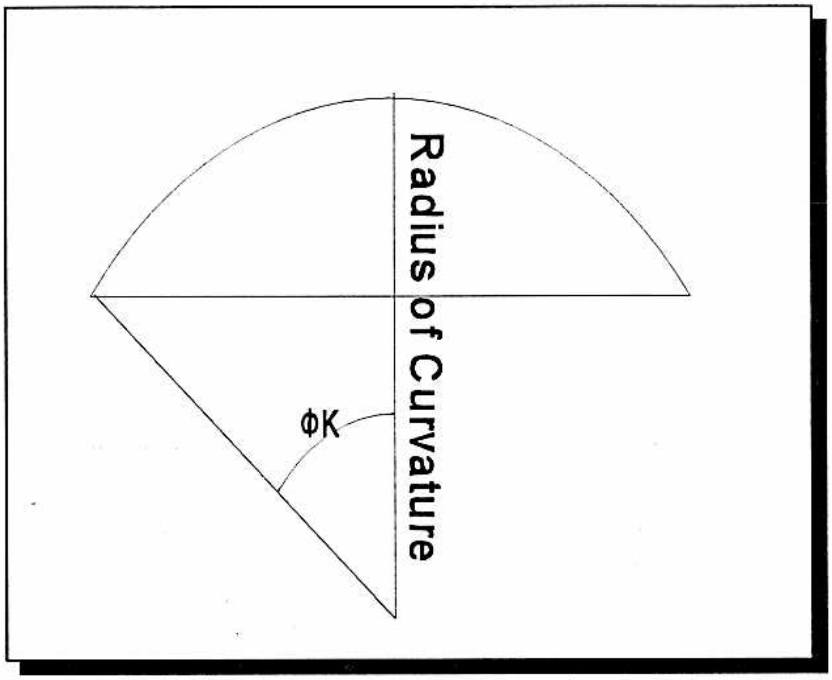

Figure 2.9 Radius of curvature

[2]David South Monolithic Constructors

only be used on hemispherical domes and not on the lower profile domes. This restricts the allowable radius of curvature for the lower profile partial hemispheres.

2.3.2 Membrane Deformations

Controlling the distortions in the membrane at critical points becomes closely related to the increased forces in the membrane. The flexibility of the membrane allows the membrane to easily conform to the shape of equilibrium, which is typically not the desired engineered shape for large-diameter low-profile air forms. A nonsupported membrane will have deflections at the apex which will cause the top radius of curvature to increase substantially (see figure 2.7), causing possible failure within the skin, as just discussed. Figure 2.8 show the forces applied to the membrane by the internal pressure, and as can be seen in the lower left hand corner each force has both a horizontal and vertical component. The lower the elevation of the apex the horizontal component increases in the lower half and the vertical component increases at the apex. This makes the forces from the "radial pressure" (see figure 2.8) build up in the apex region, causing possible tension failure in the membrane. It has been recommended that the top elevation of the finished structure be at ±3%[3] of the theoretical height (5). The amount of elevation loss at the apex of the air form directly affects the final shape of the concrete dome, effectively increasing the radius of curvature beyond the previously set bounds. The loss of elevation at the apex is critical due to the problems that it causes within the final concrete structure.

---

[3]The "finished structure" refers to the actual concrete structure.

In preparing to model an air form, the assumption that the deformation at the apex of the dome is directly related to the deformations at the 30° point simplifies some of the problem. This assumption means that if the bulge at the lower point on the dome is forced into place, then the deflection at the apex will be negligible. So if the deflection at the lower point can be controlled, the deflections at the apex of the dome will be correctable as well.

Over the last 20 years, hundreds of domes have been erected using the current[4] air form construction method. Overcoming the current size limits has been a difficult process; due to the large apex deflections in the low-profile 300+ ft dome spans. In the 1990 ACI publication, Dr. Arnold Wilson wrote that "as larger domes are planned, designed and constructed, care must be taken to understand the dome better to maintain a strong structure and safe working environment. The larger dome structures will take time to make them work, but by careful attention to details the larger domes will be feasible using air forms."

2.3.3 Membrane Solutions

The use of a cable net will ultimately be able to limit deflections sufficiently to support the membrane and maintain it at the designed profile. Geodesic cable-membrane systems have previously been used to redistribute membrane forces successfully(9).

---

[4]South Developed Method (Dome Technology)

2.3.3.1 Radial-Horizontal Cable Net

The study of using different cable nets to support large-diameter domes, is not a new area of research, but one in which there is much yet to be learned. Hatch (9) of Brigham Young University researched the idea of using a geodesic net (see figure 2.10) (9) and a net consisting of just lateral cables (see figure 10) to provide the membrane support from deflections. The lateral cable net had many problems and was rightfully deemed incompetent in Hatch's (9) analysis. The lateral net alone was considered as a weak alternative, to the geodesic cable net. However, in later considerations of the shape and form of the Pantheon (figure 2.1), the lateral cable system with added horizontal cables again became a viable alternative. The Pantheon domical roof was constructed of masonry, using a system of radial and horizontal cables spaced in equal leg dimensions horizontally and vertically. Following this pattern, the support cables on the membrane should be able to control the deflections and make the larger dome feasible, using the very uncomplicated lateral-horizontal cable net.

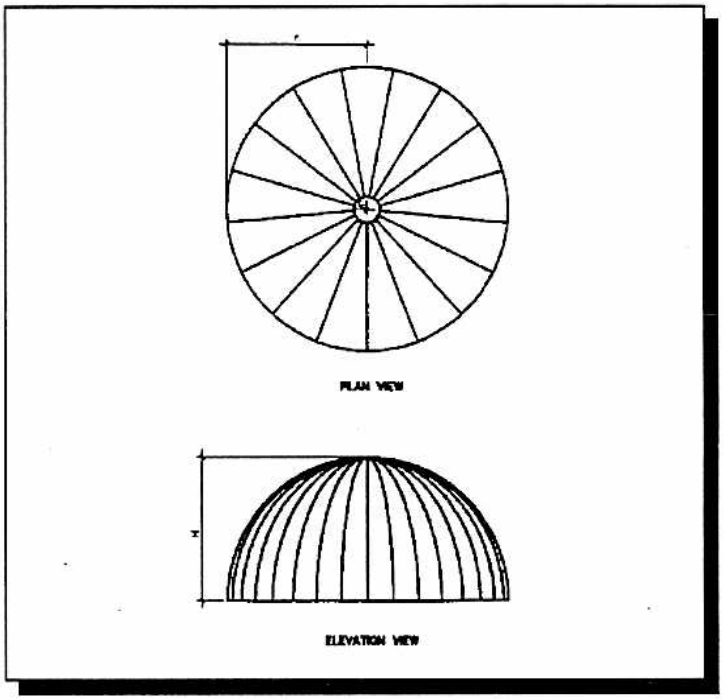

Figure 2.10 Hatch Radial cables

2.3.3.2 Geodesic Cable Net

Hatch's (9) research showed that the geodesic cable net (figure 1) is a very strong alternative. This cable system (9) "*can be projected from five platonic solids, whose vertices lie in a circumscribed sphere. These platonic solids include the tetrahedron, hexahedron (cube), octahedron, do-decahedron, and the icosahedron.*" Typically, the icosahedron is used for the main cables, and the area within is further broken down to full and partial pentagons. The pentagons or five-sided areas are favorable because they completely cover the dome in a series of larger to smaller sized pentagons. The pentagons effectively transfer the tensions within the membrane to the ring beam or foundation. The geodesic also provides a very pleasing architectural pattern in the actual concrete finished product.

The weakness of geodesic cable nets lies in the extreme complexity of the dimensions and assembly of the system. Another unknown in the use of geodesic cable nets is whether or not the nonhorizontal beam layout would cause an equilibrium problem during construction. Associated with the complexity of the cable-net pattern is that as the patterns progress up the side of the dome, the legs of the pentagon shapes differ in length. The overall complexity of the geodesic cable system adds up to a costly and time-consuming assembly operation.

2.3.3.3 Cable Membrane Interaction

The construction of a large-diameter dome with a membrane air-forming system, has been limited because of deformations at critical locations and high membrane stresses.

Using a cable net system the membrane forces are reduced as previously shown, by reducing the local radius of curvature. This is accomplished as the membrane "pillows" out between the cables. The forces in the membrane are then easily transfered to the cables, the foundation and into the ground. Thus this system alleviates the apex distortions with the cable support system by minimizing the actual forces into the membrane with the pillowing action between the cables. The cables will still be oriented in the big radius of curvature and will be required to completely carry the forces from the membrane, even though the membrane is still considered to carry a large portion of the forces. The smaller radius of curvature would effectively lower the local tensions within the membrane, allowing for the required pressures in the larger-diameter air form systems. The radial-horzontal cable net will be tested to verify, its ability to hold the membrane in the proper profile and effectively transfer the forces from the membrane to the foundation.

2.4 Summary

The limitations associated with the large-diameter dome with out cables, can be counteracted by use of a cable-net system. The model on which this research is based uses both cable net systems discussed (geodesic and radial-horizontal cable nets) earlier to alleviate the deformations and to localize the membrane tensions. Chapter 4 will further demonstrate exactly how feasible it is, using cable-net systems, to eliminate large-diameter air-form limitations.

Chapter 3
Model Procedures

A model was constructed in the Department of Civil Engineering structural lab, located in room 208 of the Clyde Building, to verify the validity of using a cable net system. Construction of the physical model will be discussed so that the reader will understand the data used for the results. The design considerations and assumptions will be throughly discussed, and the specific purpose of the tested physical model will be clarified.

3.1 Location of Model and Specific Responsibilities

An exact scaled-down model thirty-six feet in diameter by 8.64 feet high will be built in the Civil Engineering's Structural Lab at Brigham Young University. Dome Technology, and Monolithic Constructors will furnish the air form, and the cable restraint systems, including the 5x5x5/16 steel angle circular ring beam, the necessary anchors for the air form. Dome Technology will also furnish

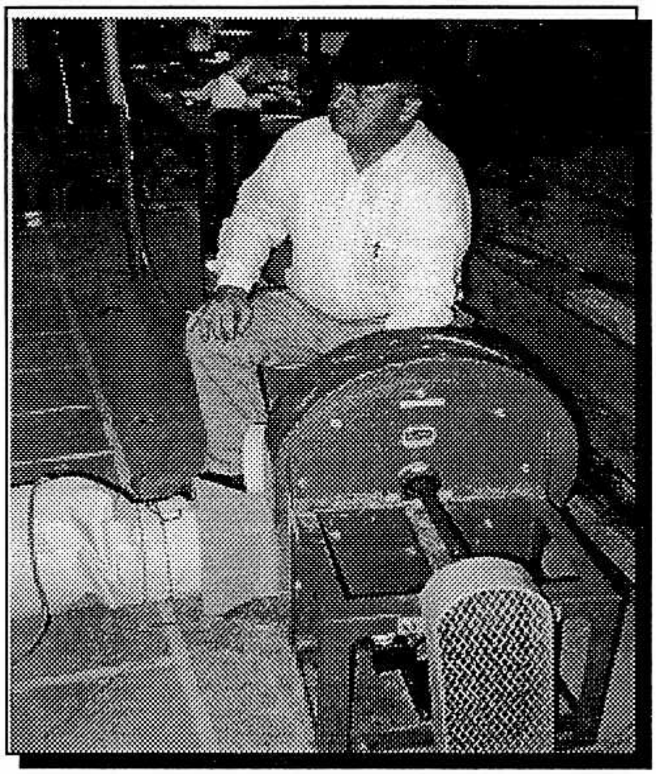

Figure 3.1 Inflation system, connected to dome opening

the air inflation system (figure 3.1) and the necessary labor to fabricate the completed thirty-six foot diameter model ready to be tested. The Brigham Young University Department of Civil Engineering will provide the structural "W" sections (figure 3.2) to fasten the ring beam to the structural floor. A graduate student will also be provided to assist in the construction of the dome, as well as perform the specified tests for the model. Dr. Arnold Wilson will oversee the entire project, providing assistance with the design and the interpretation of the data presented in the results section.

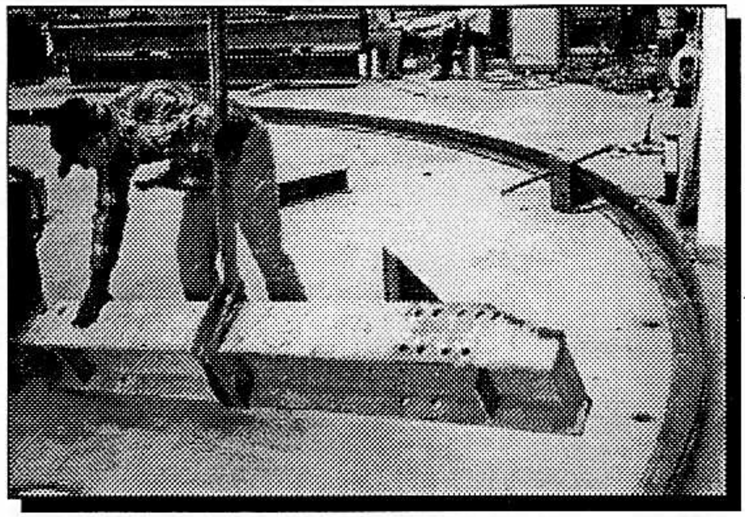

Figure 3.2 Ring beam and "W" Sections

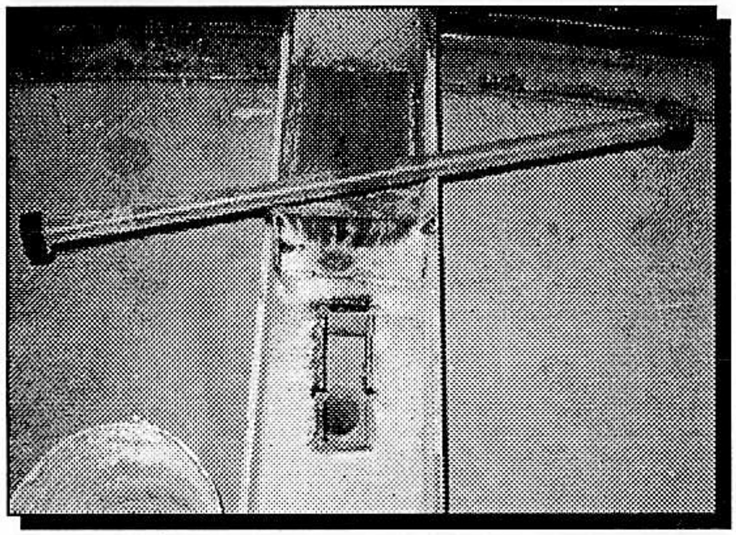

Figure 3.3 All thread and Nuts

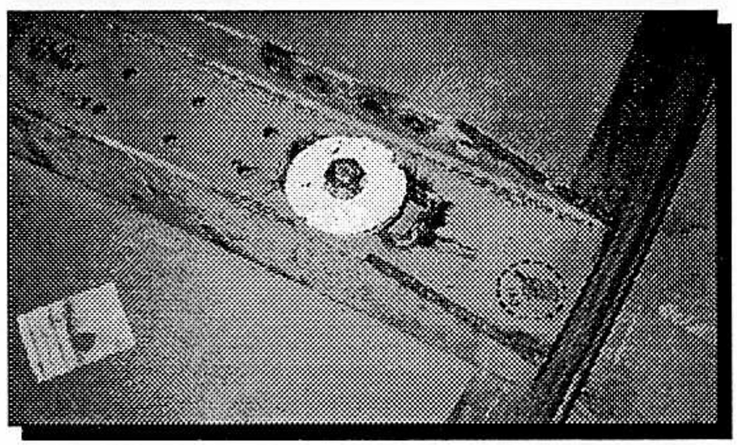

Figure 3.4 Bolted "W" Section and Wooden Washer

In the Brigham Young University Department of Civil

Engineering Structural Lab (hereafter referred to as the *structural lab*) a 26 inch structural floor was available specially designed with 2 1/2 inch holes located every three feet O.C., used to tie the ring beam to the floor. The dome outline was laid out on the floor, and the ring beam was set in place and welded together. Steel W10x's sections will be used to mount the ring beam to the floor, by bolting (figure 3.3) 2 inch diameter all threads through the holes and fastening them on both the top and bottom of the floor with

appropriate nuts and washers. The W10x sections provided will be placed at a maximum spacing of five feet on center, in order to carry the 73,000 lb expected uplift load into the structural floor. On the top side of the floor around the bolt and mounting hole, a

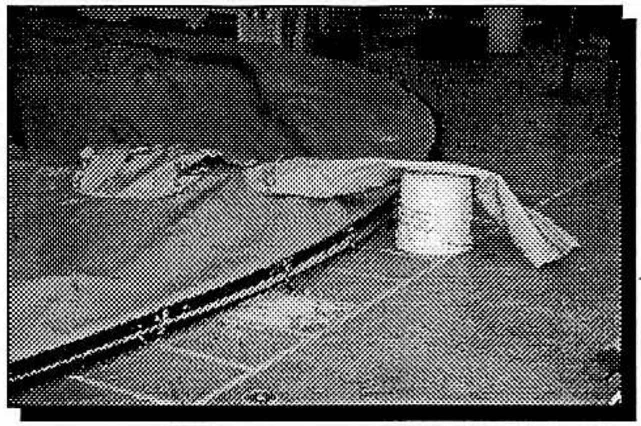

Figure 3.5 Inflation and Man Holes

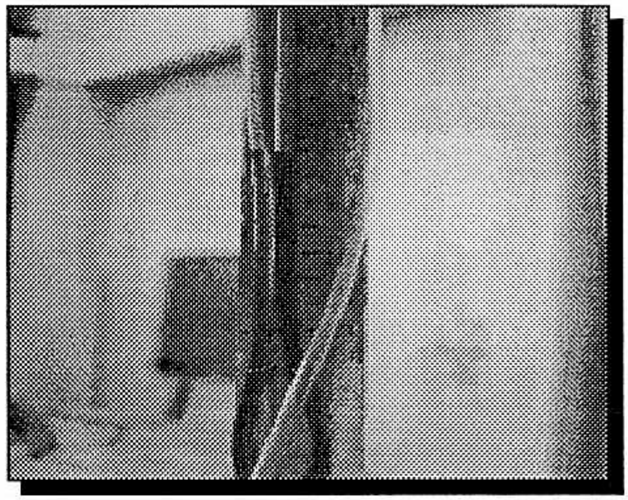

Figure 3.6 Water Pressure Gage

Figure 3.7 Radial-Horizontal Cable Net System

wooden washer will be used; (figure 3.4) urethane foam will be used to seal off the floor.

The skin will then be set in place with the manhole and air input hole (figure 3.5) to the west side of the ring beam. One of the small sleeves protruding from the side of the skin will be hooked up to an air fan (figure 3.1) for inflation of the air form. A water pressure gage (figure 3.6) will be placed in a 3/8 inch hole for measuring the fluid pressure on the membrane. The lateral-horizontal cable-net system (figure 3.7) will then be constructed and placed on the skin in order to run the specified measurements. Two foot long chains will be welded to the side of the ring beam for connection of the cables. Upon completion of the web-net tests, the geodesic cable net will also be constructed and placed on the skin for its specified measurements.

3.2 Preconstruction Assumptions

In order to actually construct the model, the physical dome properties discussed in this section were calculated, which will be verified with the results of chapter 4. Each component of the model was calculated and tested to verify adequacy of the design theory. Parts of the dome are understood only on the basis of mathematics and theory, so assumptions as to the validity of these particular characteristics were made and verified with the model results.

3.2.1 Membrane Considerations

An air form membrane is a very dynamic forming system that allows for construction of concrete-reinforced domes in a very short period of time. The desire to use an air forming system for larger diameter domes is not unfounded, because air forms have substantially reduced the time and forming costs in smaller diameter domes. The model will aid in more clearly understanding some of the dynamic characteristics of an air-forming system, especially the interaction between the cable and membrane.

In designing the model, the weight of the membrane was neglected, since the interior air pressure is so much larger than the actual membrane weight. The forces from the air pressure are assumed to go into the membrane, and then transferred through the cables into the ring beam. The air pressure also creates uplift on the membrane equal to the actual air pressure times the dome surface area footprint at the ring beam. The vertical uplift force for the model at the maximum of 13.87 inches (.5 psi) of water pressure covering a surface area of the dome footprint (1017 ft^{2}) is 73,400 lb. A component (figure 3.8) of the uplift force is taken by the vertical cables and the membrane, creating a state of equilibrium in that the uplift force must have an equal and opposite reaction force from the ring beam,

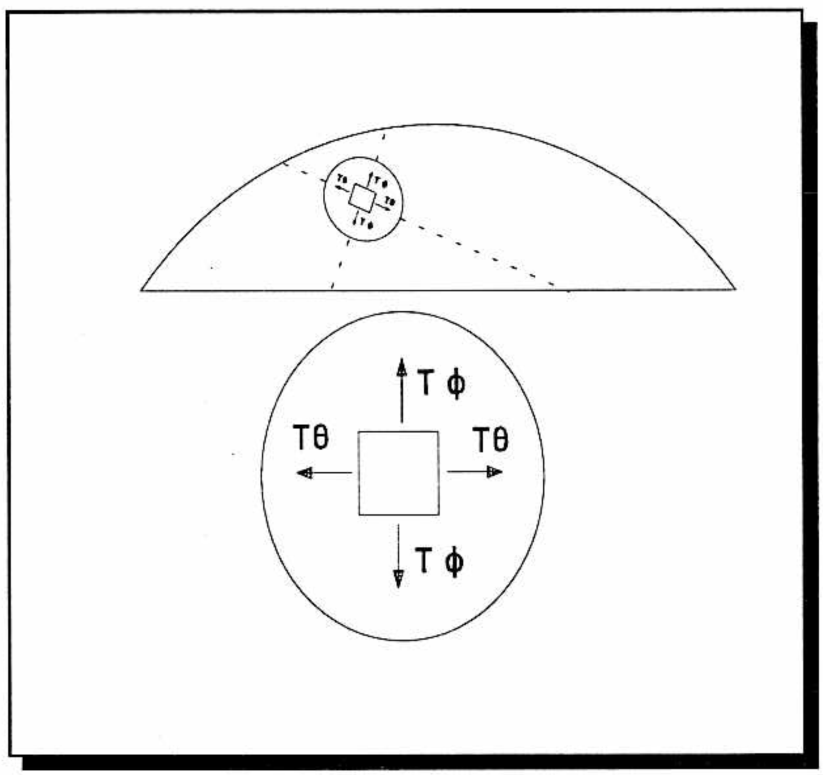

Figure 3.8 Membrane Force Components

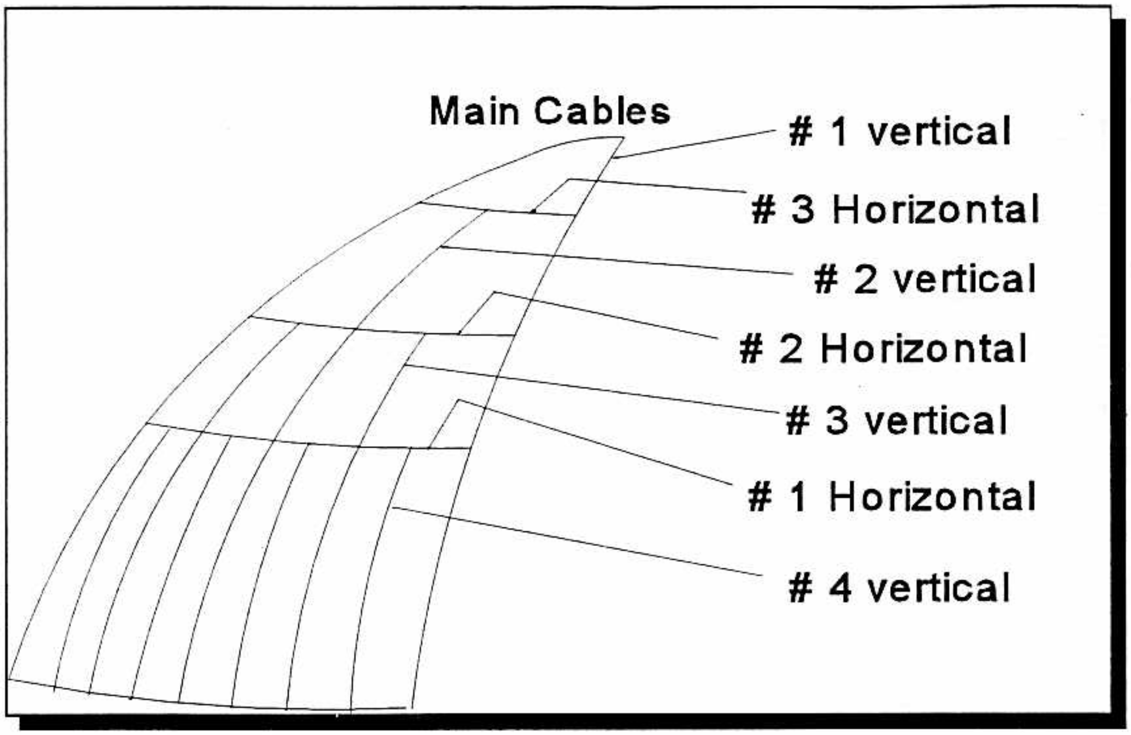

Figure 3.9 Radial-Horizontal Cable Numbers

cable net and membrane. The forces are broken up into 2 components within the plane of the membrane. The T_ϕ component is carried by the vertical cables and the T_θ component is carried by the horizontal cables. Each of these forces correspond to the lateral circumference of the spherical

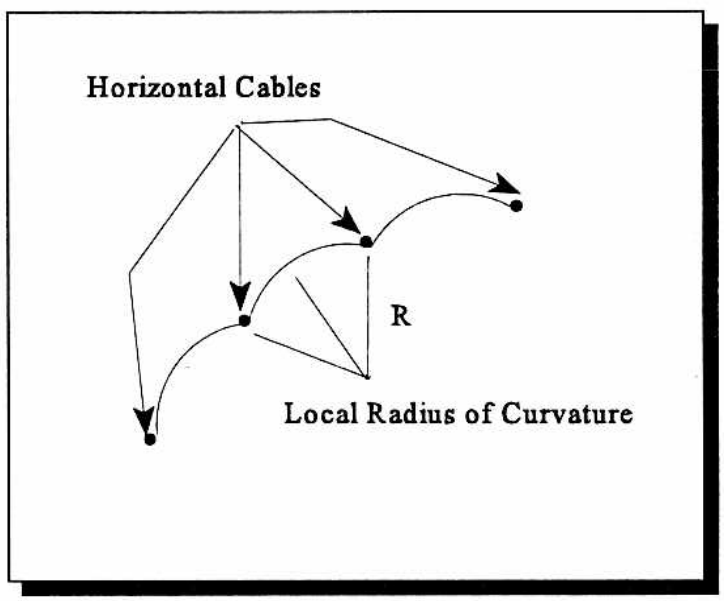

Figure 3.10 Membrane Pillowing Effect

shape (figure 3.8). Because the membrane is directly connected to the ring beam, it is reasonable to expect that some of the uplift force is actually carried to the ring beam directly in the membrane. As the horizontal circumference of the membrane gets smaller, the forces with in the membrane change proportionally with

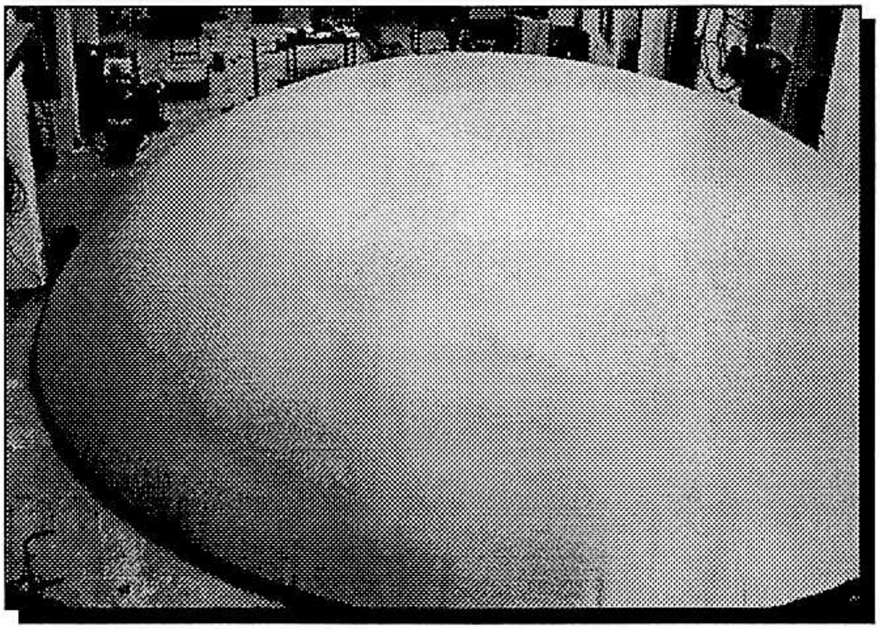
Figure 3.11 Membrane Model

the ratio of small circumference to the equator circumference[1]. Assuming that the forces within the membrane are totally transferred to the cables, the forces in the membrane will be directly proportional to the local radius of curvature. Adjustment factors have been used in the horizontal cables to correct the tension value, with a ratio of the actual horizontal circumferences to the circumference of the great circle. This is based on the theory that as the membrane pillows, and the radius of curvature decreases, the forces will also decrease. This means that the membrane will carry the local stresses to the cables, and the cables will carry the stresses to the ring beam. Based on this theory, the forces in the cables should be proportional to the tributary area on the surface of the membrane times a ratio of the horizontal cable circumference to that of the equator.

The prototype for the specified model was based on a dome 250 feet in diameter,

[1] The length of the great circle, or where the radius of curvature is equal to half of the diameter of the sphere.

$$P_{cr}=0.10E\frac{h^2}{R^2} \qquad \text{Equation 3}$$

and 60 feet in height from the apex (figure 3.12) of the dome to the finished floor. The D/H ratio equal to .24 represents a maximum low dome profile, which represents the 52° limit given by Billington (1). This ratio represents the minimum height for a specific diameter corresponding to a minimum ϕ_k. As the radius of curvature increases the concrete shell thickness must increase to handle the buckling problem. As the thickness of the concrete increases the shell dead load, eventually overcomes the potential of the shell to carry the critical buckling load within the thickness of the concrete dome. For this reason, beam-columns are used to reduce the dead load while effectively increasing the buckling capacity. As equation 3 shows, the allowable critical buckling substantially decreases proportionally to the inverse of the radius of curvature squared. The beam-columns in air form construction also are completely on the interior of the shell, allowing for a constant shell thickness over the top. The beam-columns are formed monolithically with the shell and eventually blend into the shell as it gets thicker near the structural supports at the bottom.

The air-form model diameter was constrained by the width of the structures lab to 36 feet in diameter. Based on the D/H ratio of .24, the height of the dome would be 8.64 feet, the feasible maximum diameter-to-height ratio limit as discussed previously for an air-forming system. The designed θ_k of 51.28° is again located just above the tension-compression (1) transition zone in a concrete dome. The radius of curvature (R), dome diameter (D), and the dome height (H) are all scaled according to the reduction factor as will be discussed latter. The air form is analyzed using a membrane analysis based on Billingtons method(1) (see appendix A), to find the specific forces in the membrane at loaded conditions. The membrane being flexible is not capable of carrying a moment. In appendix A Billington's (1) method of moment analysis is used to calculated the forces in the 36 ft diameter dome. This analysis shows that the moments in the base of the membrane are nonexistent, and that only a membrane analysis is necessary. A dimensional analysis will also be performed in order to accurately predict the vertical deflections in a prototype air form.

Based on these assumptions and analysis the physical model will be tested to verify the assumptions and mathematical analysis of the model air form. This information will be used to correct the assumptions and provide accurate information for a prototype air form or one of a much larger diameter.

3.2.2 Membrane Analysis

Billington's coverage of thin shell analysis is used to approximate the stresses in the membrane. The analysis in appendix A shows that only equations 4 and 5 need be

$$N'_{\varphi} = \frac{\pi a^2 p \sin^2\varphi}{2a\sin^2\varphi} = \frac{ap}{2} \qquad \text{Equation 4}$$

considered. The air forming system, is a flexible membrane and is analyzed following the

$$N'_{\theta}=a(p-\frac{ap}{2a})=\frac{ap}{2}$$ Equation 5

method that Flugge (see appendix A) developed and Billington uses as the primary solution of forces. Equation 4 and 5 are the forces T_{ϕ} and T_{θ} respectively, and are applied to the cables as previously explained. The membrane method of analysis takes into consideration the geometry of the membrane, and breaks down the forces being applied to a single finite stress block. The validity of the analysis will be verified in this model, with the measurement of forces in the cables.

3.2.3 Cable Design

The pressure loads applied to the dome membrane are calculated to find what cable sizes are needed based on the tension in the cables. Assuming that the cables are able to take all the forces in the membrane, the tension will be equal to the forces in the membrane. The membrane force being proportional to the tributary area of each specific cable, times the ratio $(C_{cable}/C_{equator})^2$ of the horizontal circumference to that of the equator. The assumption that the vertical cables will take the T_{ϕ} component and that the horizontal

---

[2] This is the correction ratio which includes the circumference of the cable divided by the equator

cables will take the T_θ component of membrane forces can be used to calculate the theoretical model cable tensions (figure 3.8). The theoretical tension[3] in the top horizontal cable (#3) (figure 3.9) is T_θ = 31.2 psf * 23.0 ft*(.25) / 2 = 89.7 lb/ft. The tension force is directed per foot around the radial direction of the membrane, thus as the horizontal tributary lengths get longer, a larger force relative to the equator is applied to the cable. A ratio of the actual diameter of the horizontal cable to the circumference of the great circle is used as an adjustment factor. The adjustment factor for each cable is included in table 1. The values for the calculated cable forces are included in table 1 for the model. The table is based on the model which consists of the following dimensions;

Diameter = 36 ft
Height = 8.64 ft
Radius of Curvature = 23.0

and assumes that all the forces in the membrane are transmitted to the ring-beam by the cable net. The actual pressure applied to the surface of the dome is taken as perpendicular

Calculated Tensions for 36 ft Model -Table 1							
Cables	Trib. Area	Adj. Factor	Tension in Cables (lb)				
pressure (psf)			10.4 psf	20.8 psf	31.2 psf	41.6 psf	52 psf
horiz 1	5.3 ft^2/ft	.62	395	791	1186	1581	1977
horiz 2	4.86 ft^2/ft	.42	246	493	739	985	1232
horiz 3	5.03 ft^2/ft	.25	149	299	448	597	746
vert 1	2.31 ft^2/ft	1.0	277	553	830	1106	1383

[3] The maximum membrane tension for this particular membrane should not go over the 49 lb/in as generally accepted by membrane manufacturers for the 34 oz fabric.

to the membrane (figure 2.8), and the pressure force can be broken down into a vertical and horizontal component, or into a hoop and radial force. For example, the force in a sample finite element block of the membrane (figure 3.8) shows tension in both directions. If considering a total sphere, N_θ and N_ϕ would have equal tension in both directions. For the low-profile domes, the radial cable tributary area is much smaller than (figure 3.9) horizontal cable #1.

Assuming that all the cables are the same size, the tributary areas should also be the same size. This allows for relative equal tension in each of the cables. The legs of the basic tributary areas should also be of equal length in the horizontal and vertical direction. The vertical and horizontal legs will be relatively equal from horizontal level to level.

The horizontal tributary areas are based on the tributary area of the membrane between horizontal cables on the dome. Each of the tributary areas should be equal; however, with just the three horizontal cables involved, they will have much larger tributary areas than the radial cables. The actual calculated tributary areas are located in appendix A. The tributary area for each cable was calculated by adding half the distance of the upper length and the lower length. For the vertical tributary area, the top and bottom cable widths of each section were averaged. The tributary area for each different vertical cable length was taken as the average of the areas through which the cable passed. This allowed the approximate cable tension calculation given in table 1.

The cables were designed so that the membrane at maximum pressure would pillow between the cables, effectively transferring the tension in the skin to the cables. As the skin pillows between the cables, the radius of curvature decreases so that based on equations 4 and 5, the tension in the skin will proportionally decrease as well. Based on the forces transferred to the cables, 1/4in diameter cables were chosen to reinforce the model. The membrane is designed to have approximately 2% stretch at full inflation so that the pillows will be able to form between the cables

Dome technology provided the manpower to assemble and place the two different cable nets. The radial-horizontal cable net shape was assembled in approximately 24 man hours, including cutting, marking, and actually clamping all of the cables together. The geodesic-net took approximately 32 hours to assemble, due to the complexity of the measuring and marking the cables. Although more cable is required for the lateral-horizontal cable net, it is a very simple pattern, and would strongly facilitate the application of a manufacturer-placed node point. During the manufacture of the membrane, connecting clamps to the membrane of cable node points would aid in the desired pillowing of the membrane.

3.3 Model Design

3.3.1 Ring beam Design

Due to the low profile of the dome, the ring beam at $\phi_k = 52°$ would have to be designed as a beam-column. The design by Dr. Arnold Wilson chose a L5x5x5/16 angle bent in about 16 ft sections to fit the circular circumference of the 36 ft diameter dome. The dome, analyzed at the maximum needed pressure of 13.87 inches of water pressure, yielded a ring beam compression value of 5.98 kips. The ring beam was designed as a beam-column, with an axial force of 5.98 kips, the maximum loading condition. The lateral bracing distance of 5, feet and r_y about the a-axis is .994 inches, then a kl/r of 60 gave an allowable axial stresses based on table C-36 (AISC-ASD) equal to $F_a = 17.43$ ksi. The actual axial stress $f_a = P/A = 5.98$ kips/3.03 inches^2 = 1.97 ksi, which is less than (<) 17.43 ksi, so the angle chosen will be more than suitable for the axial stresses. The bending moment about the x-axis is calculated as follows:

uplift force F = π 36ft^2/4 * .5 psi 144in^2/ft^2 = 73,287 lbs
uplift force/ft F = 73,287 lbs / 36 ft π = 648 lbs/ft
Moment on beam column ≈ wl^2/10 = 648lbs/ft (5ft)^2/10 = 1620 lb-ft

The compressive bending stress in the 5 ft beam-column section f_{bx} = 1620 lb/ft 12/2.04in^3 = 9.52 ksi is less than $F_{bx} \approx 18$ ksi, so the bending stresses are acceptable. The bending stresses in the y direction are due to the eccentricity of the arched beam-column. An eccentricity of 2.08 inches times the axial loading of 5.98 kips is 12.44 kip-in. Therefore the actual stresses in the y direction are f_{by}= 12.44 kip-in/2.04 in = 6.1 ksi which is also

$$\frac{f_a}{F_a} + \frac{C_m f_{bx}}{(1 - \frac{f_a}{F'_{by}})F_{bx}} + \frac{C_m f_{by}}{(1 - \frac{f_a}{F'_{ey}})F_{by}} \leq 1.0 \qquad \text{Equation 6}$$

less than $F_{by} \approx 18$ ksi and the angle is adequate in the y direction. Placing all of these values in the unity equation (Equation. 6) H1-1 & H1-2 (AISC-ASD) gives a value of 1.08, showing that the L5x5x5/16 is adequate.

3.3.2 Anchorage Design

The ring beam was anchored to the structural floor with two-inch diameter "all thread" (figure 3.3) and secured by bolts and washers both on the top and bottom of the floor. The tie-down holes in the structural floor are located 3 ft on center in both directions, limiting the maximum cantilever to 3 ft. The uplift force on the ring beam of 648 lbs/ft times the 5 ft brace spacing, times a 3 ft cantilever gives a maximum moment of 9720 lb-ft which the "W" section must adequately carry. Calculating the section modulus requirement using this moment and an allowable stress of 22 ksi will verify if the W10x30 steel beams will be sufficient. The required section modulus is equal to $S_x = M/F_b = 5.3$

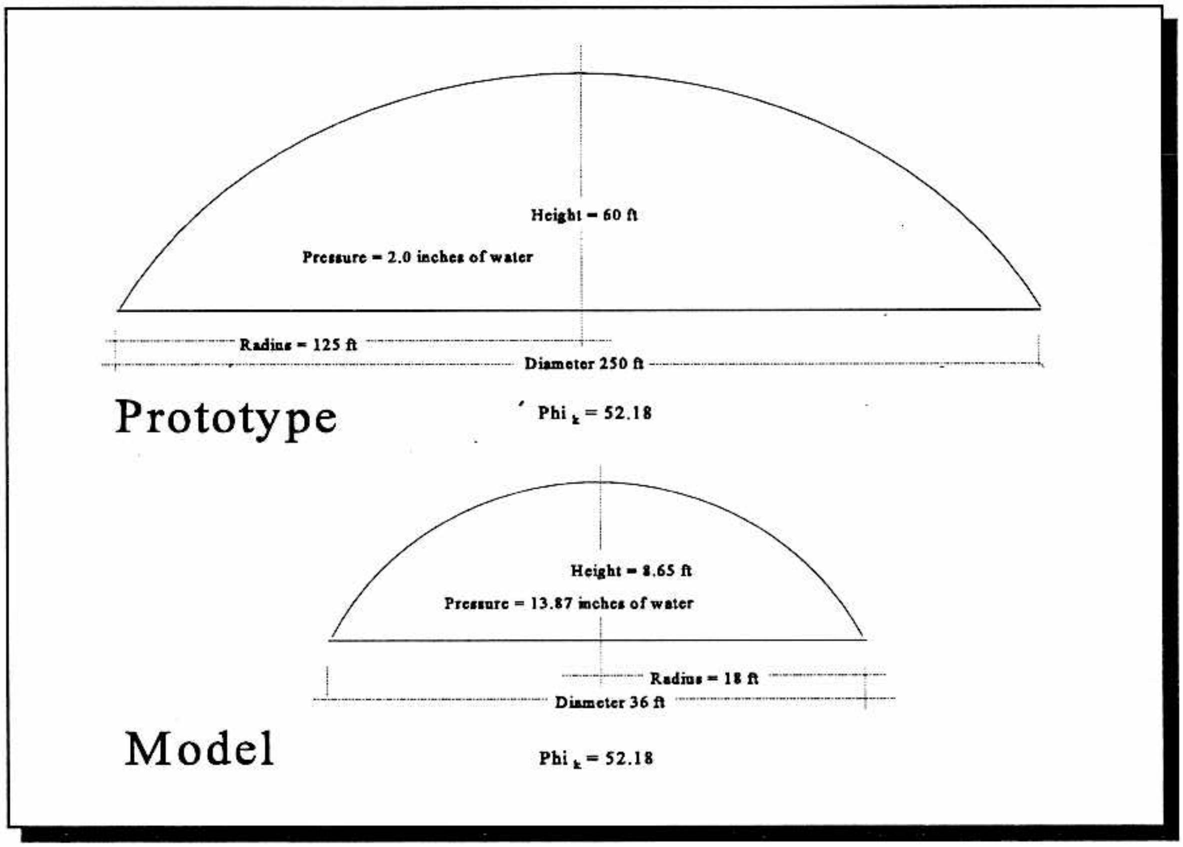

Figure 3.12 dimensions of prototype and model

in^3. The section modulus of the W10x30 is 5.75 in^3, when bending about the weak axis, therefore adequate to carry the vertical uplift force of 648 lb/ft.

3.3.3 Scaling factor

The model was based on a dome prototype membrane 250 ft in diameter with a 160 ft radius of curvature, and 60 feet high. The limited space in the structures lab allowed for a maximum diameter of 36 feet in diameter, and thus a minimum height of 36 ft times .24 equals 8.64 ft. The reduction factor was equal to the diameter of the prototype divided by the diameter of the model, or 6.944. All the prototype dimensions were divided by the reduction factor, and can be found in figure 3.12. The air pressure needed to model the prototype accurately will be the 2 inches times 6.944 = 13.87 inches of water pressure or .5 psi.

3.4 Model Tests

The main purpose of this research was to determine the feasibility of using a radial-horizontal cable net to support a low-profile dome, air-forming system. The cables will theoretically reduce or eliminate the top and side deflections in the larger diameter membranes. Maintaining the proposed radius of curvature minimizes the concrete distortion problems. The cables control the local radius of curvature by directing the forces of the big radius to the ring beam and into the foundation. The membrane will take the force applied correlating to the reduced radius of curvature and transfer it to the cable net. The tension and radius of curvature, being locally smaller, allow larger pressures to be used, making larger-diameter domes feasible with an air forming system.

The first cable net structure tested will be the radial-horizontal cable net system. The cables will be tested with two setups, with profiles (figure 3.13) taken at four, eight and ten inches of water pressure. The two membrane setups will consist of all the horizontal and vertical cables; the second will be with just the vertical (figure 3.15) cables. A tensiometer will be placed in each of the horizontal and two major vertical cables in order to find the forces which the cables are required to carry. The second cable geometry tested will be a geodesic cable net system. This system will be set up and tested by putting the tensiometer in several of the different cables, as well as measuring the profiles at four, eight and ten inches of water pressure. The pressure will be measured by placing a "U" tube filled with a water into a slot in the dome membrane. The pressure will be measured by the differential level of water in the tube, as shown in figure 3.6. The specified data will be compiled, analyzed and presented in an appropriate manner.

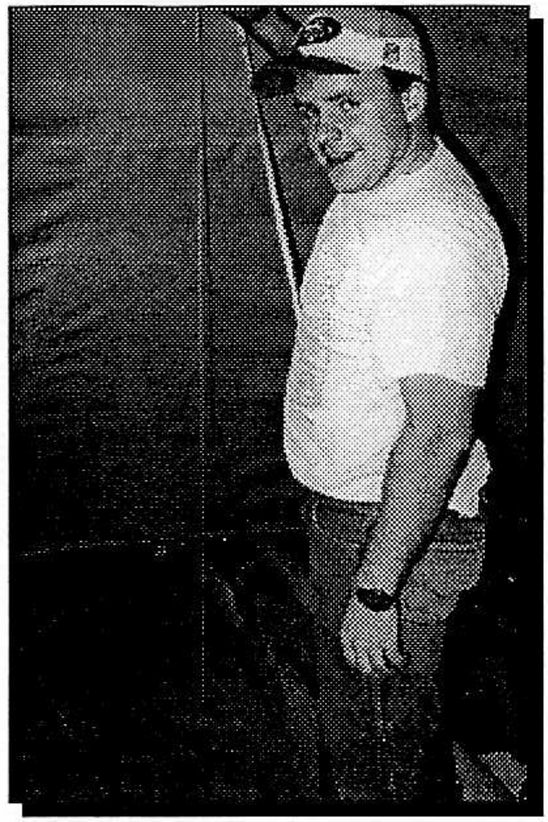

Figure 3.13 Taking Deformation measurements

3.5 Radial-horizontal cable net design program

To design an effective radial-horizontal cable net, the cables must be evenly distributed over the surface area of the dome, based on tributary area. The horizontal cables especially in the lower regions of the membrane, must restrict the deflections, thus forcing the membrane to equilibrium at the designed profile. The design spreadsheet took the entire surface area of the dome and divided it by eight main sections (figure 3.15). The eight equal area sections were again divided into subsections. Each of these subsections was of equal area, so as to maintain a constant force in each of the cables. The radial lengths of each cable and the angle α from apex to the horizontal cable were calculated. The vertical cable lengths, and number required for the entire net system were also calculated. Between the main horizontal cables, secondary cables are placed, each with equal tributary areas. The tributary leg

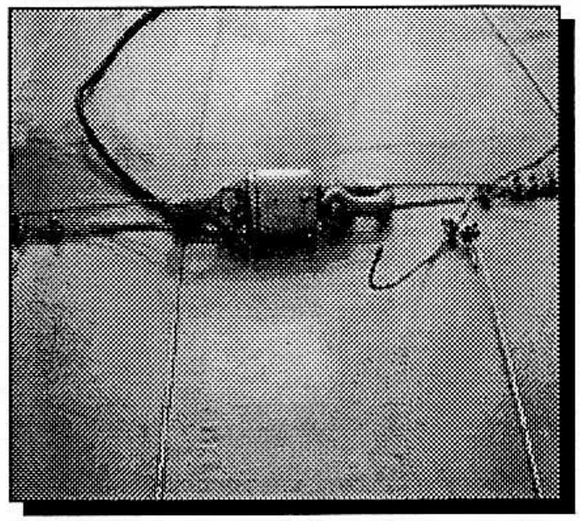

Figure 3.14 Tensiometer tests

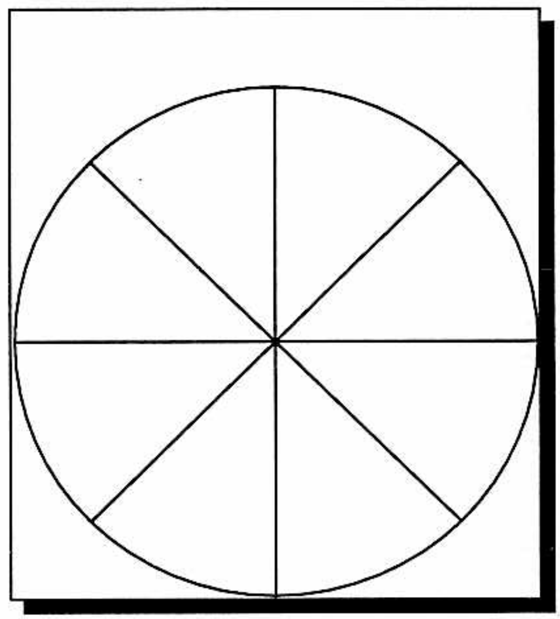

Figure 3.15 Main lateral cables

$$\varphi_n = 2[\sin^{-1}(\frac{A_n 2^n}{\pi R^2} + \sin^2\frac{\varphi_{n-1}}{2})^{1/2}] \qquad \text{Equation 7}$$

lengths, both horizontal and vertical, must be relatively equal, to assure equal forces in each cable. The program requires that the diameter, dome height and approximate vertical spacing at the ring beam be input. The number of horizontal cables can be adjusted to make the ratio of horizontal to vertical leg lengths closer to 1 in each main section. To create the program, an equation for ϕ_n was derived in terms of equal tributary areas. Equation (7) was then used to calculate the angle ϕ_n for each horizontal cable. The angles for the main horizontal model cables were $\phi_1 = 14.33°$, $\phi_2 = 25°$, $\phi_3 = 38.5°$, $\phi_k = 51.28°$ (figure 3.16). The value of A_n was found by dividing the area of the 1/8 section by the total number of areas in that section. The angles to each cable can then be used to calculate the vertical distances from the center of the dome to the horizontal cable. The distances are as follows for the model: $h_1 = 5.7$ ft, $h_2 = 9.75$ ft, $h_3 = 14.4$ ft and $h_4 = 18$ ft (figure 3.16).

Then h_x can be used to solve for the circumference of each main horizontal cable, which is the actual cable length needed. The lengths used for the model are as

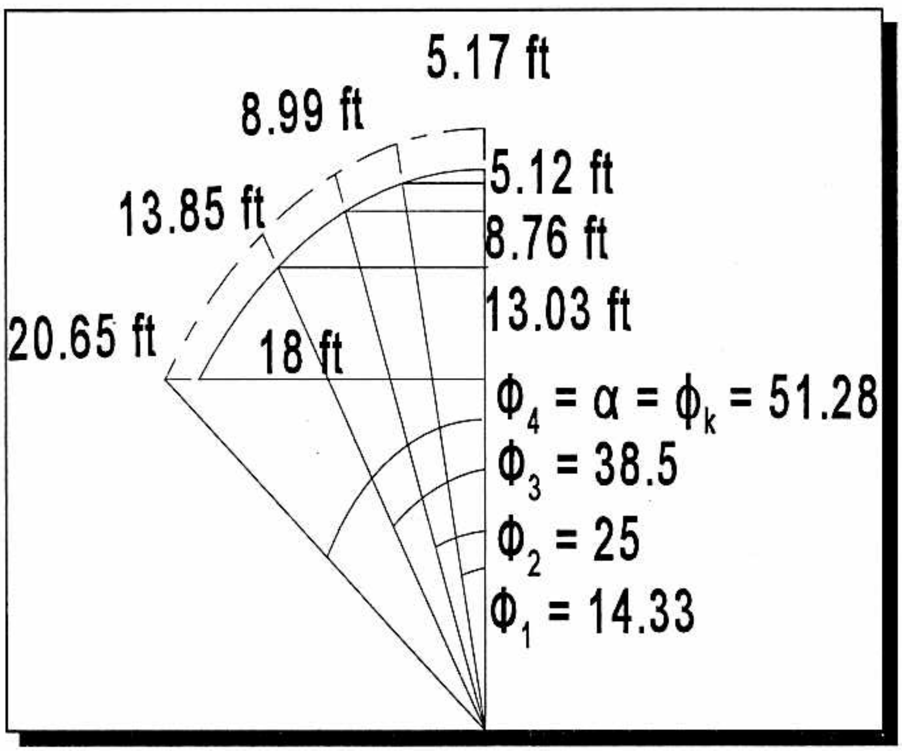

Figure 3.16 Program dimensions of main horizontal cables

follows: c_1 = 35.8 ft, c_2 = 61.3 ft, c_3 = 90.5 ft, (ring beam)c_4 = 113.1 ft (figure 3.16). The model has 3 horizontal main cables with no secondary cables. The vertical cables are calculated to show both a length and number of cables for each section of the radial-horizontal cable net system.

Upon completion of the project it was recognized that the distance between the horizontal and vertical cables, each respectively had to have equal spacing. The program was rewritten to include a manual adjustment of the horizontal and vertical spacing between the horizontal and vertical cables. The ability to add a tension ring at the apex of the dome was also included, so an odd number of main vertical cables could be designed for the dome. The cables were designed to have the main vertical cable # 1 (see figure 3.9) go completely over the apex to the other side of the ring beam or attach to the tension ring at the apex. Vertical cables two, three and four start on the respective main horizontal cable and run to the ring beam or foundation. The output of the spreadsheet includes the dimensions and locations of each cable.

The approximate horizontal deflection at the apex, with and without the cables attached to the membrane are also included, and are based on the dimensional analysis equations derived from this project. The stretch of the membrane may change the size of the air form, however in this case it is considered negligible. The spread sheet is meant to aid in the design of the cable dimensions and location of the cables on the air form.

Chapter 4
Results

The model has proven that the horizontal and vertical cable pattern found in the Pantheon, will mitigate the membrane deformations sufficiently to use the air form cable system in large diameter, low-profile domes. The model as a whole seemed to answer many questions, and in the process many new questions were raised that need to be addressed in further research. The problem is no longer whether the cables can restrain the air form sufficiently; it involves working out the connection problems and designing the correct cables to work for a particular project. As will be shown throughout this section, the cable nets did work, but the process of perfecting the cable-membrane interaction will be an ongoing process.

The data retrieved from this experiment showed that the relative deflections at the apex and at lower points was successfully mitigated, using a cable net system. The interaction taking place between the cables and the membrane in transferring the membrane tensions to the cables was highly dependent on the placement of the cables. The first time the net was placed on the membrane and inflated, the pillows were uneven everywhere, causing wrinkles in some spots and nothing in other locations. The adjustments in the cables made it possible to eliminate the wrinkles but added a degree of error into the cable tensions measured with the tensiometer. This problem encountered on the small air forms will be multiplied many times with the larger diameter air forms and cables, but can be easily taken care of by fixing each cable node point to the membrane. The fixed cable node point will clamp the cable to an exact location on the membrane, allowing for a precise pre-designed pillow between each node point. The clamp at each node will also assure that each tributary area takes an equal share of the load, and will also provide a better transfer point of the membrane forces to the cables.

The membrane deformations were measured at 2, 4, 6, 8, 10 inches of water pressure, from the inside of the membrane (figure 3.13). The data from the deflections are tabled in appendix A, with the corresponding profile measurement superimposed on the designed profile. The worst-case apex deflections were taken from the measurements of the net with only the four main lateral cables attached to the air form, and the full cable radial-horizontal cable net at 10 inches of water pressure. These values were used to solve the dimensional analysis equations for comparisons in future large-diameter low-profile air forms. The tension in each horizontal and vertical cables was also taken at different water pressure levels of inflation. The tension in the cables was directly related to the placement of the cables. Tensiometer readings were taken at the correct length, as well as at other adjusted cable positions. The overall purpose was to make a comparison of shape changes between the cables and the membrane, and to predict accurately what will happen in larger-diameter domes. A set of dimensional analysis equations were derived and solved using the model deformations. These equations are included in a spread-sheet program, used to design the cable diameters, lengths and positions, correlating with the membrane.

4.1 Dimensional Analysis

Dimensional analysis itself is a method of using the dimensions (7) of a model system, and formatting the variables in such a way that a reasonable prediction can be made in terms of a prototype system. The analysis is based on two axioms (7):

> *1. Absolute numerical equality of quantities may exist only when the quantities are similar qualitatively.*
>
> *2. The ratio of the magnitudes of two like quantities is independent of the units used in their measurement, provided that the same units are used for evaluating each .*

Axiom 1 states that only compatible units can be compared, such as in the case that the dome ϕ_k can not be compared to the radius of curvature. The equations are not based on laws of nature, but on the interrelationships between the principal variables. Axiom 2 says that the units must be compatible and make it necessary to keep data retrieved in consistent units. The dimensional analysis equations were developed to be used in the future to predict deflections based on the data collected during the testing of this model. The equations themselves are of no value without combining them with the results of a physical model. The information is included in appendix A for future reference. There are two sets of data, one in which the deflections with no cables can be predicted and one in which the deflections with a full set of cables can be predicted.

Eliminating apex deflections was the major purpose of this study, and that was demonstrated using the air form model. The deflections at the apex of a dome are assumed to be connected to the deflections at the lower portions of the dome. This is believed to be true because if the side deflections are controlled, the top section will also conform to the design profile. With these assumptions in mind, the variables involved with the membrane and cables were compiled and considered for use in creating the dimensional analysis equations.

4.1.1 Variables

The variables first considered were as follows: T-tension in the cables, F_t -stress in the cables, A_{cables}-area of each cable, H-height of the dome at midpoint, D-diameter of the dome, R-radius of curvature, u-deflection at the apex of the dome from designed profile to actual membrane profile, P-pressure applied to interior of the membrane, C_a - tributary area of the cable sections. These variables represent many of the possible dimensions in dealing with the dome; however, many of these variables are functions of the other variables. The variables involved were simplified to root variables. The final list of variables included the tributary area of each section of the cable net, height of the dome, diameter of the dome, tension in the number-one horizontal cable, and the internal pressure on the membrane. The process of deriving the dimensional analysis equations follows a simple pattern, which is easier to perform with fewer variables.

4.1.2 Equations

The first step is show the deflections as a function of the variables, as previously defined (equation 8). A constant "C" is multiplied into the equation, and an exponent is

$$u=f(T,C_a,H,D,P) \qquad \text{Equation 8}$$

$$u=CC_a^{c1}H^{c2}D^{c3}T^{c4}P^{c4} \qquad \text{Equation 9}$$

added to each of the dome variables, c_1, c_2, etc....(equation 9). From table 2, dimensional

$$L \propto \left(\frac{ML}{T^2}\right)^{c_1} (L^2)^{c_2} (L)^{c_3} (L)^{c_4} \left(\frac{M}{LT^2}\right)^{c_5} \qquad \text{Equation 10}$$

equivalents the dome variables (equation 10). Equation 10 is then resolved into component equations, and since almost all the variables are "L" or length units, the equation becomes very simple: L: ($1 = c_1 + 2c_2 + c_3 + c_4 - c_5$). For the "M" mass variable the component equation is M: ($0 = c_1 + c_5$); the component equation for "T" T: ($0 = -2c_1 - 2c_5$). These equations then can be further simplified, making the equations useable with the desired effect. The final equations (Equation 11) are taken by combining the like variables and setting each set equal to the displacement (u).

$$\frac{u}{D} = C\left(\frac{C_a}{D^2}\right)^{c_2} = C\left(\frac{H}{D}\right)^{c_3} = C\left(\frac{PD^2}{T}\right)^{c_5} \qquad \text{Equation 11}$$

Dimensional Analysis Parameters - Table 2	
Characteristic	Dimension
Length	L
Area	L^2
Volume	L^3
Mass	M
Force	ML/T^2
Pressure	M/LT^2

The results of the dimensional analysis equations are based on the model and a specified prototype; table 3-a,b shows data comparisons between the model and prototype air forms. The model dome is based on the following dimensions:

$D = 36$ ft
$H = 8.64$ ft
$P = 72\ lb/ft^2$
$C_a = 13\ ft^2$
$u = 7.3$ in

The prototype dome is based on the following:

$D = 250$ ft
$H = 60$ ft
$P = 10.4\ lb/ft^2$
$C_A = 503\ ft^2$

Dimensional Analysis Exponents Table 3-a			
u (def.)	Eq. 1 (exp)	Eq. 2 (exp.)	Eq. 3 (exp.)
7.3	.846	2.862	-1.160
.8	1.305	4.412	-1.789

The dimensional analysis equations are derived and solved using the deformation values from the model to solve for the exponents (Table 3-a).

Prototype deflection values Table 3 - b		
	W/out cables	W/cables
Eq 1	50.65 in	5.55 in
Eq 2	50.53 in	5.53 in
Eq 3	47.70 in	5.06 in

This example will use the first equation of $u = D * (C_a/D^2)^{C_2}$ to demonstrate solving for the exponent and using the information on a larger dome membrane. First, all the known values are inserted into the first dimensional analysis equation, making C_2 the only unknown. The constant exponent is easily solved for $C_2 = \log(u) / \log(D * C_a/D^2) = 2.862$. The deformation can then be solved using the same equation, but this time everything is known except u. Setting $u = D * (C_A/D^2)^{C_2}$ ($C_2 = 2.862$) equals 50.53 inches, compared to 50.69 inches (7.3 inches * 6.944 = 50.69 inches)[1] for the deformation in the 250 ft diameter dome. Each equation is covered in depth in appendix A. The exponents due to deformations with cables is 0.8 (see table 3-a) inches, and the deformations with only the vertical cables is 7.8 inches.

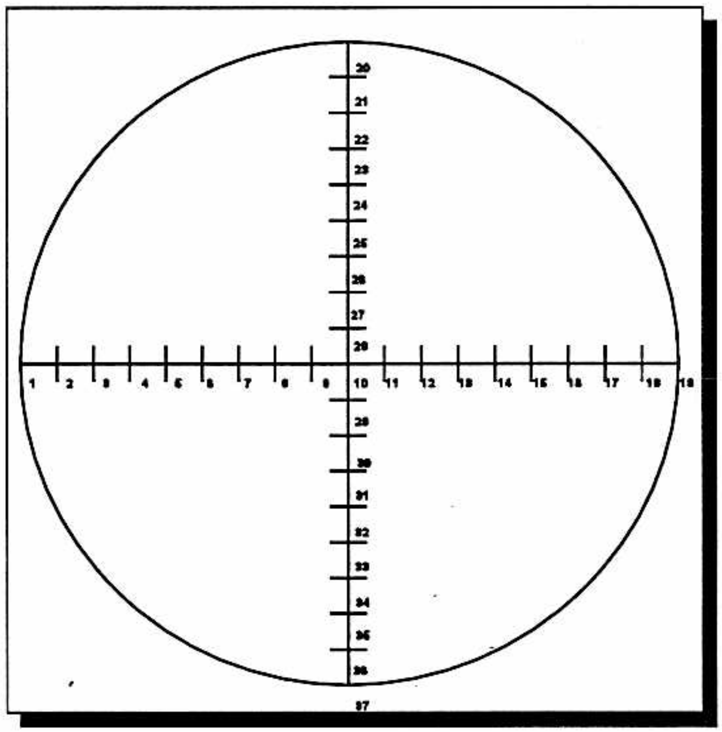

Figure 4.1 Membrane layout for measurement

4.2 profile measurements

The measurement system changed and improved during the testing process. The

---

[1]This is the model deformations times the reduction factor as a comparison of deformations in the membrane.

optimum system was found to be a surveying story pole with a 25 ft tape measure connected at the top and a 3 ft level to plumb the story pole. Two people were required to conduct a profile reading. The first person would place the story pole on the pre laid mark, then person 2 would plumb the story pole and take a measurement with the tape measure. This process was the same for every profile measurement taken. Figure 4.1 shows the permanent layout for measuring the membrane profiles.

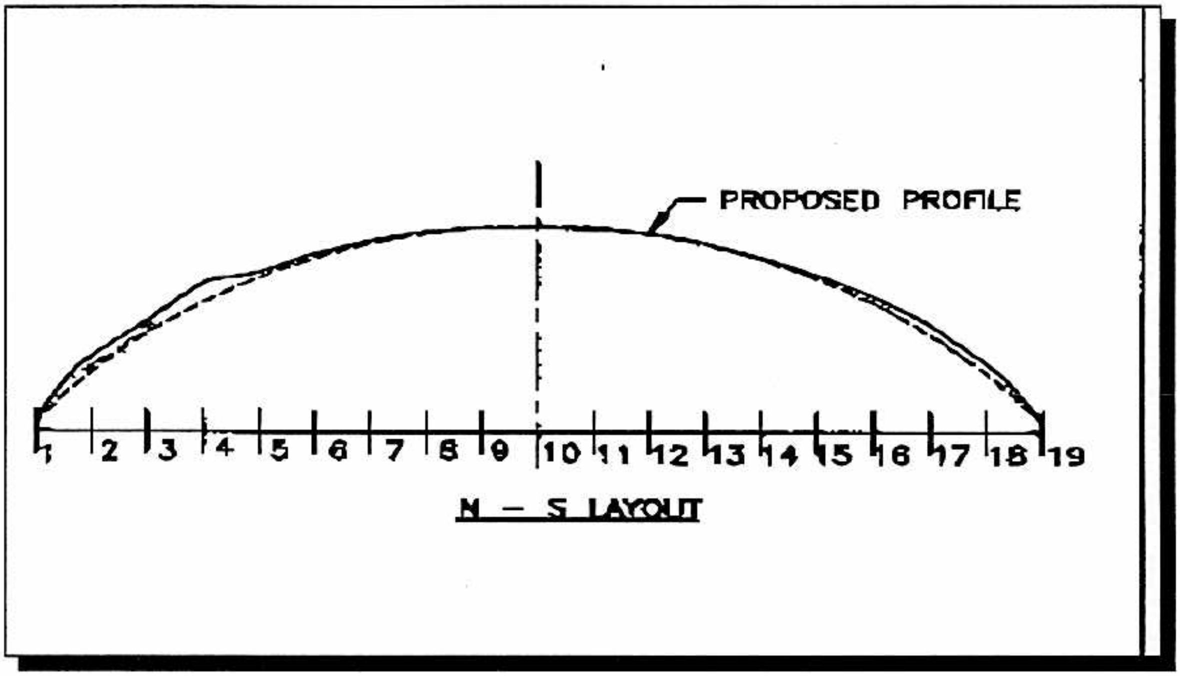

Figure 4.2 Membrane profile with full radial-horizontal cable system

4.2.1 measurement layout

A grid (figure 4.1) was set up on the concrete floor, directly correlated to the placement of the main vertical cables in the radial-horizontal cable net. This was done so that the deflections would be considered as consistent as possible, lying directly along the path of the main vertical cables. The points were marked (figure 4.1) and numbered with

1 - 19 running east and west, and 20 - 37 running north and south. The two grids were also set up perpendicular to each other, to verify in two directions the deformations of the membrane. The two grids were laid out two feet on center, to give enough points for an accurate profile. The profile measurements generally were very successful in verifying what the membrane was doing during inflation. As the air pressure increased without cables the apex elevation dropped, but with the cables, securely attached, the apex elevation rose slightly. Allowing for the errors made during adjustments of the cables, the profile in figure 2.7 shows what happened to the membrane with only the radial cables; and figure 4.2[2] is the profile with all of the main horizontal cables. In each of the profiles taken, the membrane below the first horizontal cable still had quite large deflections due to the large radial span between cables. Toward the top, the vertical deflection came within three quarters of an inch, which translates to 5.5 inches on the large diameter dome with dimensional analysis. Using a very limited horizontal cable network, the results were within allowable deflections.

4.3 tensiometer tests

A tensiometer (acquired from the department of Civil & Environmental Engineering at Brigham Young University) was placed at various times in each of the horizontal cables, as well as in several of the vertical cables. The tension readings were taken correlating to the internal pressure of the dome which varied from 0 to 10 inches of water pressure. To get a more accurate picture of what tensions the cables were required

---

[2] This is the profile with 10 inches of water pressure

to carry, the readings were taken at the correct cable length; then the cable was shortened so that the maximum pillow between cables was created. This allowed an accurate measurement of the forces in the membrane being transferred to the cables.

Readings were taken in all three main horizontal cables as well as in two vertical cables, at every inch of water pressure. The vertical cable data (figure 4.3) looked very

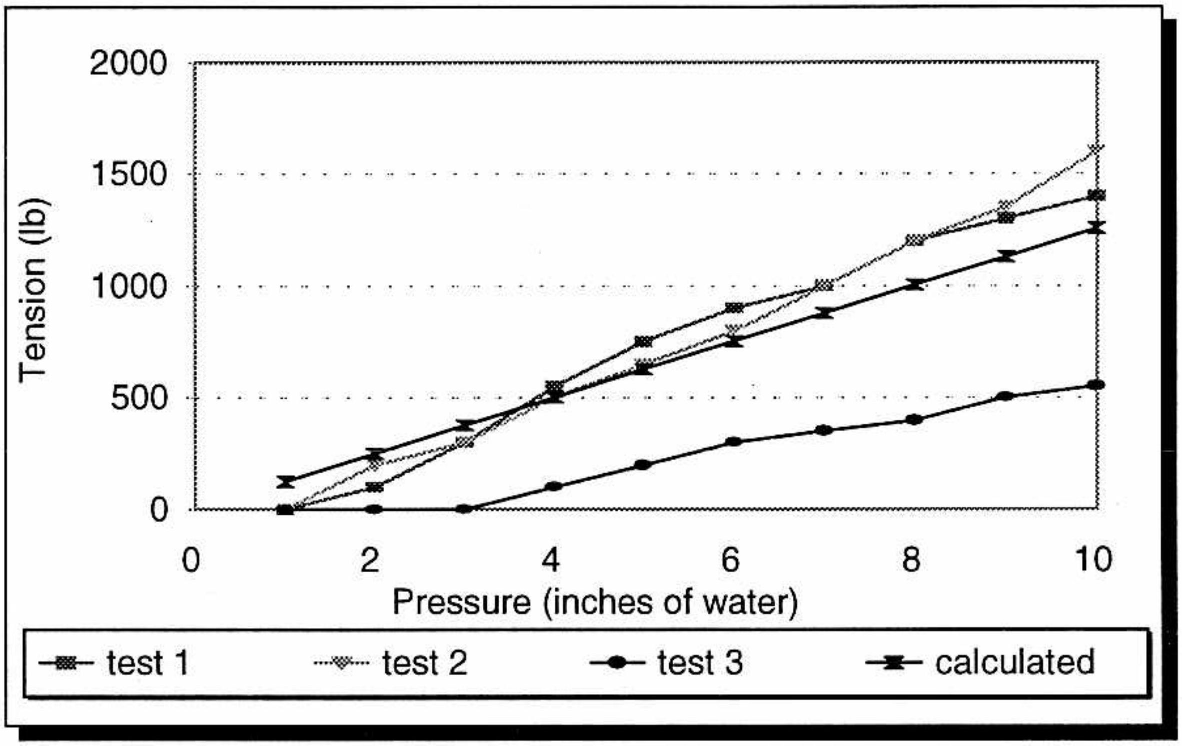

Figure 4.3 Vertical Cable forces to inches of water

close to the theoretical values. However, test values for vertical cable # 2 (figure 3.9) did not pick up any of the tension until 3 inches of water pressure. Due to the flexibility of the horizontal cables the vertical cables directly attached did not pick up the tributary forces until the horizontal cables became taught. The horizontal cable # 1 results marked very close to theoretical values, no matter how the cable was adjusted. Cable # 1 is the closest

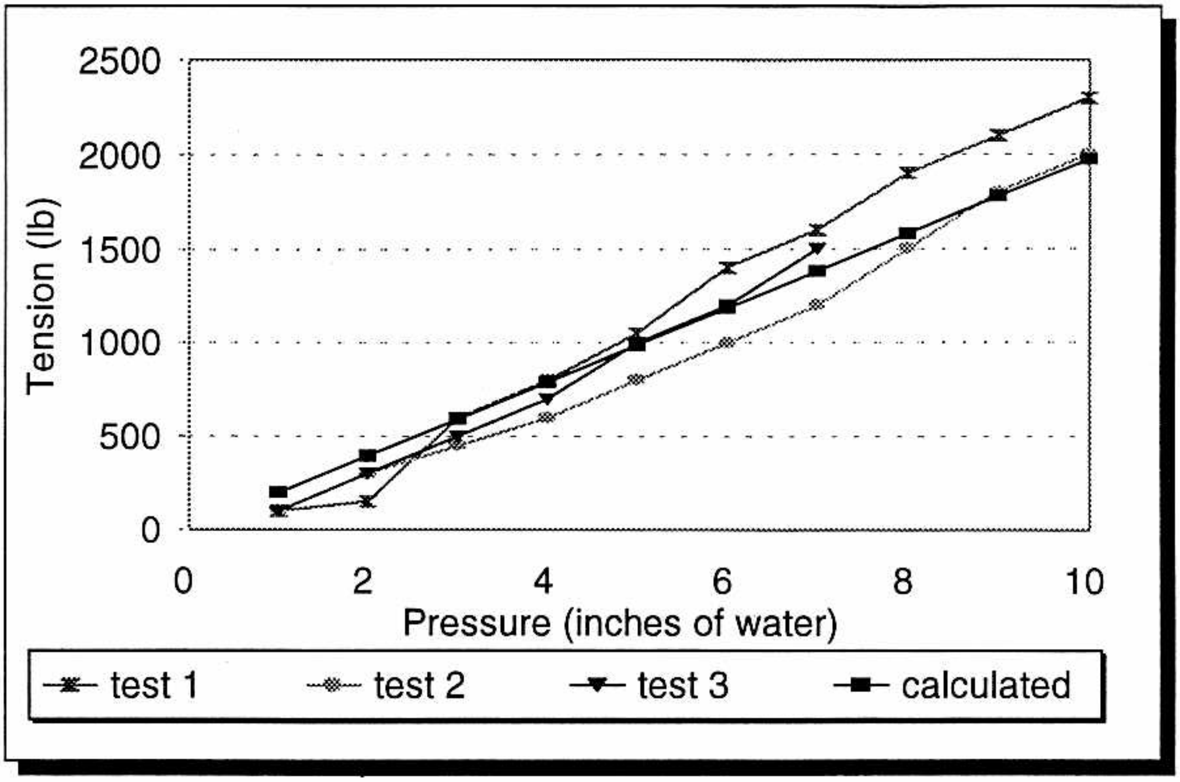

Figure 4.4 Horizontal Cable # 1 Force to inches of water

in circumference to the equator[3], so it has the largest circumference adjustment ratio. Figure 4.4 shows just how close the forces measured were to those of the calculated values. The graphs for horizontal cables # 2 and # 3 were not as close as horizontal cable # 1 to the calculated values. Both graphs wandered, depending on the movement of the cable net and the tributary area the cable was carrying. The distribution factor relating the circumferences of the actual cable to the equator is based on a linear distribution. The graphs (figure 4.5) show that the factor is not a linear relationship. However, these data also show that as the cable is pulled tighter onto the membrane, it picks up more force within the cable. This is another reason that the cables must be very carefully placed with

[3]The diameter of the sphere at midpoint.

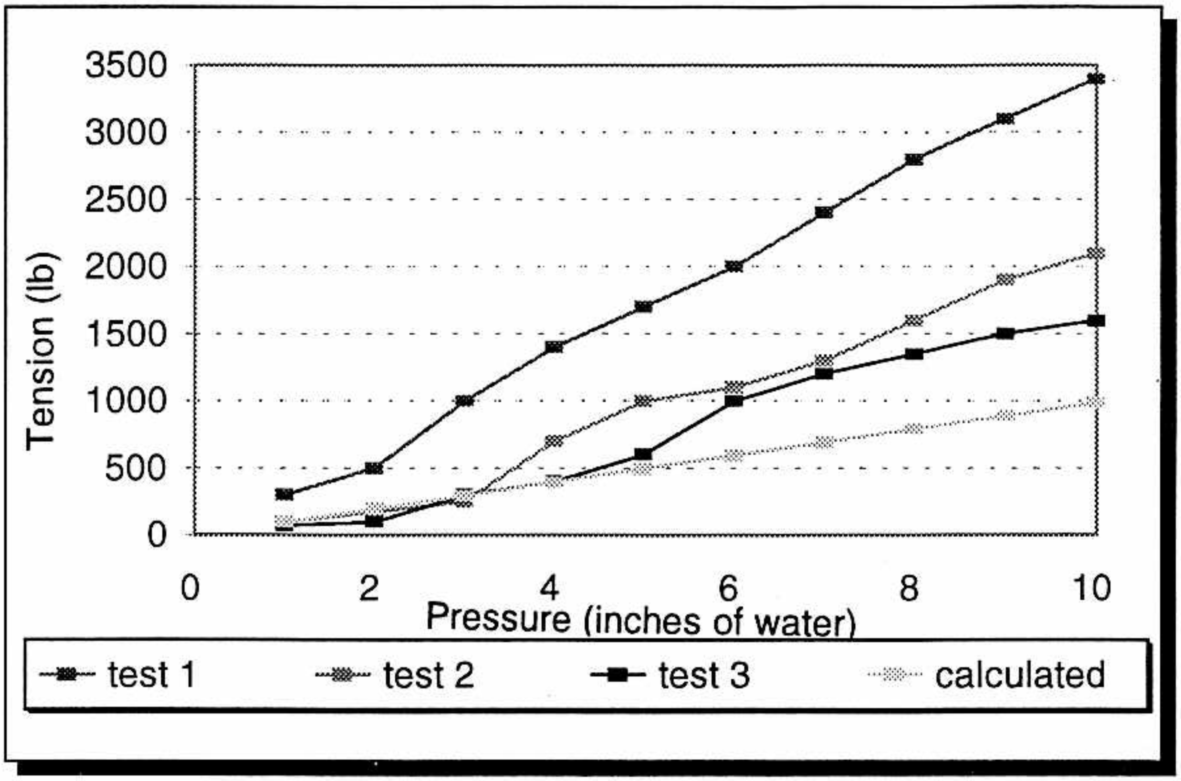

Figure 4.5 Horizontal Cable # 2 forces to inches of water

even leg lengths both horizontal and vertical in order to evenly carry the forces in the membrane. The remaining graphs for the horizontal cables and the vertical cables are located in appendix C. Only two cables were measured in the geodesic cable net, showing that the tensions were relatively close, independent of which cable is measured. During the testing process, horizontal cable # 2 failed at a cable splice three times at higher pressures. This area seems to be a critical location for transferring forces from the membrane to the cable net systems. The upper cables are highly susceptible to movement in that the forces increase substantially when they are tightened or lowered on the profile of the dome, whereas horizontal cable # 1 had very little variation. The vertical cables were very stable, because of the consistent location around the membrane circumference. The horizontal cables based, on the same principle, will be more stable, with a more consistent placement in equal leg lengths up the profile of the membrane.

4.4 Cable nets

The radial-horizontal cable net performed very well overall; and with the addition of the secondary cables and fixed membrane-cable node points, the system will be extremely stable. The secondary cables are place between the main cables, at spacing close to that of the bottom vertical spacing. The radial-horizontal cable net was able to reduce the deflections in the apex of the dome membrane substantially; and as the pressure increased, the apex actually rose slightly above the engineered profile. During the placement of the radial-horizontal cable net, many lessons were learned, making the placement of the next cable net (geodesic-net) a much easier process. The radial-horizontal cable net points could be easily placed on the membrane at pre-designed points. The membrane-cable node points will be a future area of research that will improve the air-forming system for large-diameter, low-profile domes.

Chapter 5

5.1 Conclusion

The recent desire to build large diameter domes using air forming techniques has required research of this kind. The costs of constructing a large-diameter dome are critical, due to high labor costs. The cost of building a large diameter roof structure could be substantially reduced from that of the Kingdome. Based on the model study and the associated research including that of Hatch (9), the cable net systems will conform to the allowable specifications of air form and dome engineering, thus making the construction of large domes feasible.

The two specific objectives of this thesis were to show that a radial-horizontal cable net can maintain the engineered profile, and show that the cable net can effectively transfer the forces in the membrane to the cables and into the ground. The geometry inspired by the Pantheon was very successful at both removing the apex deformation and transferring the membrane forces into the ground. This technology, based on mathematical and physical model data collected during the research presented here, using the radial-horizontal and geodesic cable net systems, will effectively control deformations throughout the membrane.

The geodesic cable system performed very well, and deformations were constrained in the membrane in every direction. This system was more difficult and time consuming to assemble; however, its strength was in its ability to redistribute the forces evenly to the cables. The cables measured with the tensiometer, differing in length and orientation, carried relatively the same tension.

The radial-horizontal cable net system sufficiently reduced the deflections at the critical locations. The cable system was successful with minimum horizontal cables, because it did reduce the apex deflection to within ±3% of the engineered profile.

The radial-horizontal cable net is an effective tool in the air-forming construction of domical low-profile roof structures. The previous model study showed that even with the minimum horizontal cables the profile was maintained. The pillowing effect between the cables was able to transfer forces from the membrane to the ground and reduce the local stresses within the membrane. Continued research is needed to understand the actual forces in the membrane, being transferred to the cables.

5.2 Recommendations

The forces within the membrane, were effectively transferred to the cables, and reduced the radius of curvature reducing the forces in the membrane. However as a recommendation for successful construction, node clamps need to be placed at specific points rigidly connected to the membrane. Monolithic Constructors, the manufacturer of the membrane, will place cable clamps directly in the membrane at the engineered location of the cable node point. The membrane node points will allow for easier field installation of the cables, and will make it possible to completely control the pillowing of the membrane between cables. This will be accomplished by placing an exact amount of material between each point and rigidly connecting the points with cables. The node point will consist of a steel plate on the bottom and top side of the membrane, rigidly connected, with the membrane material. A bolt will be threaded through the top side of the membrane, with a clamp to connect the cables. This makes it easier for the cables to be laid out, marked and connected to the membrane using the quick cable clamps. This will allow for the exact designed stretch to take place between each node point in the membrane. This will also help develop the transfer of forces from the membrane to the cables, allowing for a more even distribution through a fixed point. The fixed node points will also help to transfer forces from the horizontal cables to the vertical cables, more effectively funneling the cable forces to the ring beam and foundation. The membrane clamps make the radial-horizontal cable system a more user-friendly construction process, and better able to match exactly the proposed profile of the dome. The time factor for assembly will also be substantially reduced, furthering the positive characteristics in favor of using the radial-horizontal cable system.

BIBLIOGRAPHY

(1) Billington, David P., Thin Shell Concrete Structures, Princeton University: McGraw-Hill Book Company, Inc., 1982.

(2) Melaragho, Michele, Introduction of Shell Structures, Van Nostrand Reinhold, New York, 1991.

(3) Irvine, H. Max, Cable Structures, Cambridge: The MIT Press, 1981.

(4) Vilnay, Oren, Cable Nets and Tensegric Shells, Ellis Horwood, 1990.

(5) Wilson, Arnold and Shaffer, Keith, Construction of Shells Using Air Supported Forms, 1996.

(6) Wilson, Arnold, "Very Large Air-Formed Concrete Shells", American Concrete Institute, 1990.

(7) Murphy, Glenn CE, PHD, Similitude in Engineering, The Ronald Press Company, New York, 1950.

(8) McAdams, William H., Heat Transmission, McGraw-Hill Book Company, 1954.

(9) Hatch, Robert J., Large Thin Shell Concrete Domes Using Air Supported Forms and Cable Nets, Thesis (BYU), 1994.

(10) "The Builders", Published by: The Book Division, National Geographic Society, Washington, D.C.

(11) Hand Written Notes (Flugge theory of membrane analysis) -- BYU Harold B. Lee Library

APPENDIX A

Membrane Analysis

Flugge derivation of membrane analysis

Model design

Dimensional analysis

Cable design - (model)

HAND WRITTEN NOTES:

MEMBRANE THEORY- SURFACE OF REVOLUTION SYMMETRICAL LOADING

A. COORDINATE SYSTEM AND GEOMETRY

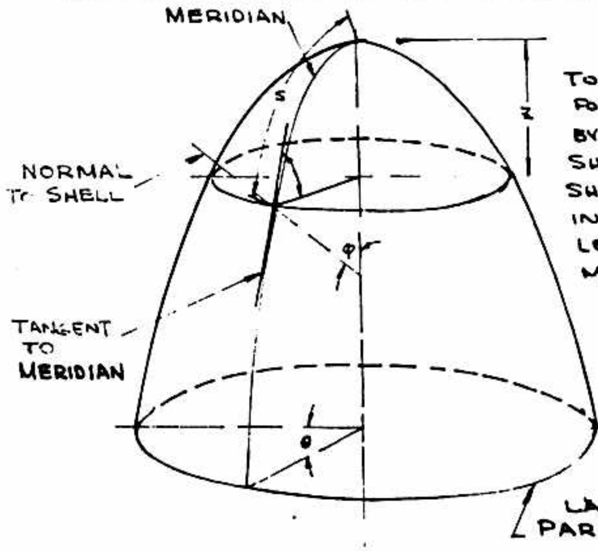

SOMETIMES IT IS POSSIBLE TO CARRY THESE NORMAL FORCES MERELY AND COMPLETELY BY FORCES IN THE PLANE OF THE SHELL. IN THIS MANNER, TRANSVERSE SHEAR AND MOMENTS MAY BE ELIMINATED FROM THE PICTURE. THIS LEADS TO THE EXTREMELY SIMPLE MEMBRANE THEORY

DEFINITION OF SHELL FLÜGGE: ANY STRUCTURE OF COMPARATIVELY THIN NATURE WHICH POSSESSES CURVATURE.

1. LOCATION OF MERIDIAN

LOCATE MERIDIAN BY AN ANGLE $\underline{\theta}$ (θ IS AN ANGLE IN THE PLANE PERPENDICULAR TO AXIS OF THE SURFACE OF REVOLUTION, AND IS MEASURED FROM SOME DATUM LINE.)

2. LOCATE POINT ON MERIDIAN - CHOICE OF COORDINATE

z - COORDINATE

a.) WE COULD USE A LINEAR COORDINATE ALONG THE AXIS OF THE SHELL. THE DISADVANTAGE OF THIS PRACTICE, IS THAT, AT THE TOP OF THE SHELL A SMALL CHANGE IN THIS COORDINATE WOULD CORRESPOND TO A LARGE CHANGE IN THE STRESSES AT THE TOP

b.) WE COULD ALSO USE CURVILINEAR COORDINATES "s" DISADVANTAGE. GEOMETRY BECOMES MESSY. (EXAMPLE: FOR AN ELLYPSE, WE GET ELLYPTIC FUNCTIONS)

c.) USE φ

φ IS THE ANGLE THAT THE TANGENT TO THE MERIDIAN MAKES WITH THE HORIZONTAL AT THE POINT IN QUESTION, OR φ IS THE ANGLE THAT THE NORMAL TO THE SHELL MAKES WITH THE VERTICAL. THIS DOESN'T WORK FOR A CONE. THIS ANGLE IS THE COMPLIMENT TO A LATTITUDE ANGLE FOR MAPPING ON THE EARTH.

EQUILIBRIUM

RESTRICT TO AXIALLY SYMMETRIC LOADING. SYSTEM IS INDEPENDENT OF ANGLE θ

BELOW IS A DIFFERENTIAL ELEMENT CONTAINED BETWEEN TWO MERIDIANS AND TWO PARALLEL CIRCLES.

USE SO CALLED MIDDLE SURFACE

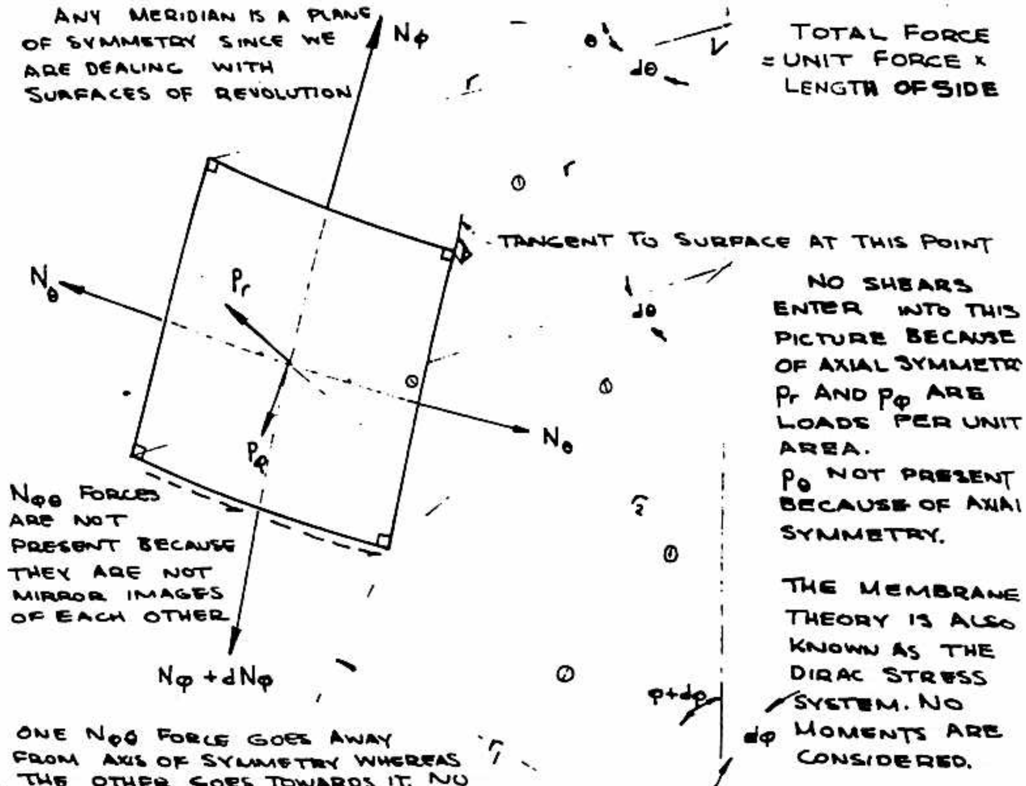

ONE $N_{\varphi\theta}$ FORCE GOES AWAY FROM AXIS OF SYMMETRY WHEREAS THE OTHER GOES TOWARDS IT. NO
(1) SUCH SYSTEM OF FORCES ARE ADMISSABLE.

$r = r_2 \sin\varphi$ – HORIZONTAL RADIUS RIGHT TRIANGLE ABOVE

r_1, r_2 ARE PRINCIPAL RADII OF CURVATURE

NOTE: N_θ IS IN THE HORIZONTAL PLANE ALL ①'S ARE IN THE SAME VERTICAL PLANE.

1. LOADS

p_φ, p_r ARE IN (psi.), $p_\theta = 0$ BY SYMMETRY

$+p_r$ IS OUTWARD

$+p_\varphi$ IS IN THE DIRECTION OF INCREASING φ,

MEMBRANE THEORY

EQUILIBRIUM

MERIDIAN FORCE N_φ - PER UNIT ARC LENGTH
HOOP FORCE $N_\theta \, r\,d\varphi$ -

N_θ, N_φ ARE POSITIVE WHEN DESCRIBING TENSION

$N_{x\varphi} = 0$ BECAUSE OF SYMMETRY. WE NEED TWO EQUILIBRIUM CONDITIONS SINCE ONLY TWO FORCES ARE ASSUMED TO REMAIN.

THERE IS NO CHANGE IN N_θ BECAUSE OF SYMMETRY. ALSO, NOTHING IS A FUNCTION OF θ, WE CAN USE WHOLE DIFFERENTIALS $d(\ )$ INSTEAD OF PARTIALS $\frac{\partial(\ )}{\partial(\ )}$

$$dA = (r_1\,d\varphi)(r\,d\theta)$$

(IF WE NEGLECT HIGHER ORDER TERMS)

THERE ARE ONLY TWO CONDITIONS OF EQUILIBRIUM NOT AUTOMATICALLY SATISFIED.) ANY PLANE OF ANY MERIDIAN MUST BE A PLANE OF SYMMETRY IN SUCH A STRESS SYSTEM.

2. $\sum F_\varphi$ DIRECTION $= 0$

a.) DUE TO p_φ:

$$+\,p_\varphi\,(r_1\,d\varphi)(r\,d\theta)$$

b.) DUE TO N_φ

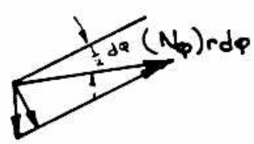

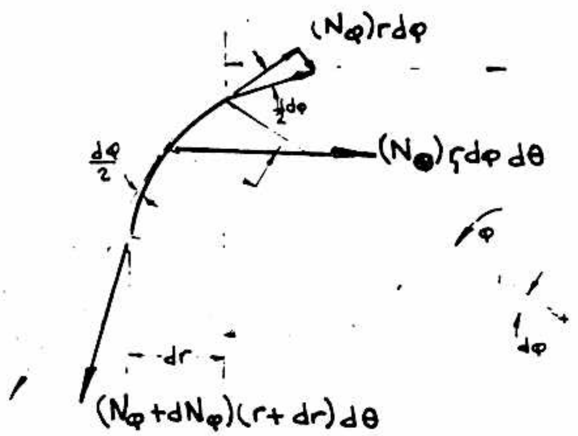

$N_\varphi\, r\, d\varphi$ IS NOT QUITE CORRECT SINCE WE NEED TO PROJECT THE RESULTANT ONTO THE TANGENT LINE. HOWEVER, $\cos\frac{1}{2}d\varphi \approx 1.0$

NOTE

$$\cos\frac{d\varphi}{2} = 1$$

$$(N_\varphi + dN_\varphi)(r+dr)\,d\theta - N_\varphi\, r\, d\theta = r\,dN_\varphi\,d\theta + N_\varphi\,dr\,d\theta$$

$$= \frac{d}{d\varphi}(N_\varphi\, r\, d\theta)\,d\varphi = \frac{d}{d\varphi}(N_\varphi r)\,d\theta\,d\varphi$$

TAKE $d\theta$ OUT, SINCE IT DOES NOT DEPEND ON φ

IN SAME DEGREE OF ACCURACY AS ABOVE

EQUILIBRIUM

c.) DUE TO N_θ

WALL ACTION
OR HOOP ACTION
(ONE CONDITION)

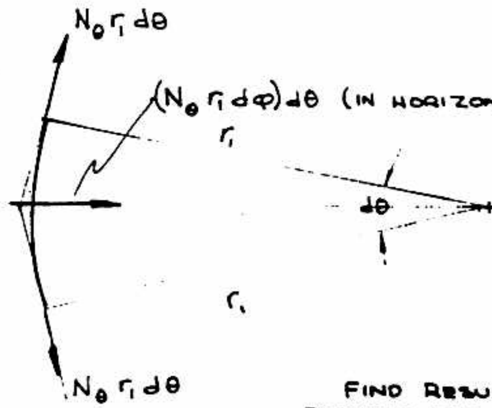

FIND RESULTANT BY DRAWING THE FORCE POLYGON
CARRY THE FORCE OVER INTO THE SIDE PLANE

FROM PRECEDING PAGE
WE NEED PROJECTION OF THIS FORCE ONTO VERTICAL

$$-(N_\theta r_1 d\phi d\theta)\cos\phi$$

MULTIPLY BY $\cos\phi$ FOR VERTICAL PART.

SUMMING ALL QUANTITIES

$$p_\varphi (r_1 d\varphi)(r d\theta) + \frac{d}{d\varphi}(N_\varphi r) d\theta d\varphi - N_\theta r_1 d\varphi d\theta \cos\varphi = 0$$

OR

ADDING VARIOUS FORCES TOGETHER

φ IS NOT AN INFINTESIMAL ANGLE BUT MAY ASSUME ANY VALUE BETWEEN 0° AND 90°

$$\boxed{\frac{d}{d\varphi}(N_\varphi r) - N_\theta r_1 \cos\varphi = -p_\varphi r_1 r} \qquad (2)$$

EQUATION OF EQUILIBRIUM

3.) NORMAL EQUILIBRIUM (+ IS OUT) RADIAL DIRECTION

SUMMING ALL FORCES.

a.) DUE TO p_r : $+p_r (r_1 d\varphi)(r d\theta)$

b.) DUE TO N_θ : (SEE SKETCH ON PRECEDING PAGE

$$-N_\theta r_1 d\varphi d\theta \sin\varphi$$

c.) DUE TO N_φ

$\frac{d\varphi}{2}$ (IN THE LIMIT) $\frac{d\varphi}{2}$ (IN THE LIMIT)

$$-(N_\varphi) r d\theta \sin\frac{d\varphi}{2} - (N_\varphi + dN_\varphi)(r + dr) d\theta \sin\frac{d\varphi}{2}$$

$$-N_\varphi r d\theta d\varphi$$

IMPORTANT: WHEN IN DOUBT AS TO WHICH TERMS TO INCLUDE AND WHICH TO DROP, INCLUDE ALL TERMS. SHRINK ELEMENT AND OBSERVE WHICH TERMS VANISH IN THE LIMIT

EQUILIBRIUM:

AGAIN, SUMMING ALL TERMS

$$p_r r_1 r d\theta d\varphi - N_\theta r_1 d\theta d\varphi \sin\varphi - N_\varphi r d\theta d\varphi = 0$$

$$N_\varphi r + N_\theta r_1 \sin\varphi = p_r r_1 r \quad (3a)$$

SUBSTITUTING $r = r_2 \sin\varphi$ AND DIVIDING BY $r_1 r$

$$\boxed{\frac{N_\varphi}{r_1} + \frac{N_\theta}{r_2} = p_r} \quad \text{EQUATION OF EQUILIBRIUM} \quad (3b)$$

HENCE:

FOR AXIAL SYMMETRY, THE PROBLEM IS OF NO HIGHER THAN FIRST ORDER.

SUMMARIZING THE EQUATIONS OF EQUILIBRIUM

$$\frac{d}{d\varphi}(N_\varphi r) - N_\theta r_1 \cos\varphi = -p_\varphi r_1 r \quad (a)$$

$$\frac{N_\varphi}{r_1} + \frac{N_\theta}{r_2} = p_r \quad (b)$$

or

$$(N_\varphi r + N_\theta r_1 \sin\varphi = p_r r_1 r)$$

THERE ARE TWO EQUATIONS AND TWO UNKNOWNS. CONSEQUEN THE PROBLEM IS STATICALLY DETERMINANT.

ELIMINATE N_θ

SUBSTITUTE $r = r_2 \sin\varphi$ IN (b)

$$N_\varphi r_2 \sin\varphi + N_\theta r_1 \sin\varphi = p_r r_1 r_2 \sin\varphi$$

$$N_\theta r_1 = -N_\varphi r_2 + p_r r_1 r_2$$

SUBSTITUTING INTO (a)

$$\frac{d}{d\varphi}(N_\varphi r_2 \sin\varphi) + N_\varphi r_2 \cos\varphi = -p_r r_1 r_2 \cos\varphi - p_\varphi r_1 r_2 \sin\varphi$$

MEMBRANE THEORY: SURFACE OF REVOLUTION

EQUILIBRIUM:

MULTIPLYING BY $\sin\varphi$

$$\sin\varphi \frac{d}{d\varphi}(N_\varphi r_2 \sin\varphi) + N_\varphi r_2 \sin\varphi\cos\varphi = p_r r_1 r_2 \sin\varphi\cos\varphi - p_\varphi r_1 r_2 \sin^2\varphi$$

THE FIRST TWO TERMS ARE

$$\frac{d}{d\varphi}(N_\varphi r_2 \sin\varphi \cdot \sin\varphi) = \frac{d}{d\varphi}(N_\varphi r_2 \sin^2\varphi)$$

THUS, WE TAKE STOCK OF EVERYTHING WE HAVE DONE SO FAR AND RESORT TO MATHEMATICAL MEANS TO FURTHER SOLVE PROBLE

$$\frac{d}{d\varphi}(N_\varphi r_2 \sin^2\varphi) = (p_r\cos\varphi - p_\varphi \sin\varphi) r_1 r_2 \sin\varphi$$

INTEGRATING AND SOLVING FOR N_φ

$$N_\varphi = \frac{1}{r_2 \sin^2\varphi}\left[\int_{\varphi_0}^{\varphi}(p_r'\cos\varphi' - p_\varphi'\sin\varphi') r_1' r_2' \sin\varphi' \, d\varphi' + C\right] \quad (4)$$

$\varphi = \varphi_0$ IS THE VALUE THE MERIDIAN BEGINS WITH, $\varphi = \varphi$ IS THE VALUE AT WHICH WE ARE COMPUTING N_φ

THE PRIMES INDICATE RUNNING VALUES AND UNPRIMED QUANTITIES $(N_\varphi r_2 \sin^2\varphi)$ INDICATE THE PLACE AT WHICH WE ARE COMPUTING N_φ. WE COULD LET THE LOWER BOUNDARY BE UNDETERMINED AND LOWER LIMIT WOULD NOT BE ZERO.

THEN:

N_θ IS FOUND FROM

$$\frac{N_\varphi}{r_1} + \frac{N_\theta}{r_2} = p_r$$

NOTE:

EVERYTHING THUS FAR IS VALID FOR VARIABLE THICKNESS AND AN-ISOTROPIC SHELL CONSTRUCTION (NO HOLES)

THE EQUATIONS OF EQUILIBRIUM JUST DERIVED APPLY TO THE FOLLOWING SURFACES OF REVOLUTION.

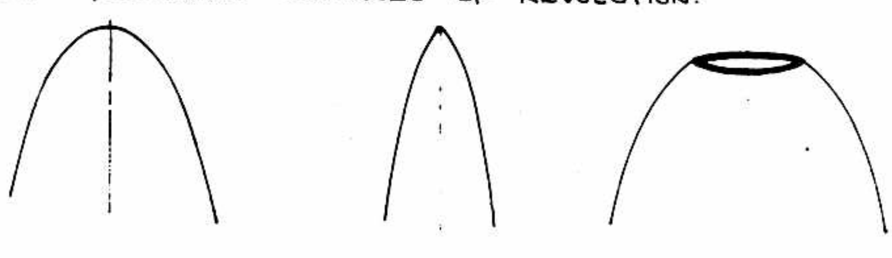

MEMBRANE THEORY SURFACE OF REVOLUTION

MECHANICAL INTERPRETATION OF N_φ EQUATION

FROM EQUATION 4

(a)

$$N_\varphi = \frac{1}{r_2 \sin^2\varphi}\left[\int_0^\varphi (p_r' \cos\varphi' - p_\varphi' \sin\varphi') r_1' r_2' \sin\varphi' \, d\varphi' + C\right]$$

WE MAY DROP THE PRIMES.

THE LOWER LIMIT 0 IS ARBITRARY AND MAY NOT BE CORRECT, THUS ADJUST FOR THIS BY ADDING THE CONSTANT C.

TAKE HORIZONTAL CUT THROUGH SHELL

MECHANICAL INTERPRETATION OF INTEGRATION

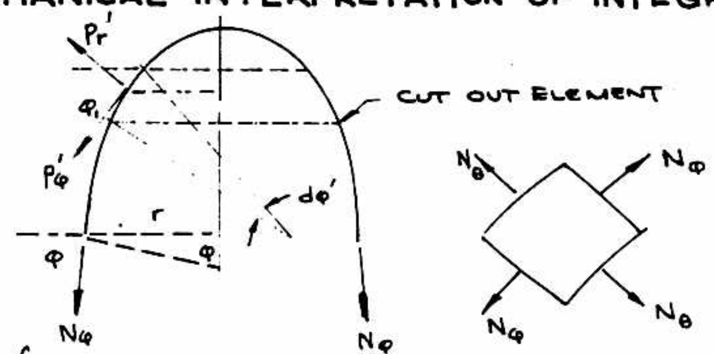

WHENEVER $\int x\,dx$ IS WRITTEN, IT IS MEANT $= \frac{x^2}{2} + C$

VERTICAL COMPONENT OF N_φ IS $(N_\varphi 2\pi r_2 \sin\varphi)\sin\varphi$ ↓

DOWNWARD RESULTANT OF N_φ FORCES

VERTICAL LOAD PER UNIT AREA OF PRESSURE FORCE IS

AREA $= r_1' d\varphi' 2\pi r'$

$p_r' \cos\varphi - p_\varphi' \sin\varphi'$

↑

BAND AREA $= (2\pi r')(r_1' d\varphi') = 2\pi r_2' r_1' \sin\varphi' d\varphi$

AFTER ONE CONTRIBUTION FROM A SINGLE ELEMENT HAS BEEN FOUND HEN, ADD UP ALL CONTRIBUTIONS.

EQUATING

$$N_\varphi = \frac{1}{r_2 \sin^2\varphi}\left[\int_0^\varphi (p_r' \cos\varphi' - p_\varphi' \sin\varphi') r_1' r_2' \sin' d\varphi\right]$$

HENCE, WE SEE THAT WE OBTAIN THE SAME EQUATION FOR φ AS BEFORE, EXCEPT FOR THE CONSTANT C.

HOWEVER, THIS CONSTITUTES A CHECK ONLY SINCE WE WISH TO STICK WITH THE MOST GENERAL METHOD OF SOLUTION AS A FOUNDATION FOR FURTHER SHELL THEORY

MEMBRANE THEORY SURFACE OF REVOLUTION

EQUILIBRIUM

IN REGARD TO CONSTANT C

1. C TAKES INTO ACCOUNT THE POSSIBILITY OF A CONCENTRATED LOAD

2. IF AN INDEFINITE INTEGRAL IS WRITTEN C IS AUTOMATICALL FIXED.

- IS THE REASON WE OBTAINED N_φ FROM THE DIFFERENTIAI ELEMENT INSTEAD OF WRITING VERTICAL EQUILIBRIUM OF FINITE PORTION OF THE SHELL.

THE REASON IS THAT, TAKING VERTICAL EQUILIBRIUM FOR A FINITE PORTION OF THE SHELL ONLY, APPLIES FOR SYMMETRICAL LOADING AND DOES NOT DEVELOP THE GENEF TECHNIQUES. C. REPRESENTS WHAT MAY ESCAPE US WHEN SOME GOES WRONG IN TOTAL LOAD

LIMITS ON INTEGRAL FOR N_φ

a.) THE UPPER LIMIT IS ALWAYS φ

b.) THE LOWER LIMIT MAY BE ANYTHING. USE THE CONSTANT C TO COMPENSATE FOR LOWER LIMIT.

LOWER LIMIT = 0, SOMETIMES USEFULL.

LOWER LIMIT = φ_1, FOR POINTED DOME

LOWER LIMIT = φ_2, FOR OPEN SHELL

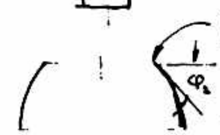

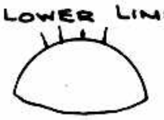

RETAIN CONSTANT FACTOR 2π

$2\pi \times N_\varphi$ = TOTAL LOAD AT SUPPORT

EXAMPLE 1 SHERICAL SHELL UNDER INTERNAL PRESSURE

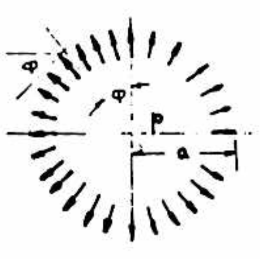

HERE $r_1 = r_2 = a$

$p_r = +p$

$p_\theta = 0$

MEMBRANE THEORY

EXAMPLE: SPHERICAL SHELL UNDER INTERNAL PRESSURE

EQUATION 4 FOR N_φ YIELDS

$$N_\varphi = \frac{1}{r_2 \sin^2\theta}\left[\int_0^\varphi (p_r \cos\varphi - p_\varphi \sin\varphi) r_1 r_2 \sin\varphi \, d\varphi + C\right]$$

$$= \frac{1}{a \sin^2\theta}\left[\int_0^\varphi (p \cos\varphi - 0) a^2 \sin\varphi \, d\varphi + C\right]$$

$$= \frac{pa}{\sin^2\varphi}\left[\int_0^\varphi \cos\varphi \sin\varphi \, d\varphi + C\right]$$

$$N_\varphi = \frac{pa}{2\sin^2\varphi}\left[\sin^2\varphi + C\right] = pa + C\frac{pa}{\sin^2\varphi}$$

PAGE 74 BUR

FOR THE REGULARITY AT $\varphi = 0$, 180°

$$[C = 0]$$

IN ORDER THAT N_φ DOES NOT BECOME INFINITE AT $\varphi = 0$, 180°

$$N_\varphi = \frac{pa}{2}$$

N_θ MAY BE COMPUTED FROM

$$\frac{N_\varphi}{r_1} + \frac{N_\theta}{r_2} = p_r$$

$$N_\varphi + N_\theta = pa$$

$$\frac{pa}{2} - N_\theta = pa$$

$$N_\varphi = N_\theta = \frac{pa}{2}$$

AS IS WELL KNOWN

Ring beam and Anchorage Design

(by Dr. Arnold Wilson)

Anchorage Design

Uplift force due to an internal force of 13.87 inches of water or 0.5 psi

$D := 36$ Diameter of Dome

$Force := \frac{\pi \cdot D^2}{4} \cdot .5 \cdot 144$ $Force = 7.329 \cdot 10^4$ (lbs of uplift)

$A := \frac{\pi \cdot D^2}{4}$ $A = 1.018 \cdot 10^3$ (Area of Dome Footprint (ft^2))

$F_p := \frac{Force}{36 \cdot \pi}$ $F_p = 648$ (Force per linear foot lb/ft of ring beam)

Assume anchor cantilevers to be 3 ft

Assume compression ring spans to be 5 ft

The force on the end of the anchor becomes:

$A_f := F_p \cdot 5$ $A_f = 3.24 \cdot 10^3$ (lbs)

The moment on the end of the anchor becomes:

$M := A_f \cdot 3$ $M = 9.72 \cdot 10^3$ (lb-ft)

Checking the section modulus for anchor design

$F_b := 22000$ (psi)

Assume non-compact (worse case) anchor section

$S_x := \frac{M \cdot 12}{F_b}$ $S_x = 5.302$ (inches)

Sy the weak direction section modulus for an W10x30 is (5.75) inches
Number of anchors (tie downs) at maximum 5 ft spacing $L := 5$ (ft)

$N := \frac{D \cdot \pi}{5}$ $N = 23$ anchors

Compression Ring Design

$p := 72.12$ psi
$R := 23.03$ ft

$T := p \cdot \frac{R}{2}$ $T = 830.462$

$P := T \cdot \cos(.895)$ $P = 519.469$ lb/ft,

$F := P \cdot \frac{R}{2}$

$F = 5.982 \cdot 10^3$ lbs Acting on ring Compression force becomes F

Axial force(lbs) in ring beam @ 13.87 inches of water or 0.5 psi

Try a 5x5x5/16 compression ring

$A_1 := 3.03$ (in^2)

$r_x := 1.57$

$r_y := r_x$

$r_z := .994$

$K := 1$

$Q := K \cdot \frac{L \cdot 12}{r_z}$ (Q=Kl/r)

$Q = 60.362$

$F_a := 17.430$ (ksi)

$f_a := \frac{F}{A_1}$ $f_a = 1.974 \cdot 10^3$ Fa > fa ok so check unity equation

Bending of Compression Ring in the x-direction

$S_x := 2.04$ (Section modulus)

$w_b := F_p$ $w_b = 648$ (lb/ft)

$$M_b := \frac{\frac{w_b \cdot L^2}{10}}{1000}$$

$M_b = 1.62$ (kip-ft, Moment in x direction of the beam)

$f_{bx} := M_b \cdot \frac{12}{S_x}$

$f_{bx} = 9.529$ (Allowable stress for unsymetric angle)

$Fex := 41.48$ (From table 8 page 5-122 ASD-AISC)

$F_{bx} := 18$

$F_{by} := F_{bx}$

(Compressive bending stress that would be permitted if bending moment alone existed, ksi)

Bending of Compression Ring in the y-direction

Find the eccentricity of beam in a five ft span

$R := 18$ ft, Radius of curvature of ring

$\theta := \left(\frac{L}{R}\right) \cdot \frac{180}{\pi}$

$\theta = 15.915$ (Angle in degrees of five ft length span between anchors)

$\theta_2 := \left(\frac{\theta}{2}\right) \cdot \frac{\pi}{180}$

$\theta_2 = 0.139$

$T := R \cdot \cos(\theta_2)$

$T = 17.827$ (ft in length of the circle radius minus the eccentricity)

$\Delta_e := (R - T) \cdot 12$

$\Delta_e = 2.08$ (inches of eccentricity for the moment in the y-direction)

$C_m := .79$ (Constant in unity equation)

$f_{by} := F \cdot \frac{\Delta_e}{S_x}$ (Allowable stress - Sx = Sy)

$U_1 := \frac{f_a}{F_a}$ $U_1 = 113.262$

$$U_2 := \frac{C_m \cdot (f_{bx})}{\left[1 - \left(\frac{f_a}{Fex}\right)\right] \cdot F_{bx}} \qquad U_2 = -0.009$$

$$U_3 := \frac{C_m \cdot f_{by}}{\left[1 - \left(\frac{f_a}{Fex}\right)\right] \cdot F_{by}} \qquad U_3 = -5.745$$

$$U := U_1 + U_2 + U_3 \qquad U = 107.508$$

(This okay because the internal pressure will not get to 13.87 inches of water (0.5 psi) that would create the full effect on the ringbeam)

Dimensional Analysis

Purpose: to determine the ΔH, ΔV deflections at the apex of the dome membrane forming system, with a given cable support. The dome will have a constant pressure applied to the interior of the membrane. These equations will identify as nearly as possible the deformations in domes larger than the 36 ft diameter model, based on the prototype properties.

The following variables were considered in the dimensional analysis outlined here:

T = Tension in the first primary horizontal cable

Ft = Stress in the same cable mentioned above

Acables = Cross sectional area of the cables

Ca = Tributary area of each primary (typical horizontal and vertical spacing) section

H = Height of the dome to the apex

D = Diameter of the dome

R = Radius of curvature

P = Pressure applied to the interior of the membrane

u = The vertical elevation change from an engineered profile

u = f(T, Ft, Acables, Ca, H, D, R, P)

u = C*(T^c1*Ft^c2*Acables^c3*Ca^c4*H^c5*D^c6*R^c7*P^c8)

Any variables that can be found in terms of one or more of the other variables are removed here:

Ft: it can be found with the force in the cables

Acables: Not related to the actual force in the cables

R: Diameter and height can be used to find the radius of curvature

reducing the equation to: u = C*(T^c1*Ca^c2*H^c3*D^c4*P^c5).
Using the dimension less parameters found in table 3.

L (proportional) (MLT^-2)^c1*(L^2)^c2*(L)^c3*(L)^c4*(ML^-1T^-2)^c5

By resolving this equation in to M, L, T components the following is found:

M: 0 = c1+c5

L: 1 = c1+2c2+c3+c4-c5

T: 0 = -2c1-2c5

These equations are used to solve for three of the five variables as shown below:

c1 = -c5

c4 = 1+2c5-2c2-c3

Plugging these known variable back into the (u) equation the unknown variables can be reduced to three from five.

u = C*(T^-c5)*(Ca^c2)*(H^c3)*(D^(1+2c5-2c2-c3))*(P^c5)

u/CD = (Ca/D^2)^c2*(H/D)^c3*(PD^2/T)^c5

The variables are calculated in terms of the deformations with and without cables. For simplicity the c coefficients are changed to c2 = c1, c3 = c2, c5 = c3.

Coefficients based on test model

Pressure	= 10 inches
Pressure	= 52 psf
Diameter	= 36 ft
Tributary Area	= 10.44 ft ^2
Cable Tension	= 2000 lb
Height	= 8.65 ft

u (max, min)	equation 1 (c1)	equation 2 (c2)	equation 3 (c3)
7.3 inches	0.846	2.862	-1.160
0.8 inches	1.305	4.412	-1.789

Note: 7.3 inches distortion is with vertical cables
0.8 inches distortion is with the three main horizontal cables
All deflections are at the apex of the membrane

Coefficients based on prototype model

Pressure	= 10.4 psf
Diameter	= 250 ft
Tributary Area	= 503 ft ^2
Cable Tension	= 18304 lb
Height	= 60 ft

	w/out cables	with cables
equation 1	50.65 in	5.55 in
equation 2	50.53 in	5.53 in
equation 3	47.40 in	5.06 in

Job Title: Model - 36 ft diameter

Calculated:		
Input: (Only input values in yellow boxes)		
Diameter	36	
Height	8.65	
Dome base circumference	113.10	ft
Radius of curvature =	23.05	ft
Phi K (degrees) =	51.33	degrees
Total surface area =	1253	ft ^2
Internal membrane pressure	10	
Apex deformations w/out cables	7.27	inches
Apex deformations w/cables	0.79	inches
*Note: These deformation values represent the theoretical maximum apex values, based on a dimensional analysis of a 36 ft diameter model. The values are then interpolated to the dimensions of the prototype specified in this module.		
Tension ring		1 if tension ring
Tension ring circumference	0.00	
Tension ring % of top section	0.05	
Primary horiz cables (3-5)	3	
Primary vertical cables	8	*Note if no tension ring must have equal number of primary vertical cables
Total vertical cables	64	
Actual vertical spacing @ ringbeam	1.77	ft

Vertical Cables:	
Actual primary cables (# 1)	4 cables
Cable lengths	41.31 ft
Secondary cable (# 2)	8 cables
Cable lengths	14.89 ft
Secondary cable (# 3)	16 cables
Cable lengths	10.60 ft
Secondary cable (# 4)	32 cables
Cable lengths	5.16 ft
Secondary cable (# 5)	0 cables
Cable lengths	0.00 ft
Secondary cable (# 6)	0 cables
Cable lengths	0.00 ft

Horizontal Cables	
Top Section	
Secondary circumference 1a	0.00 ft
Secondary circumference 2a	0.00 ft
Secondary circumference 3a	0.00 ft
Secondary circumference 4a	0.00 ft
Secondary circumference 5a	0.00 ft
Secondary circumference 6a	0.00 ft
Primary circumference (# 1)	35.85 ft
Secondary circumference 1b	0.00 ft
Secondary circumference 2b	0.00 ft
Secondary circumference 3b	0.00 ft
Secondary circumference 4b	0.00 ft
Secondary circumference 5b	0.00 ft
Secondary circumference 6b	0.00 ft
Primary circumference (# 2)	61.22 ft
Secondary circumference 1c	0.00 ft
Secondary circumference 2c	0.00 ft
Secondary circumference 3c	0.00 ft
Secondary circumference 4c	0.00 ft
Secondary circumference 5c	0.00 ft
Secondary circumference 6c	0.00 ft
Primary circumference (# 3)	90.17 ft
Secondary circumference 1d	0.00 ft
Secondary circumference 2d	0.00 ft
Secondary circumference 3d	0.00 ft
Secondary circumference 4d	0.00 ft
Secondary circumference 5d	0.00 ft
Secondary circumference 6d	0.00 ft
Ringbeam	0.00
ringbeam =	113.10 ft
	0.00 ft
	0.00 ft
	0.00 ft
	0.00 ft
	0.00 ft
	0.00 ft
	0.00
	0.00 ft
	0.00 ft
	0.00 ft
	0.00 ft
	0.00 ft
	0.00 ft
Ring beam	113.10 ft

Secondary horizontal cables

Note if nothing is input in manual cable cells, the number of cables needed will be figured automatically, and if no secondary cables are desired place a "1" in the manual cable number (long yellow box).

*Note if nothing is input in the yellow Phi box, the angle for each cable will be manually figured.

Average vertical cable spacing	2.24	
Average horizontal cable spacing	5.77	
Manual Phi - 1	14.33	14.33
Number of horizontal cables top section		
1	0	

Average vertical cable spacing	3.03	
Average horizontal cable spacing	4.29	
Manual Phi - 2	25	25
Number of horizontal cables		
1	0	

Vertical cable spacing	2.82	
Horizontal cable spacing	5.43	
Manual PHi - 3	38.5	38.5
Number of horizontal cables		
1	0	

Vertical cable spacing	1.88	
Horizontal cable spacing	5.16	
Manual Phi - 4		51.333815
Number of horizontal cables		
1	0	

Vertical cable spacing	0.00	
Horizontal cable spacing	0.00	
Manual Phi - 5		0
Number of horizontal cables		
	0	

Vertical cable spacing	0.00	
Horizontal cable spacing	0.00	
Manual Phi - 6		0
Number of horizontal cables		
	0	

General Cable Net Calculations		
Diameter	36	
Height	8.65	
Dome base circumference	113.097	ft
Adjusted # of Cables	64	Vertical cables
Actual vertical spacing	1.77	ft spacing/cable @ ringbeam
Radius of curvature =	23.053	ft
1/2 arc length	20.654	ft ^2
Phi K (radians) =	0.896	radians
Phi K (degrees) =	51.334	degrees
Total surface area =	1252.939	ft ^2
Main horizontal cables	3	Main cables
Main vertical cables	8	Main cables
Average tributary area	10.4411551	

Number of Cable Calculations			
Ring beam circumference	113.0973355292 ft		
Radius of curvature	23.0533		
Horizontal rings	Input primary vertical cables	Vertical cables	Vertical spacing
3	8	64	2

Calculated tensions	Cable number	# 3	# 2	# 1			ring beam
Horizontal cables		5.0	4.9	5.3	2.6	0.0	2.6
tributary area (ft)	adjust factor	0.2	0.4	0.6	0.0	0.0	0.8
pressure (in-water)	pressure (psf)			tension (lb)			
1	5.2	74.6	123.2	197.7	0.0	0.0	120.8
2	10.4	149.2	246.3	395.3	0.0	0.0	241.7
3	15.6	223.8	369.5	593.0	0.0	0.0	362.5
4	20.8	298.5	492.7	790.7	0.0	0.0	483.3
5	26	373.1	615.9	988.4	0.0	0.0	604.2
6	31.2	447.7	739.0	1186.0	0.0	0.0	725.0
7	36.4	522.3	862.2	1383.7	0.0	0.0	845.8
8	41.6	596.9	985.4	1581.4	0.0	0.0	966.7
9	46.8	671.5	1108.5	1779.1	0.0	0.0	1087.5
10	52	746.1	1231.7	1976.7	0.0	0.0	1208.3

Vertical cables	tributary area (ft)						tension (lb)					
# 6	0.00	[redacted]	0	0	0	0	0	0	0	0	0	0
# 5	0.00		0	0	0	0	0	0	0	0	0	0
# 4	1.59		95	190	286	381	476	571	666	761	857	952
# 3	1.98		118	237	355	474	592	711	829	948	1066	1185
# 2	2.33		140	279	419	558	698	838	977	1117	1256	1396
# 1	2.31		138	277	415	553	691	830	968	1106	1244	1383

Uplift						Uplift (kips)					
area (ft^2)	Total force (kips)	5	11	16	21	26	32	37	42	48	53
1017.88						Uplift per cable (lbs)					
	Force/cable (lbs)	83	165	248	331	414	496	579	662	744	827

Tributary Areas

Horizontal cables

	above	below	tributary area per foot	Actual circum (ft)	adjustment for non-linearity	equator circum (ft)	horizontal cable ratio
ring beam	2.58		2.58	113.10	1	144.85	0.78
	0.00	0.00	0.00	0.00	1	144.85	0.00
	2.58	0.00	2.58	0.00	1	144.85	0.00
# 1	2.72	2.58	5.30	90.17	1	144.85	0.62
# 2	2.15	2.72	4.86	61.22	1	144.85	0.42
# 3	2.88	2.15	5.03	35.85	1	144.85	0.25

Vertical cables

	top section (ft)	second section (ft)	Third section (ft)	fourth section (ft)	fifth section (ft)	sixth section (ft)	average width (ft)	tributary area per foot
# 6						0.00	0.00	0.00
# 5					0.00	0.00	0.00	0.00
# 4				1.59	0.00	0.00	1.59	1.59
# 3			2.37	1.59	0.00	0.00	1.98	1.98
# 2		3.03	2.37	1.59	0.00	0.00	2.33	2.33
# 1	2.24	3.03	2.37	1.59	0.00	0.00	2.31	2.31

Design of horizontal cables			
Radius of curvature	23.053	ft	
Primary horizontal cables	3		
	radians	degrees	
Phi K (radians) =	0.896	51.334	
Initial Phi values	0.224	12.833	

Arc legnths	
Total legnth	20.654
s1	5.766
s2	10.059
s3	15.491
s4	20.654
s5	0.000
s6	0.000

horizontal radius of arc length		
h1	5.706	ft
h2	9.743	ft
h3	14.351	ft
h4	18.000	ft
h5	0.000	ft
h6	0.000	ft

horizotal circumference		
c1	35.851	ft
c2	61.215	ft
c3	90.170	ft
c4	113.097	ft
c5	0.000	ft
c6	0.000	ft

Angles of cables from apex to ringbeam	Calculated	Input		
Phi 1	0.250	14.33	14.330	From apex to first primary horizontal cable
Phi 2	0.436	25	25.000	From first primary cable to the second
Phi 3	0.672	38.5	38.500	From second primary cable to the third
Phi 4	0.896	0	51.334	From third primary cable to the fourth
Phi 5	0.000	0	0.000	From fourth primary cable to the fifth
Phi 6	0.000	0	0.000	From fifth primary cable to the sixth

Cable Tributary lengths	
Cable 1	5.029
Cable 2	4.862
Cable 3	5.298
Cable 4	2.582
Cable 5	0.000
Cable 6	0.000

	Horiz-1	Horiz-2	Horiz-3	Horiz -4	Horiz -5	ring beam
Horizontal Primary Cable lengths	35.851	61.215	90.170	0.000	0.000	113.097

Secondary Horizontal Cables				
Number Vertical Cables	64			
Circumference of ring beam	113.097			
Spacing between cables	1.77			
	0			
Top Tension ring	0.000			
	caculated		corrected	input
Number secondary cables top section	3.263		0	1
Spacing of cables above top horizontal sectio	5.766	ft		
Number secondary cables in second section	2.429		0	1
Spacing of cables in second section	4.293	ft		
Number secondary cables in third section	3.074		0	1
Spacing of cables in third section	5.432	ft		
Number secondary cables in fourth section	2.922		0	1
Spacing of cables in fourth section	5.164	ft		
Number secondary cables in fifth section	0.000		0	0
Spacing of cables in fifth section	0.000	ft		
Number secondary cables in sixth section	0.000		0	0
Spacing of cables in sixth section	0.000	ft		

	circumferences of secondary cables				ringbeam	
Tension ring (ft)	cable number	Top	second	third	fourth	fifth
0.000	Primary Cable	35.85	61.22	90.17	113.10	0.00
Secondary	1	0.00	0.00	0.00	0.00	0.00
Secondary	2	0.00	0.00	0.00	0.00	0.00
Secondary	3	0.00	0.00	0.00	0.00	0.00
Secondary	4	0.00	0.00	0.00	0.00	0.00
Secondary	5	0.00	0.00	0.00	0.00	0.00
Secondary	6	0.00	0.00	0.00	0.00	0.00

Design of Vertical cables

Radius of curvature	23.053	ft

Primary Vertical Cables (Cable # 1)

	radians	degrees
Phi k	0.896	51.334
Tension ring	0	1 if tension ring
Cable length	41.309	ft
Number of cables	4	

Secondary Vertical Cables

Cable # 2		
	radians	degrees
Phi k-Phi 1	0.646	37.004
Cable length - 2	14.889	ft
Number of cables	8	

Cable # 3	1	
	radians	degrees
Phi k-Phi-2	0.460	26.334
Cable length - 1	10.596	ft
Number of cables	16	

Cable # 4	2	
	radians	degrees
Phik-Phi-3	0.224	12.834
Cable length - 1	5.164	ft
Number of cables	32	

Cable # 5	3	
	radians	degrees
Phik-Phi-4	0.000	0.000
Cable length - 1	0.000	ft
Number of cables	0	

Cable # 6	4	
	radians	degrees
Phik-Phi-5	0.000	0.000
Cable length - 1	0.000	ft
Number of cables	0	

Deformations

* The constant numbers are based on a 36 ft diameter model @ 10 inches of water pressure

Pressure	10	inches
Pressure	52	psf
Diameter	36	ft
Tributary area	10.44	ft^2
Cable tension	1976.74	lb
Height	8.65	ft

equation 1 (c1)	equation 2 (c2)	equation 3 (c3)	
0.846	2.862	-1.160	deflections with only vertical cables
1.305	4.412	-1.789	deflections with main horizontal cables
equation 1 (in)	equation 2 (in)	equation 3 (in)	
7.30	7.30	7.20	w/out cables
0.80	0.80	0.78	w/ cables

APPENDIX B

Profile Results and Deformation Plots

Profile Results Data Sheet

Test proposed profile

Date

point #	x (ft)	y (ft)	z (in)
1	-18	0	0
2	-16	0	27.6
3	-14	0	46.68
4	-12	0	64.8
5	-10	0	78.36
6	-8	0	90
7	-6	0	96
8	-4	0	100.8
9	-2	0	102.6
10	0	0	103.8
11	2	0	102.6
12	4	0	100.8
13	6	0	96
14	8	0	90
15	10	0	78.36
16	12	0	64.8
17	14	0	46.68
18	16	0	27.6
19	18	0	0

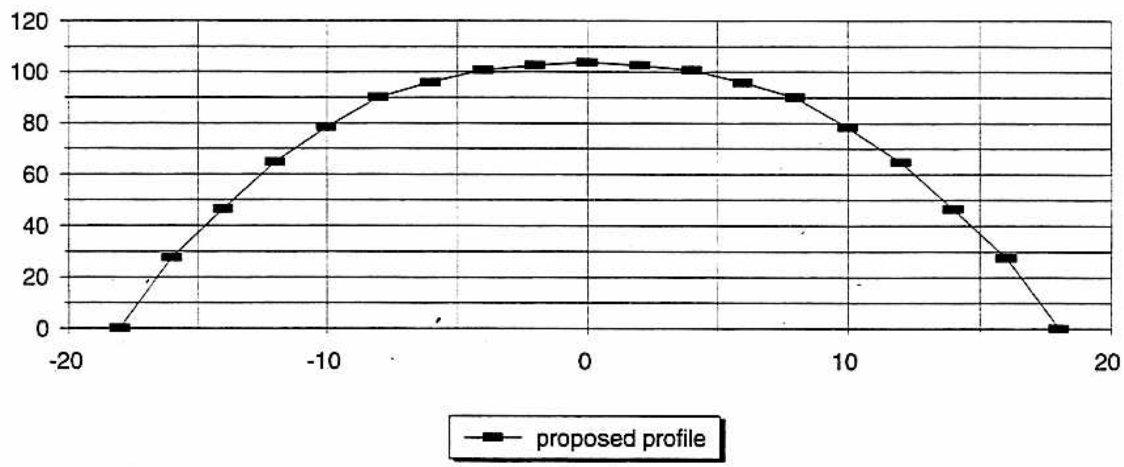

Profile Results Data Sheet

Test			1			
Date			03/15/96			
Internal pressure		4in		** water pressure **		
				measured	prop. profile	Difference
point #	x (ft)	y (ft)		z (in)	in	in
1	-18		0	0	0	0
2	-16		0	33	27.6	-5.4
3	-14		0	52.625	46.68	-5.945
4	-12		0	67.5	64.8	-2.7
5	-10		0	79.625	78.36	-1.265
6	-8		0	87.875	90	2.125
7	-6		0	93.875	96	2.125
8	-4		0	97.25	100.8	3.55
9	-2		0	99	102.6	3.6
10	0		0	99.25	103.8	4.55
11	2		0	99	102.6	3.6
12	4		0	97.125	100.8	3.675
13	6		0	93.5	96	2.5
14	8		0	87.25	90	2.75
15	10		0	78.875	78.36	-0.515
16	12		0	67.25	64.8	-2.45
17	14		0	51.375	46.68	-4.695
18	16		0	31	27.6	-3.4
19	18		0	0	0	0

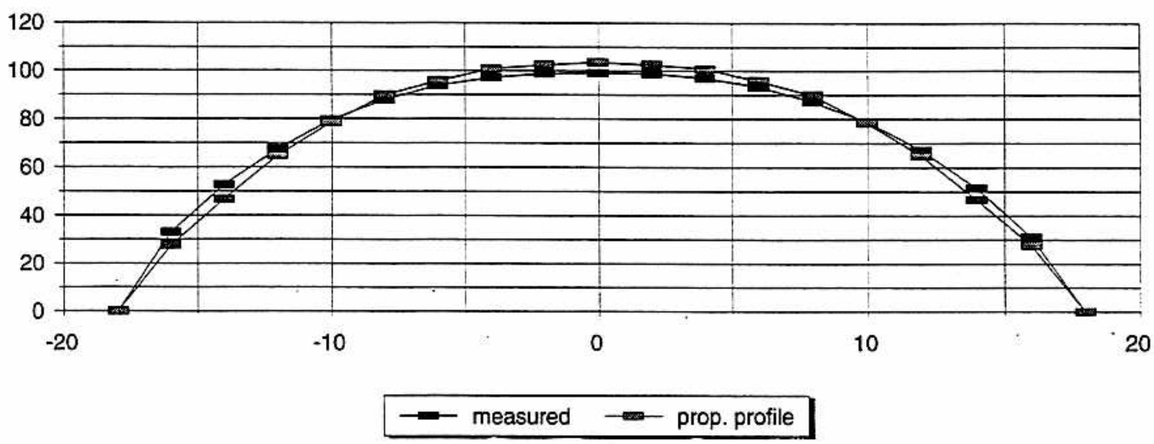

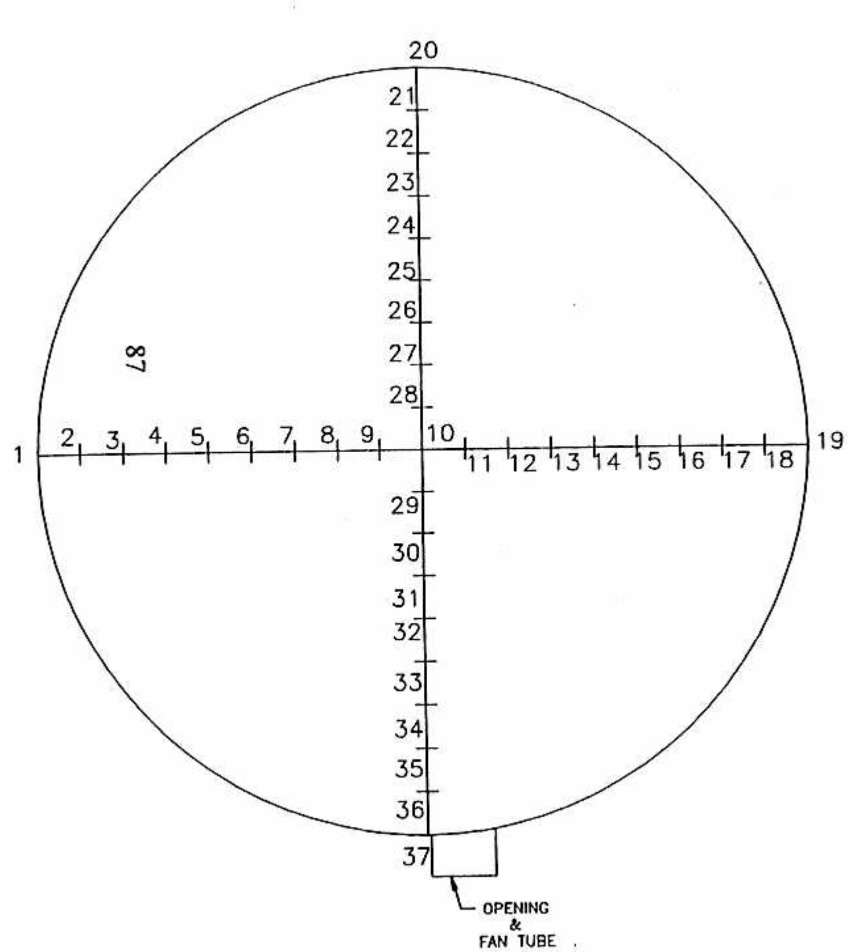

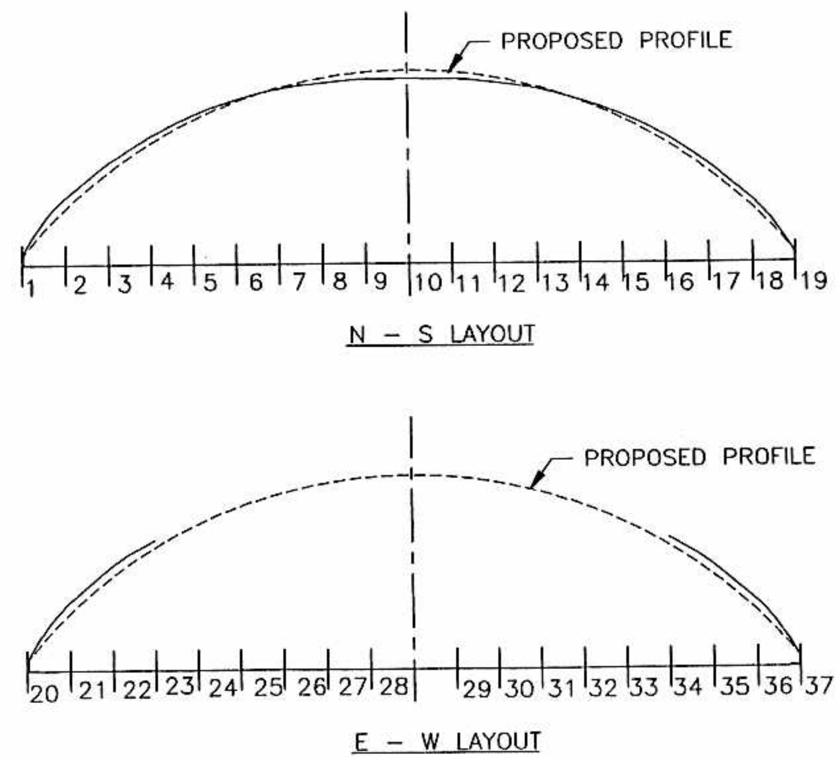

INTERNAL PRESSURE = 4"	TEST 1	WEB METHOD	15 MARCH 1996 9:30

Profile Results Data Sheet

Test 2

Date 03/14/96

Internal pressure 8 in ** water pressure **

point #	x (ft)	y (ft)	measured z (in)	prop. profile in	Difference in
1	-18	0	0	0	0
2	-16	0	28.25	27.6	-0.65
3	-14	0	47.75	46.68	-1.07
4	-12	0	57.875	64.8	6.925
5	-10	0	76.875	78.36	1.485
6	-8	0	86.625	90	3.375
7	-6	0	94.25	96	1.75
8	-4	0	99.325	100.8	1.475
9	-2	0	101.875	102.6	0.725
10	0	0	102.25	103.8	1.55
11	2	0	101.875	102.6	0.725
12	4	0	99.325	100.8	1.475
13	6	0	94.125	96	1.875
14	8	0	85.325	90	4.675
15	10	0	75.325	78.36	3.035
16	12	0	62.5	64.8	2.3
17	14	0	47	46.68	-0.32
18	16	0	27	27.6	0.6
19	18	0	0	0	0

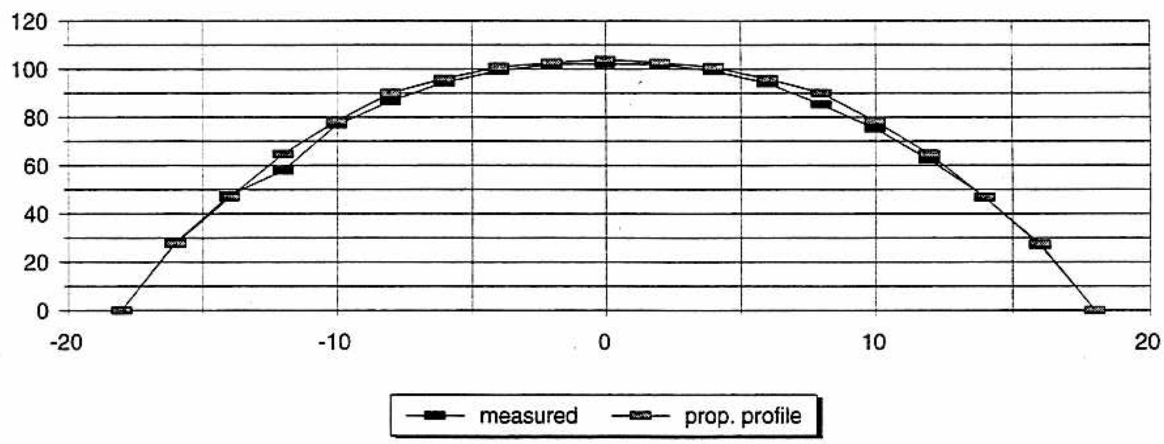

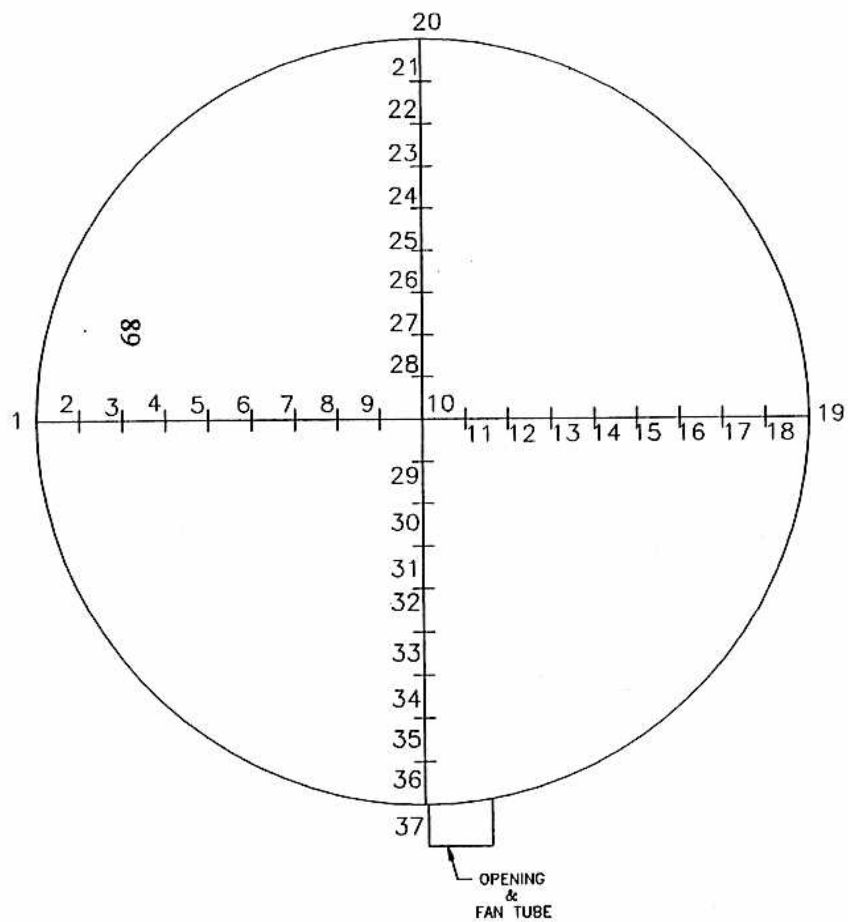

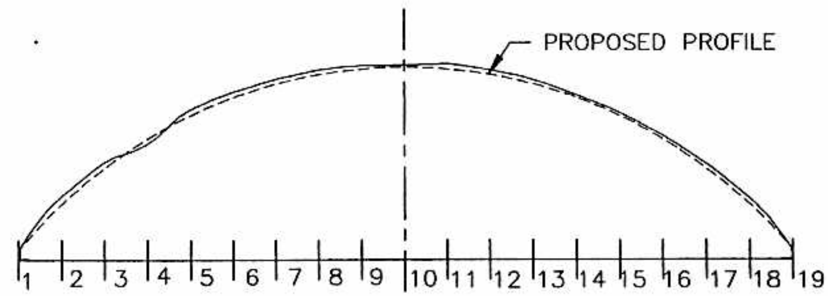

N – S LAYOUT

900lb – #3 HORZ

INTERNAL PRESSURE = 8"	TEST 2	WEB METHOD	14 MARCH 1996 7:00

Profile Results Data Sheet

Test 3 adjusted cables

Date 03/15/96

Internal pressure 4 in ** water pressure **

point #	x (ft)	y (ft)	measured z (in)	prop. profile in	Difference in
1	-18	0	0	0	0
2	-16	0	33.8	27.6	-6.2
3	-14	0	53	46.68	-6.32
4	-12	0	68	64.8	-3.2
5	-10	0	79	78.36	-0.64
6	-8	0	88.5	90	1.5
7	-6	0	95.625	96	0.375
8	-4	0	99.75	100.8	1.05
9	-2	0	100.5	102.6	2.1
10	0	0	100.8	103.8	3
11	2	0	100.4	102.6	2.2
12	4	0	99.5	100.8	1.3
13	6	0	95.625	96	0.375
14	8	0	87	90	3
15	10	0	79	78.36	-0.64
16	12	0	66.8	64.8	-2
17	14	0	51.2	46.68	-4.52
18	16	0	31.4	27.6	-3.8
19	18	0	0	0	0

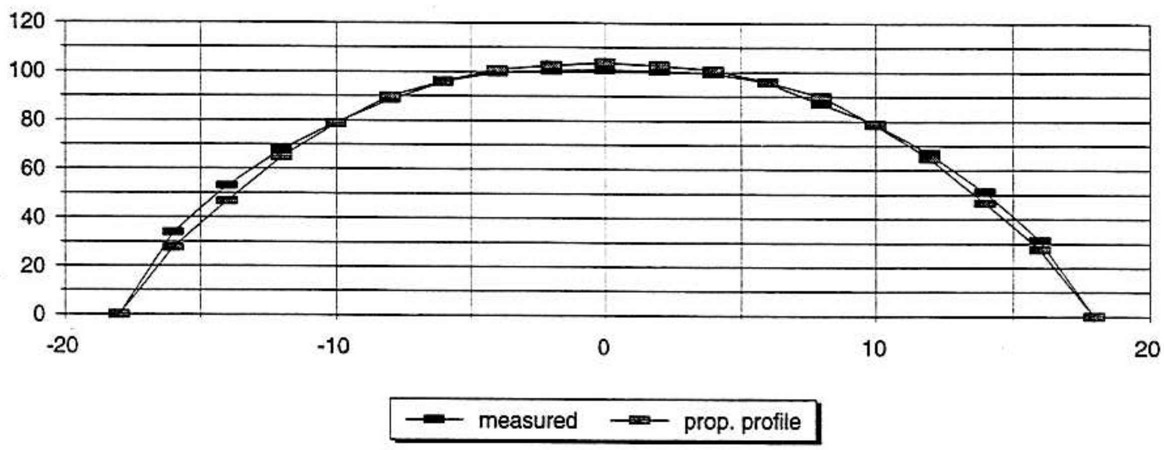

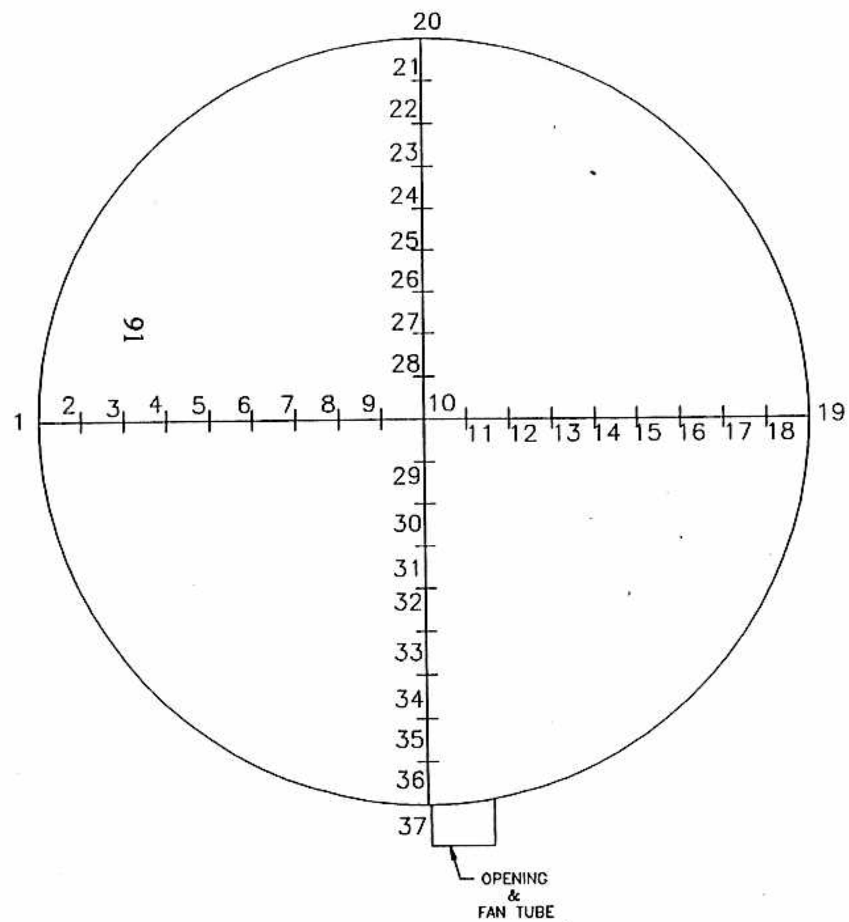

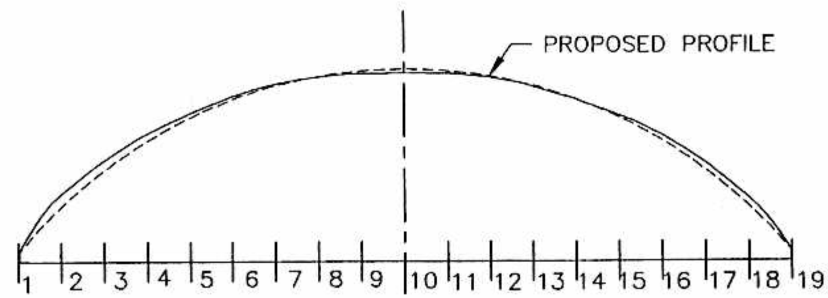

N – S LAYOUT

INTERNAL PRESSURE = 4"	TEST 3	WEB METHOD	15 MARCH 1996 7:30

Profile Results Data Sheet

Test 4 adjusted cables

Date 03/15/96

Internal pressure 10 in ** water pressure **

point #	x (ft)	y (ft)	measured z (in)	prop. profile in	Difference in
1	-18	0	0	0	0
2	-16	0	35	27.6	-7.4
3	-14	0	53.96	46.68	-7.28
4	-12	0	74	64.8	-9.2
5	-10	0	79.5	78.36	-1.14
6	-8	0	89	90	1
7	-6	0	96	96	0
8	-4	0	100.5	100.8	0.3
9	-2	0	102.75	102.6	-0.15
10	0	0	103	103.8	0.8
11	2	0	102.75	102.6	-0.15
12	4	0	100.25	100.8	0.55
13	6	0	96	96	0
14	8	0	87.75	90	2.25
15	10	0	79	78.36	-0.64
16	12	0	67.4	64.8	-2.6
17	14	0	52.4	46.68	-5.72
18	16	0	32	27.6	-4.4
19	18	0	0	0	0

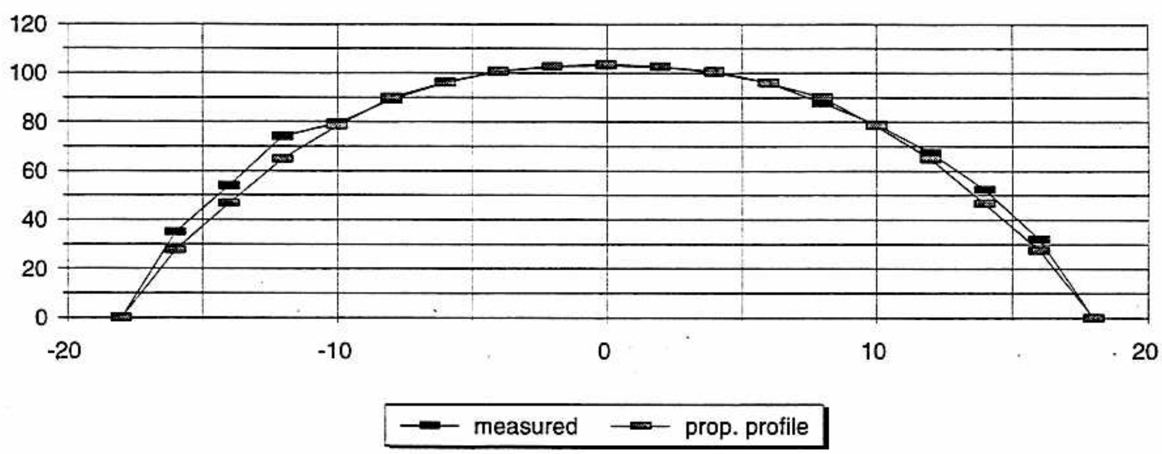

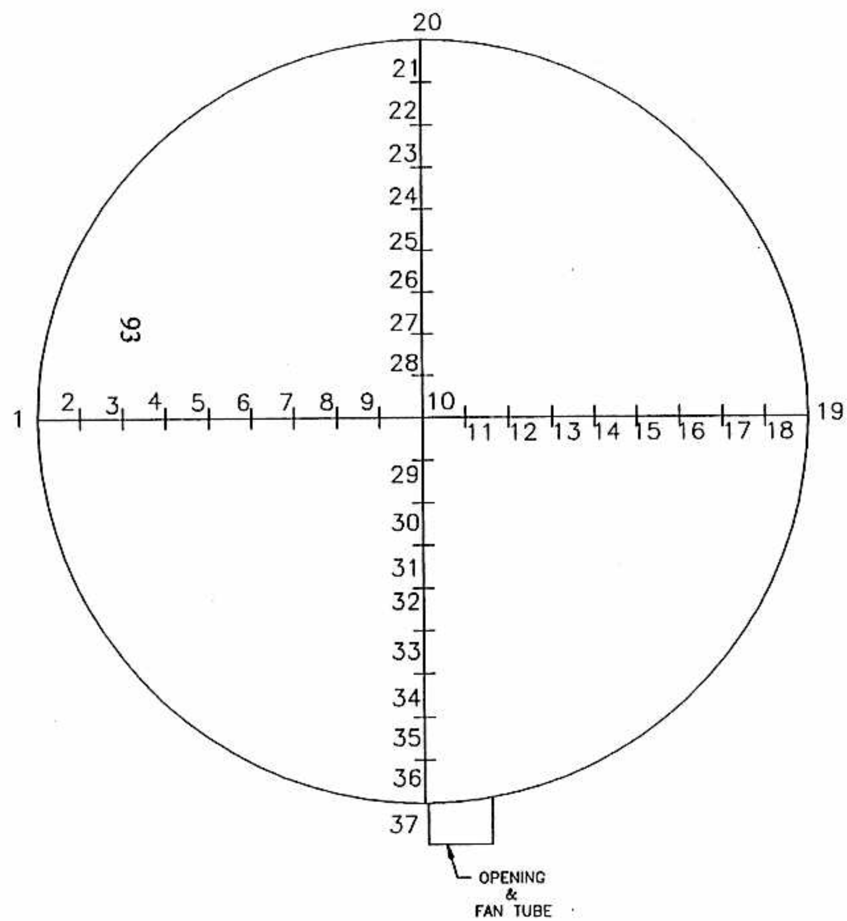

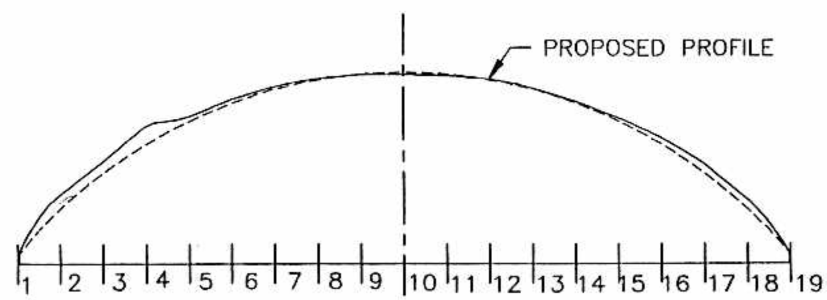

N – S LAYOUT

INTERNAL PRESSURE = 10"	TEST 4	WEB METHOD	15 MARCH 1996 8:00

Profile Results Data Sheet

Test	5		**0 horizontal rings - 8 main lateral cables			
Date		03/19/96				
Internal pressure	4 in		** water pressure **			
			measured	prop. profile	Difference	
point #	x (ft)	y (ft)	z (in)	in	in	
1	-18	0	0	0	0	
2	-16	0	31.325	27.6	-3.725	
3	-14	0	52.125	46.68	-5.445	
4	-12	0	67	64.8	-2.2	
5	-10	0	78.125	78.36	0.235	
6	-8	0	86	90	4	
7	-6	0	91.25	96	4.75	
8	-4	0	94.5	100.8	6.3	
9	-2	0	95.875	102.6	6.725	
10	0	0	95.75	103.8	8.05	
11	2	0	96	102.6	6.6	
12	4	0	94.625	100.8	6.175	
13	6	0	91	96	5	
14	8	0	85.875	90	4.125	
15	10	0	77.625	78.36	0.735	
16	12	0	67	64.8	-2.2	
17	14	0	51	46.68	-4.32	
18	16	0	29.625	27.6	-2.025	
19	18	0	0	0	0	

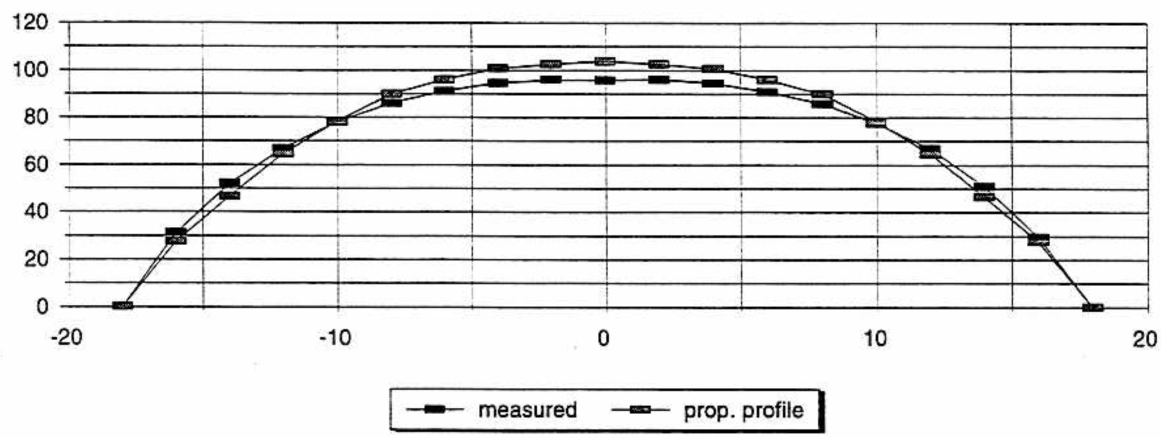

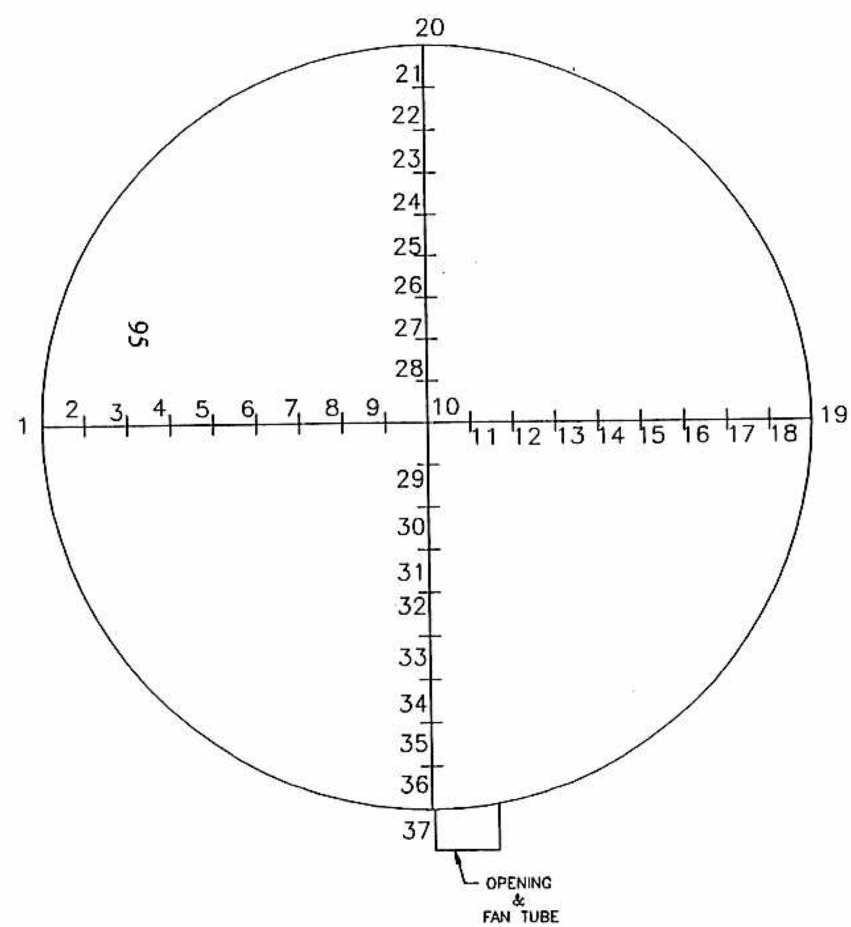

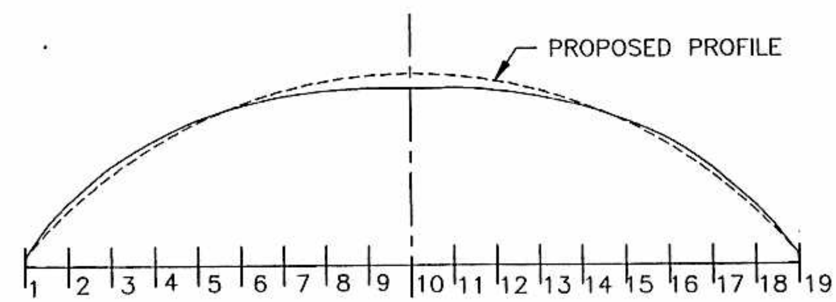

N – S LAYOUT

INTERNAL PRESSURE = 4"	TEST 5	8 LATITUDE LINES	19 MARCH 1996

Profile Results Data Sheet

Test		6	**0 horizontal rings - 8 main lateral cables			
Date		03/19/96				
Internal pressure		6 in	** water pressure **			
			measured	prop. profile	Difference	
point #	x (ft)	y (ft)	z (in)	in	in	
1	-18	0	0	0	0	
2	-16	0	31.75	27.6	-4.15	
3	-14	0	52.25	46.68	-5.57	
4	-12	0	67.325	64.8	-2.525	
5	-10	0	78.325	78.36	0.035	
6	-8	0	86.325	90	3.675	
7	-6	0	91.5	96	4.5	
8	-4	0	94.5	100.8	6.3	
9	-2	0	96	102.6	6.6	
10	0	0	95.875	103.8	7.925	
11	2	0	96	102.6	6.6	
12	4	0	94.625	100.8	6.175	
13	6	0	91.325	96	4.675	
14	8	0	85.875	90	4.125	
15	10	0	77.75	78.36	0.61	
16	12	0	66.625	64.8	-1.825	
17	14	0	51.75	46.68	-5.07	
18	16	0	29.75	27.6	-2.15	
19	18	0	0	0	0	

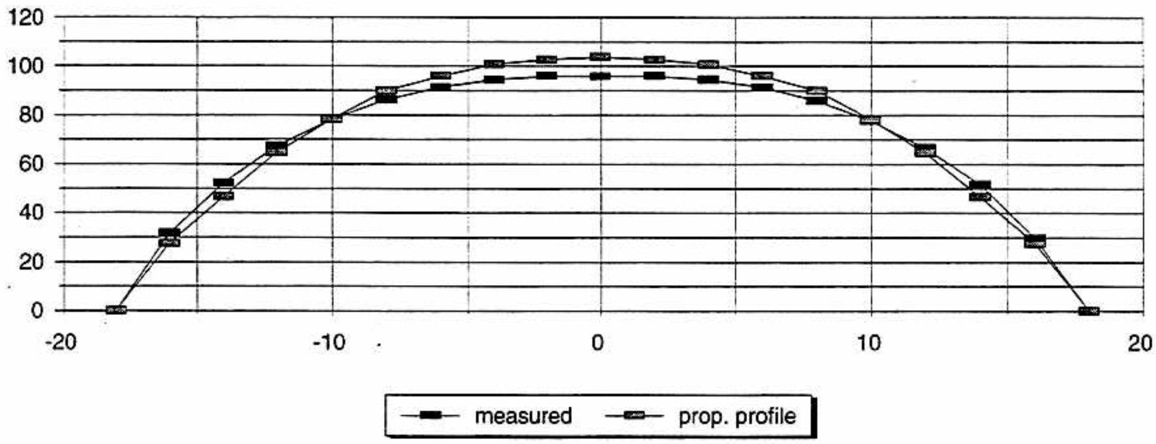

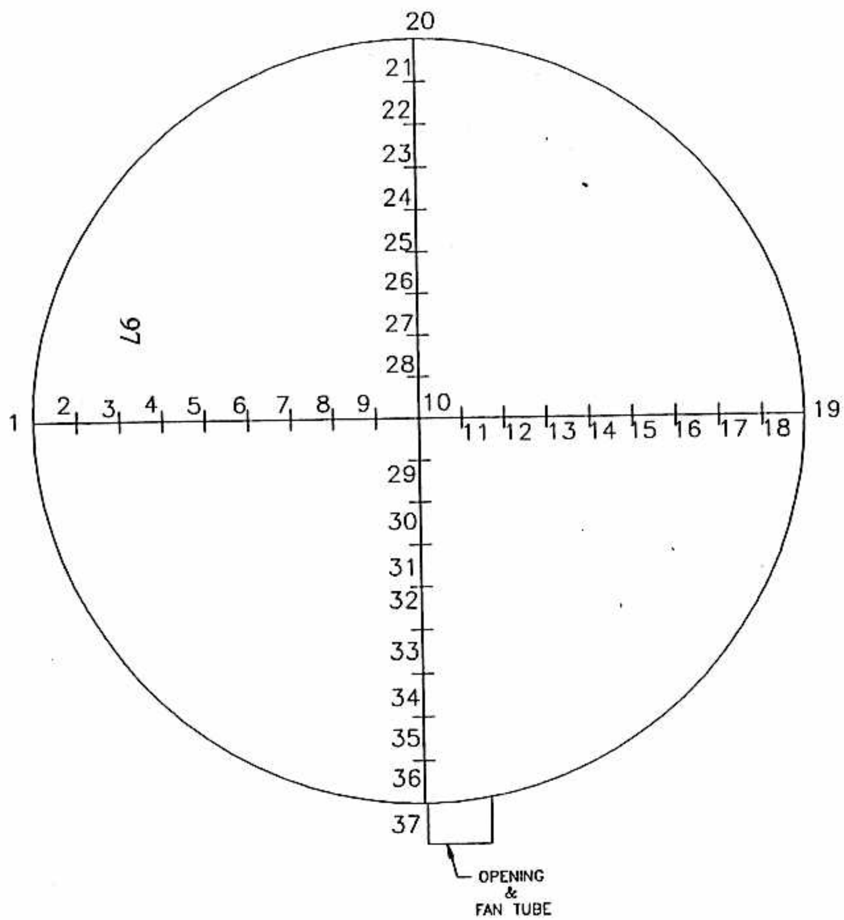

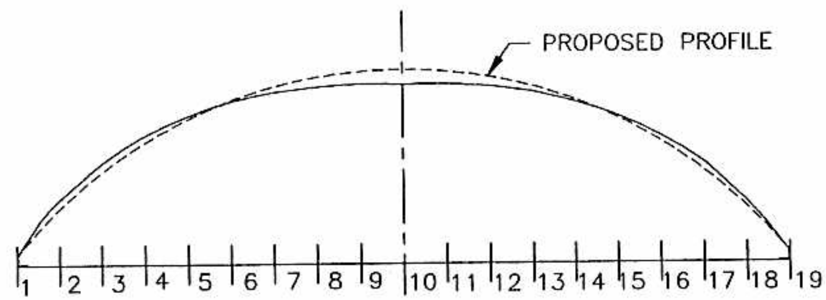

N – S LAYOUT

INTERNAL PRESSURE = 6"	TEST 6	8 LATITUDE LINES	19 MARCH 1996

Profile Results Data Sheet

Test	7		**0 horizontal rings - 8 main lateral cables			
Date		03/19/96				
Internal pressure	8 in		** water pressure **			
			measured	prop. profile	Difference	
point #	x (ft)	y (ft)	z (in)	in	in	
1	-18	0	0	0	0	
2	-16	0	32	27.6	-4.4	
3	-14	0	52.875	46.68	-6.195	
4	-12	0	68.25	64.8	-3.45	
5	-10	0	79.25	78.36	-0.89	
6	-8	0	87.125	90	2.875	
7	-6	0	92.25	96	3.75	
8	-4	0	95.325	100.8	5.475	
9	-2	0	96.625	102.6	5.975	
10	0	0	96.5	103.8	7.3	
11	2	0	96.625	102.6	5.975	
12	4	0	95.125	100.8	5.675	
13	6	0	92	96	4	
14	8	0	86.75	90	3.25	
15	10	0	78.875	78.36	-0.515	
16	12	0	67.25	64.8	-2.45	
17	14	0	52	46.68	-5.32	
18	16	0	30	27.6	-2.4	
19	18	0	0	0	0	

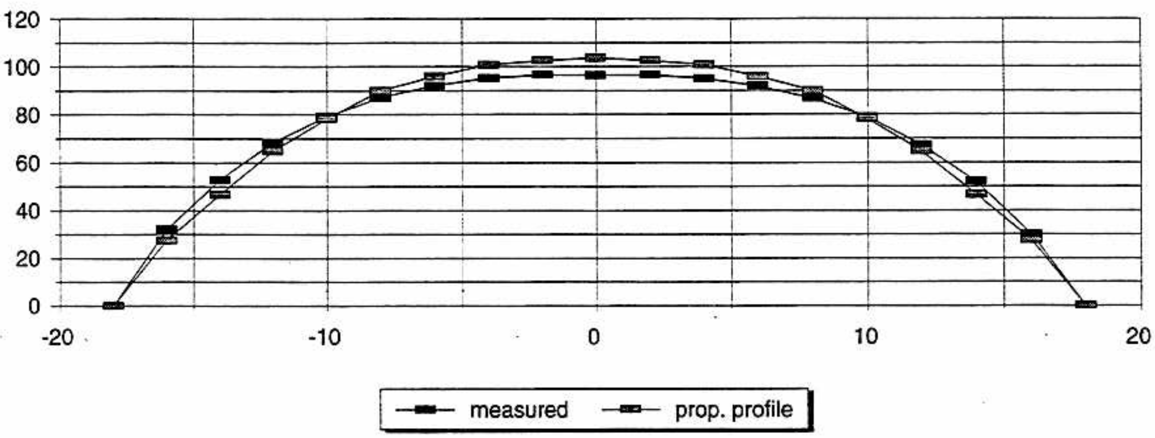

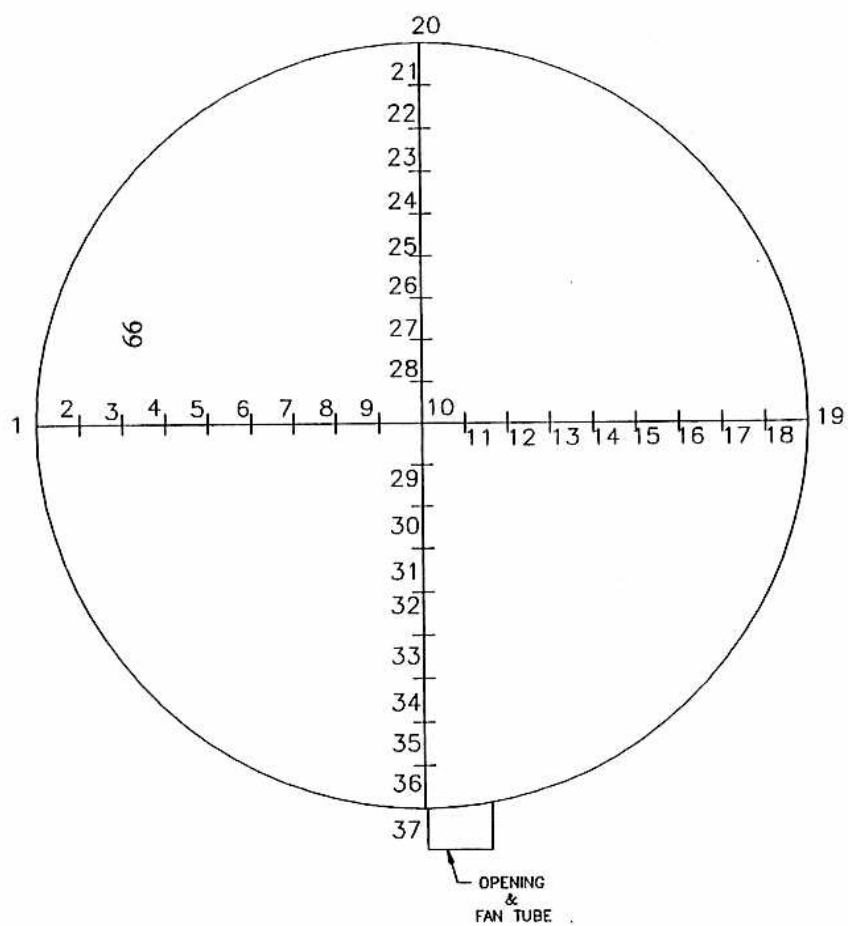

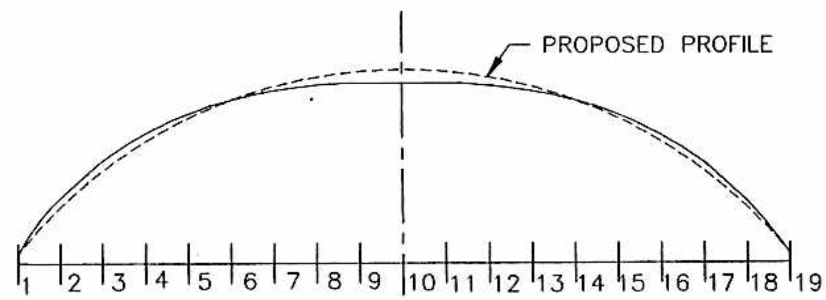

N - S LAYOUT

INTERNAL PRESSURE = 8"	TEST 7	8 LATITUDE LINES	19 MARCH 1996

Profile Results Data Sheet

Test		8	**0 horizontal rings - 8 main lateral cables		
Date		03/19/96			
Internal pressure		10 in	** water pressure **		
			measured	prop. profile	Difference
point #	x (ft)	y (ft)	z (in)	in	in
1	-18	0	0	0	0
2	-16	0	32	27.6	-4.4
3	-14	0	53.25	46.68	-6.57
4	-12	0	68.75	64.8	-3.95
5	-10	0	80	78.36	-1.64
6	-8	0	87.75	90	2.25
7	-6	0	92.75	96	3.25
8	-4	0	95.75	100.8	5.05
9	-2	0	96.125	102.6	6.475
10	0	0	96.5	103.8	7.3
11	2	0	97.125	102.6	5.475
12	4	0	95.75	100.8	5.05
13	6	0	93.625	96	2.375
14	8	0	87.125	90	2.875
15	10	0	79	78.36	-0.64
16	12	0	67.875	64.8	-3.075
17	14	0	52.5	46.68	-5.82
18	16	0	30	27.6	-2.4
19	18	0	0	0	0

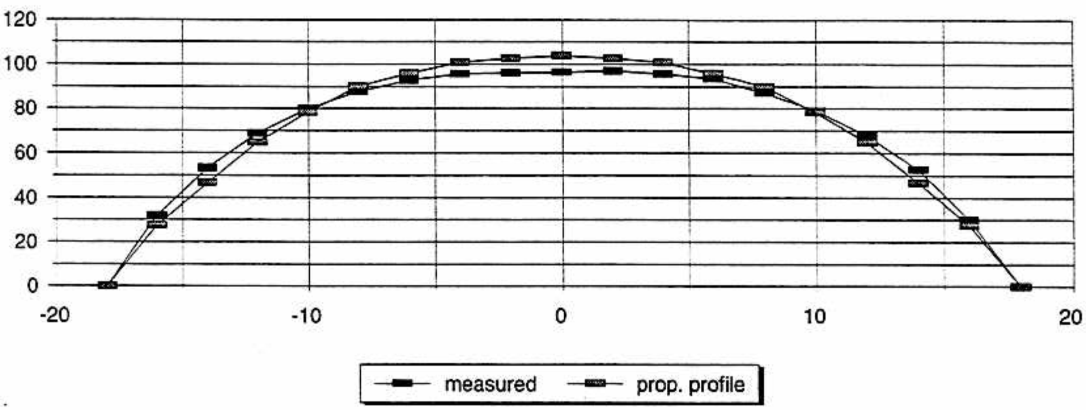

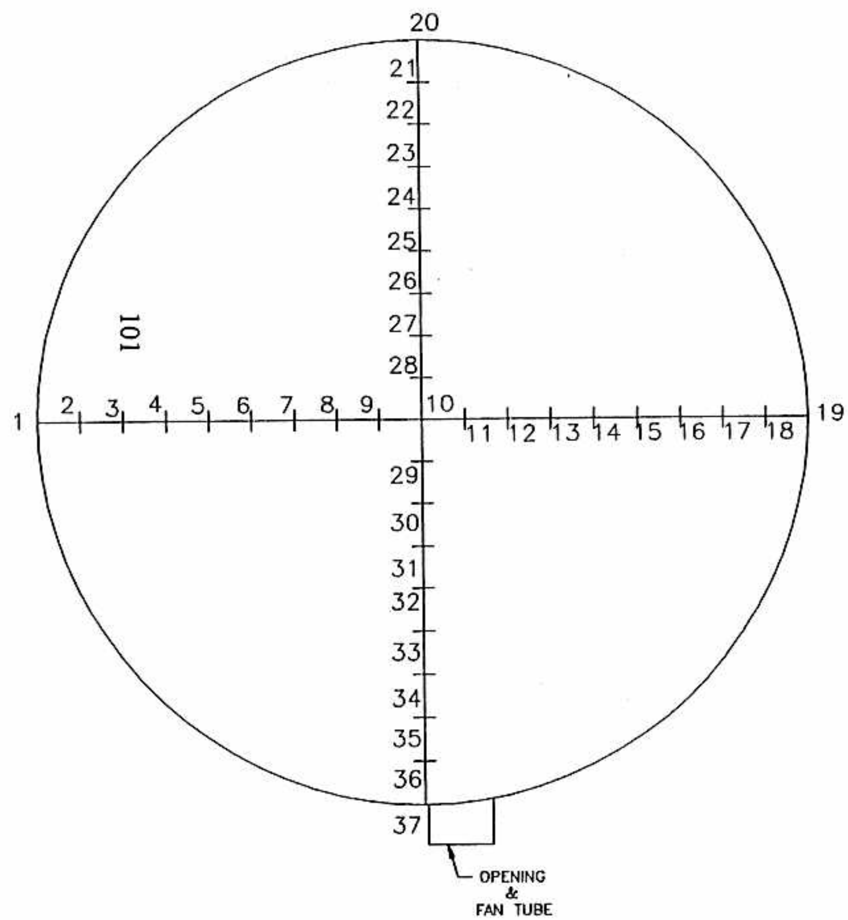

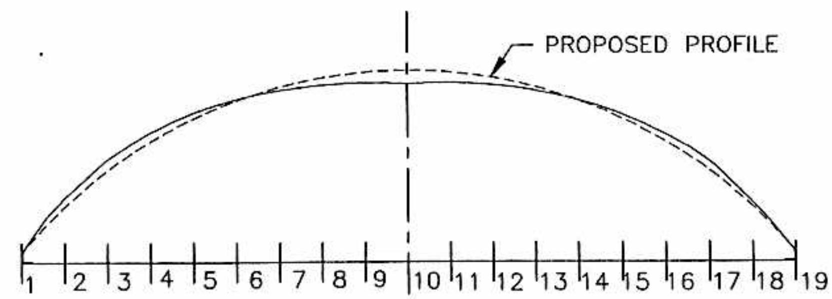

N – S LAYOUT

INTERNAL PRESSURE = 10"	TEST 8	8 LATITUDE LINES	19 MARCH 1996

Profile Results Data Sheet

Test 9 ** Geodesic cable net **

Date 03/20/96

Internal pressure 8 in ** water pressure **

point #	x (ft)	y (ft)	measured z (in)	prop. profile in	Difference in
1	-18	0	0	0	0
2	-16	0	29.5	27.6	-1.9
3	-14	0	46.75	46.68	-0.07
4	-12	0	64.25	64.8	0.55
5	-10	0	76.25	78.36	2.11
6	-8	0	86.25	90	3.75
7	-6	0	92.75	96	3.25
8	-4	0	98.25	100.8	2.55
9	-2	0	102.5	102.6	0.1
10	0	0	100.5	103.8	3.3
11	2	0	99.5	102.6	3.1
12	4	0	99.25	100.8	1.55
13	6	0	91.5	96	4.5
14	8	0	85.5	90	4.5
15	10	0	74.5	78.36	3.86
16	12	0	63.25	64.8	1.55
17	14	0	45.75	46.68	0.93
18	16	0	26.125	27.6	1.475
19	18	0	0	0	0

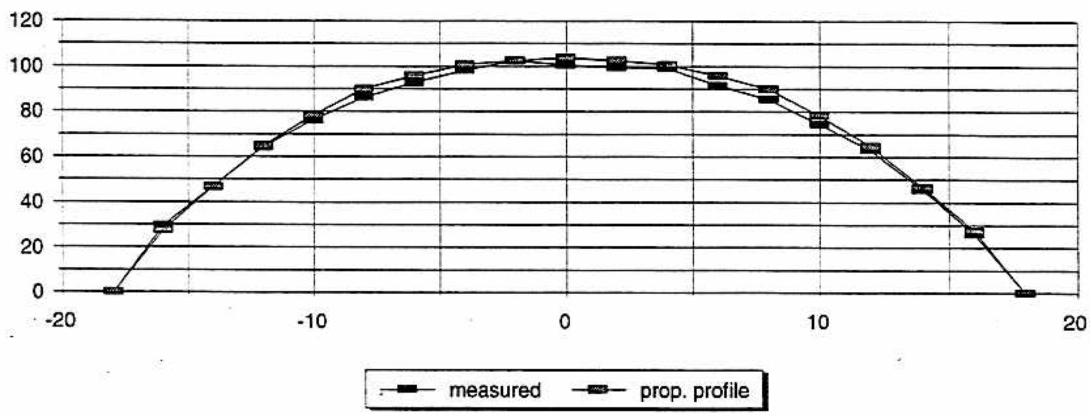

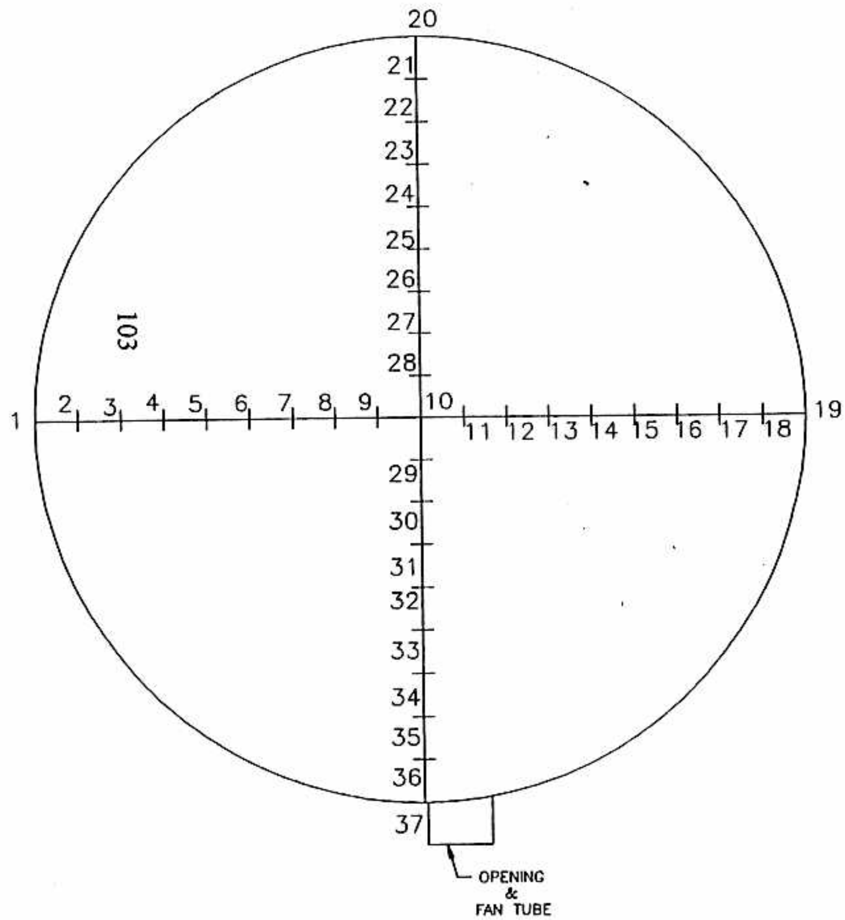

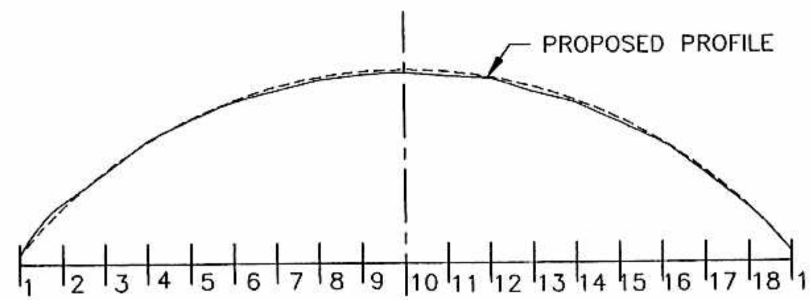

N – S LAYOUT

INTERNAL PRESSURE = 4"	TEST 9	GEODESIC	20 MARCH 1996

Profile Results Data Sheet

Test	10		** Geodesic cable net **			
Date		03/20/96				
Internal pressure		10 in	** water pressure **			
			measured	prop. profile	Difference	
point #	x (ft)	y (ft)	z (in)	in	in	
1	-18	0	0	0	0	
2	-16	0	30.325	27.6	-2.725	
3	-14	0	48.5	46.68	-1.82	
4	-12	0	66.625	64.8	-1.825	
5	-10	0	77.625	78.36	0.735	
6	-8	0	88.5	90	1.5	
7	-6	0	94	96	2	
8	-4	0	99.625	100.8	1.175	
9	-2	0	102	102.6	0.6	
10	0	0	102.75	103.8	1.05	
11	2	0	101.625	102.6	0.975	
12	4	0	100.125	100.8	0.675	
13	6	0	93.75	96	2.25	
14	8	0	87.625	90	2.375	
15	10	0	76.625	78.36	1.735	
16	12	0	64.875	64.8	-0.075	
17	14	0	47.625	46.68	-0.945	
18	16	0	28	27.6	-0.4	
19	18	0	0	0	0	

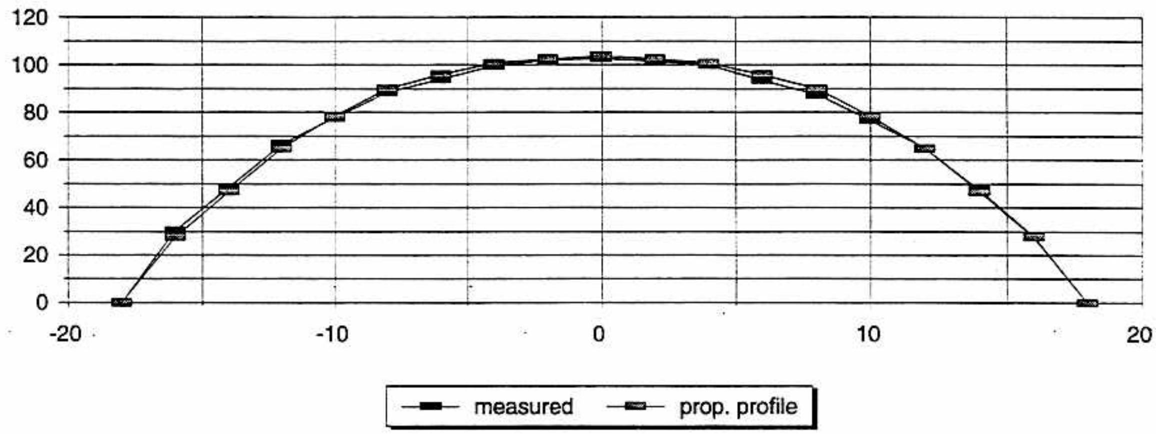

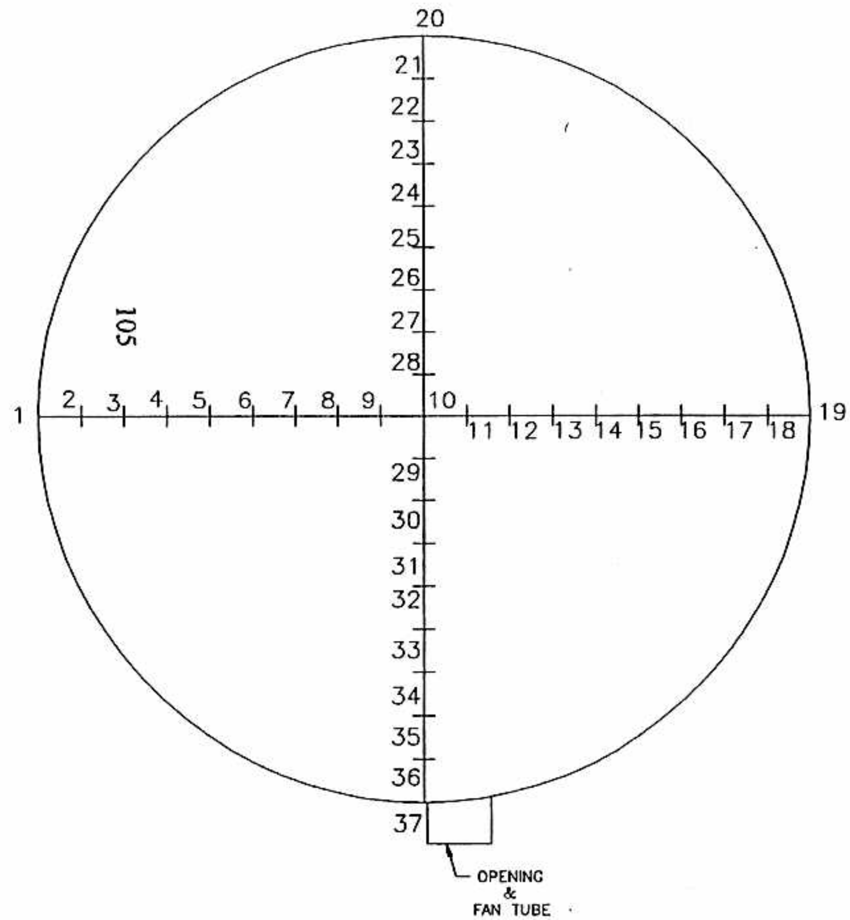

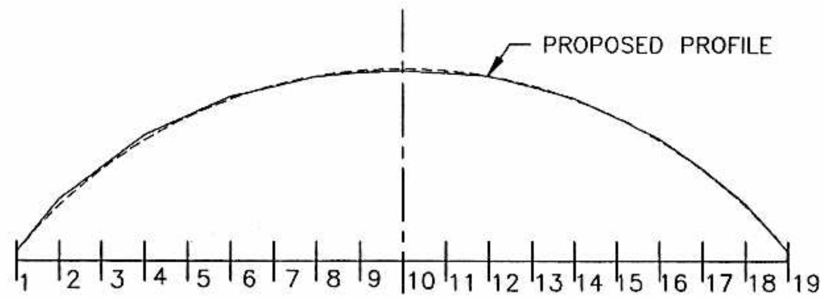

N – S LAYOUT

INTERNAL PRESSURE = 10"	TEST 10	GEODESIC	20 MARCH 1996

APPENDIX C

Cable Tension Data and Comparison Plots

Cable tension data sheets

Horizontal cable # 1 vert. down 2" adjusted short cab 2"

pressure inches water	pressure (psi)	test 1 measured tension (lb)	test 2 measured tension (lb)	test 3 measured tension (lb)	tension calculated
1	5.2	100	100	100	198
2	10.4	150	300	300	396
3	15.6	600	500	450	593
4	20.8	800	700	600	791
5	26	1050	1000	800	989
6	31.2	1400	1200	1000	1187
7	36.4	1600	1500	1200	1384
8	41.6	1900		1500	1582
9	46.8	2100		1800	1780
10	52	2300		2000	1978

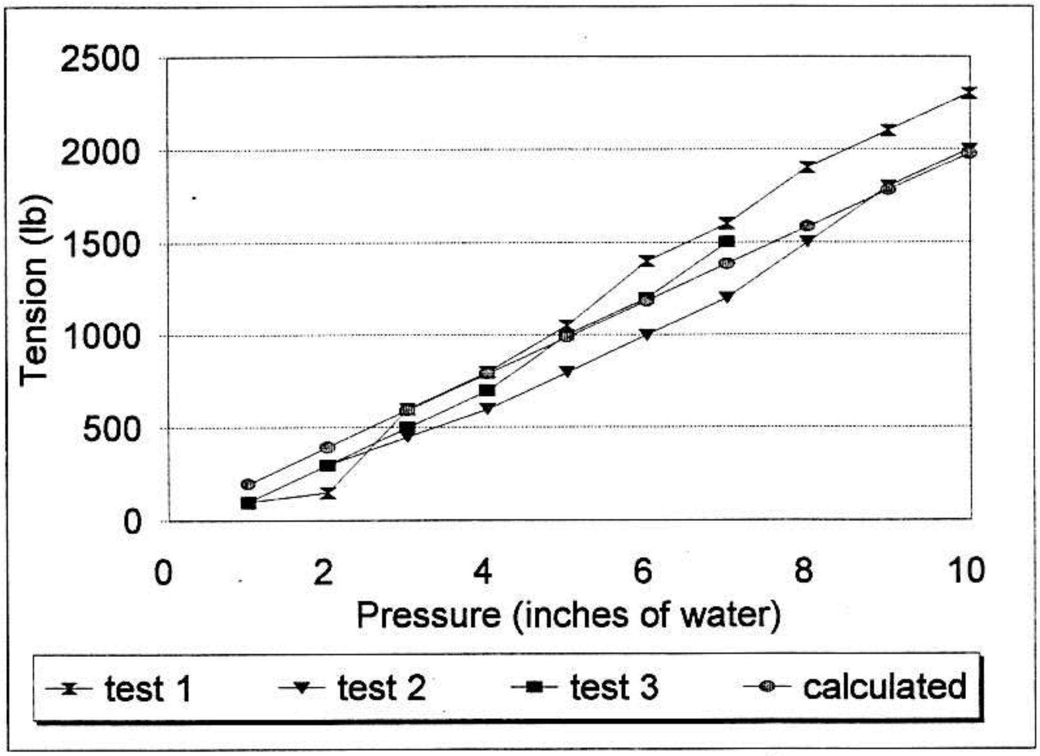

Cable tension data sheets

Horizontal cable # 2 vert. down 2" short cab 2" adjusted

pressure inches water	pressure (psi)	test 1 measured tension (lb)	test 2 measured tension (lb)	test 3 measured tension (lb)	tension calculated
1	5.2	300	100	75	123
2	10.4	500	175	100	247
3	15.6	1000	250	300	370
4	20.8	1400	700	400	493
5	26	1700	1000	600	617
6	31.2	2000	1100	1000	740
7	36.4	2400	1300	1200	864
8	41.6	2800	1600	1350	987
9	46.8	3100	1900	1500	1110
10	52	3400	2100	1600	1234

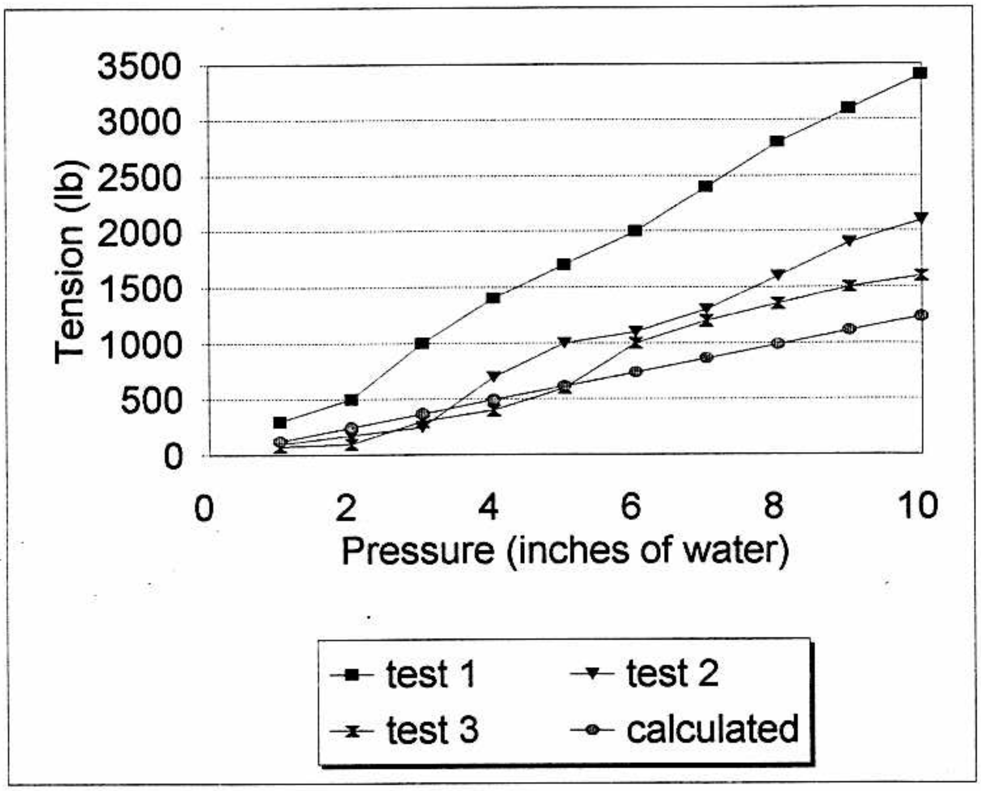

Cable tension data sheets

Horizontal cable # 3		short cab 2"	adjusted	
pressure		test 1	test 2	
inches water	pressure (psi)	measured tension (lb)	measured tension (lb)	tension calculated
1	5.2	75	0	75
2	10.4	100	0	149
3	15.6	250	0	224
4	20.8	400	100	298
5	26	550	200	373
6	31.2	700	300	448
7	36.4	800	400	522
8	41.6	1000	500	597
9	46.8	1300	600	672
10	52	1400	800	746

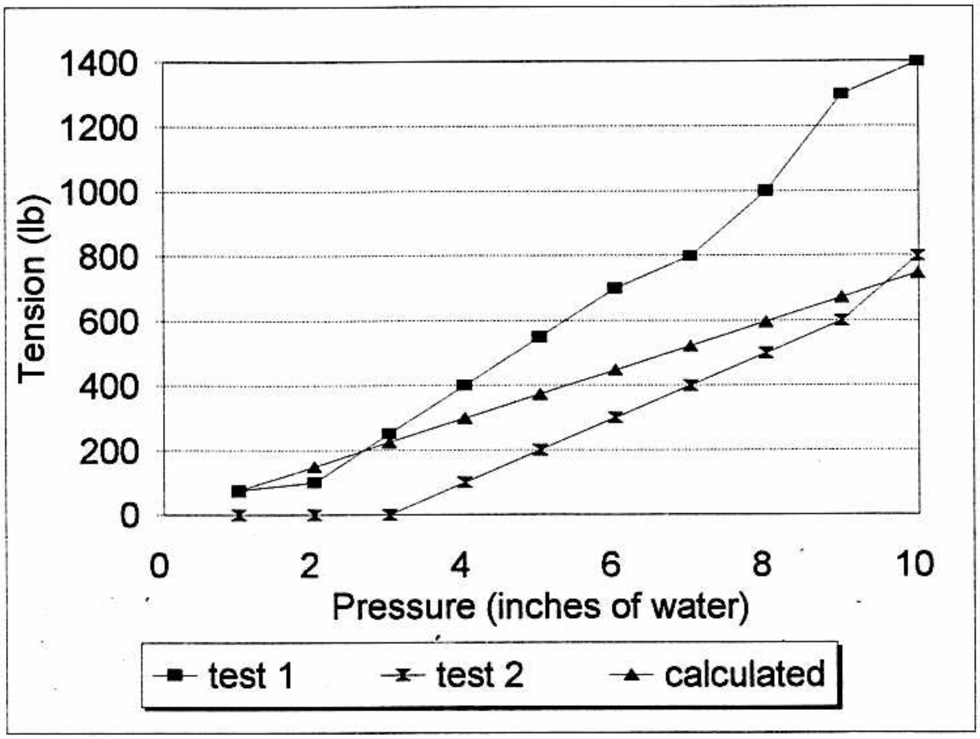

Cable tension data sheets

Vertical cable # 1 vert. down 2" only vert cab vertical cable # 2

pressure inches water	pressure (psi)	test 1 measured tension (lb)	test 2 measured tension (lb)	test 3 measured tension (lb)	tension calculated
1	5.2	0	0	0	138
2	10.4	100	200	0	276
3	15.6	300	300	0	414
4	20.8	550	500	100	552
5	26	750	650	200	690
6	31.2	900	800	300	828
7	36.4	1000	1000	350	966
8	41.6	1200	1200	400	1104
9	46.8	1300	1350	500	1242
10	52	1400	1600	550	1380

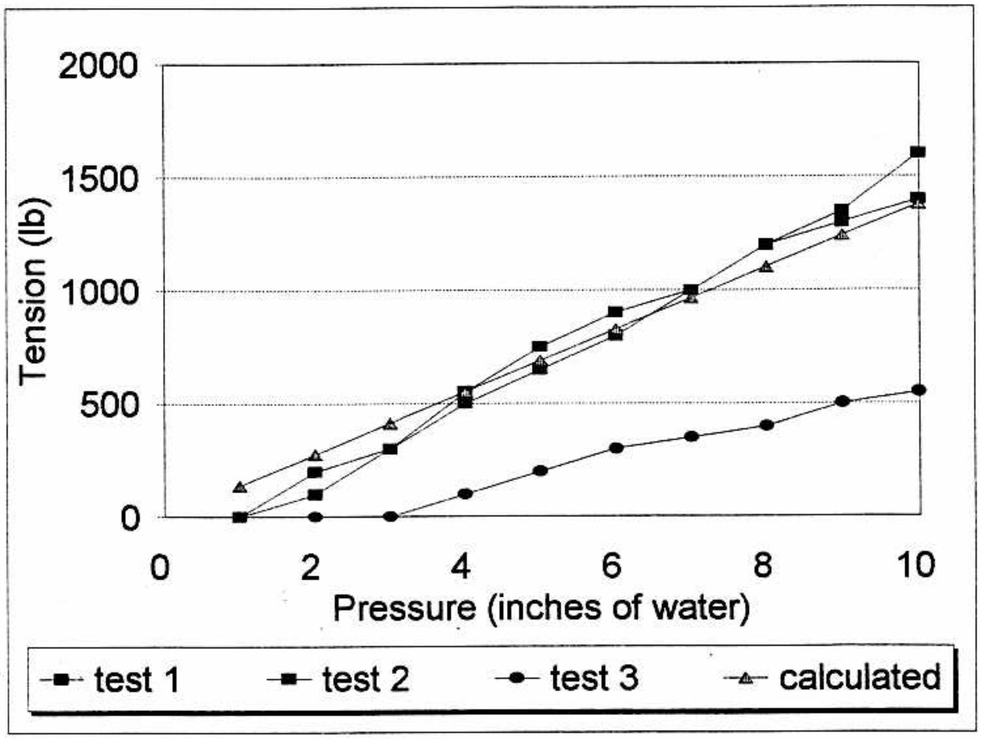

Geodesic cable net

pressure inches water	pressure (psi)	hoizontal test 1 measured tension (lb)	vertical test 2 measured tension (lb)
1	5.2	100	200
2	10.4	300	300
3	15.6	550	400
4	20.8	800	500
5	26	1000	550
6	31.2	1200	650
7	36.4	1400	700
8	41.6	1650	800
9	46.8	1850	900
10	52	2000	950

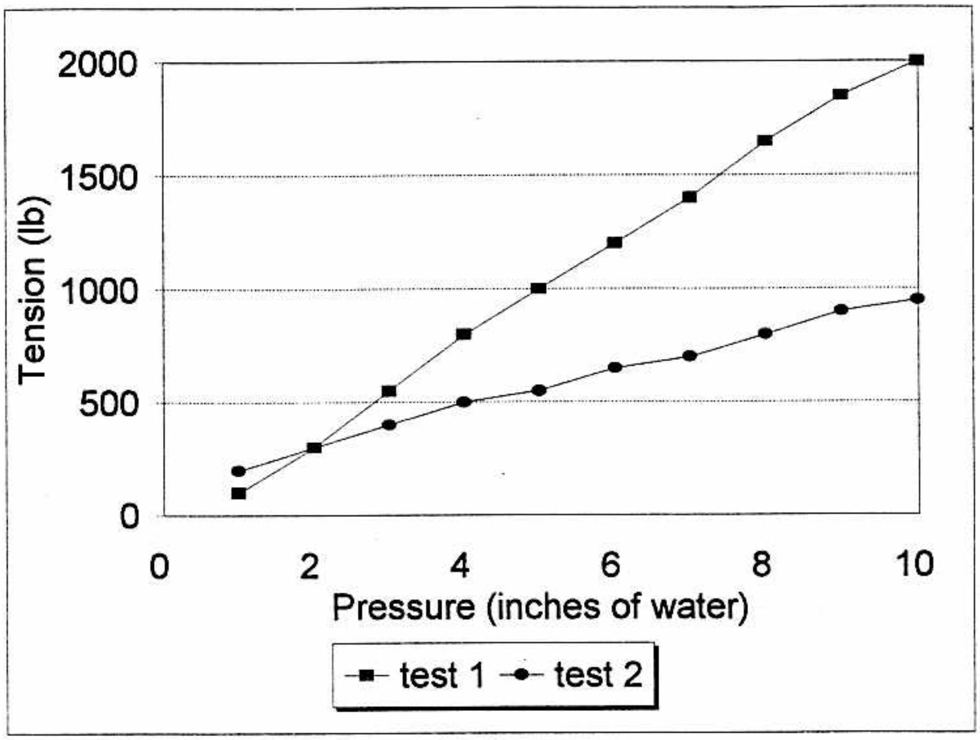

Calculations of tributary areas for each cable

Horizontal cables

	above	below	tributary area per foot	circum (ft)	equator circum (ft)	horizontal cable ratio
# 3	2.88	2.15	5.03	35.85	144.5	0.248
# 2	2.15	2.72	4.87	61.22	144.5	0.424
# 1	2.72	2.58	5.3	90.17	144.5	0.624
ring beam	2.58	0	2.58	113.1	144.5	0.783

Vertical cables

	top section (ft)	second section (ft)	Third section (ft)	fourth section (ft)	average width (ft)	tributary area per foot
# 4	0	0	0	1.59	1.59	1.59
# 3	0	0	2.37	1.59	1.98	1.98
# 2	0	3.03	2.37	1.59	2.33	2.33
# 1	2.24	3.03	2.37	1.59	2.31	2.31

Calculated tensions

pressure (in-water)		1	2	3	4	5	6	7	8	9	10
pressure (psf)		5.2	10.4	15.6	20.8	26	31.2	36.4	41.6	46.8	52
Rad. curv	23 ft										
Diameter	36 ft										

Horizontal cables

	tributary area (ft)	adjust factor	tension (lb)									
# 3	5.0	0.248	75	149	224	298	373	448	522	597	672	746
# 2	4.9	0.424	123	247	370	493	617	740	864	987	1110	1234
# 1	5.3	0.624	198	396	593	791	989	1187	1384	1582	1780	1978
ring beam	2.6	0.783	121	241	362	483	604	724	845	966	1087	1207

Vertical cables

	tributary area (ft)	[redacted]	tension (lb)									
# 4	1.6		95	190	285	380	475	570	666	761	856	951
# 3	2.0		118	237	355	474	592	710	829	947	1066	1184
# 2	2.3		139	279	418	557	697	836	975	1115	1254	1393
# 1	2.3		138	276	414	552	690	828	966	1104	1242	1380

Uplift	area (ft^2) 1017.876	Uplift (kips)									
		5	11	16	21	26	32	37	42	48	53
force per vertical cable (lbs)		83	165	248	331	414	496	579	662	744	827

APPENDIX D

Pictures of 36 ft Air Form Model Construction